UNIVERSITY OF TECHNOLOGY, SYDNEY
Faculty of Engineering and Information Technology

MODELLING AND CONTROL OF OFFSHORE CRANE SYSTEMS

by

R.M.T. Raja Ismail

A Thesis Submitted
in Partial Fulfillment of the
Requirements for the Degree

Doctor of Philosophy

Sydney, Australia

2015

Certificate of Authorship/Originality

I certify that the work in this thesis has not previously been submitted for a degree nor has it been submitted as a part of the requirements for other degree except as fully acknowledged within the text.

I also certify that this thesis has been written by me. Any help that I have received in my research work and in the preparation of the thesis itself has been fully acknowledged. In addition, I certify that all information sources and literature used are quoted in the thesis.

Production Note:
Signature removed
prior to publication.

R.M.T. Raja Ismail

July 15, 2015

ABSTRACT

MODELLING AND CONTROL OF OFFSHORE CRANE SYSTEMS

by

R.M.T. Raja Ismail

Cranes are widely used in transportation, construction and manufacturing. Suspended payloads in crane system are caused to swing due to actuator movement, external disturbance such as wind flows, and motion of the crane base in the case of portable cranes. Recently, offshore cranes have become a new trend in stevedoring and in offshore construction as they can help to avoid port congestion and also to exploit ocean engineering applications. For crane operations, it is important to satisfy rigorous requirements in terms of safety, accuracy and efficiency. One of the main challenges in crane operations has been identified as the sway motion control, which is subject to underactuation of crane drive systems and external disturbances. Particularly in offshore cranes, the harsh conditions can produce exogenous disturbances during the load transfer at various scenarios of offshore crane operations in practice. Therefore, it is interesting as to how to design robust controllers to guarantee high performance in the face of disturbances and parameter variations in offshore cranes.

The motivation for this thesis is based on recent growing research interest in the derivation of dynamic models and development of control techniques for offshore cranes in the presence of, for example, the rope length variation, sway, ocean waves and strong winds in offshore crane systems. Accordingly, the work for this thesis has been conducted in the two main themes, namely analytical modelling and control design, for which new results represent its contributions.

Dynamic models of two types of offshore crane systems, namely the offshore gantry crane and offshore boom crane, are derived in the presence of vessel's ocean

wave-induced motion. The effect of wind disturbances on the payload sway is also considered in the modelling. In the control context, sliding mode control techniques for a generic form of underactuated mechanical Lagrangian systems are presented, including the conventional first-order, second-order and adaptive fuzzy sliding mode controllers. The major component in this part of the thesis is the design of sliding mode control laws based on the developed offshore crane models for trajectory tracking problems, in the presence of persistent disturbances in severe open-sea conditions. Extensive simulation results are presented to demonstrate the efficacy of the models and robustness of the designed controllers.

Acknowledgements

This thesis could not have been completed without the enormous support of numerous people. I would like to acknowledge all those people who have made contribution to the completion of my thesis.

First of all, I would like to express my sincere thanks to my PhD supervisor, Associate Professor Quang Ha, for his guidance, advice, encouragement and support in the course of my doctoral work. Regular meetings in his research group and friendly discussions during lunch time at the University of Technology, Sydney (UTS) helped me reaffirm my research direction.

I would like to take this opportunity to gratefully acknowledge Universiti Malaysia Pahang and the Ministry of Education Malaysia for the financial support of my research and study at UTS.

Most importantly, my thesis could not have been completed without the encouragement and support from my family. I would like to dedicate my thesis to my parents, Siti Khodijah and Raja Ismail, and my beloved wife Mazni and daughter Aufa, who have been a source of care, love, support and strength during my graduate study.

My brothers and sisters and many friends whose concerns and support have helped me overcome obstacles and concentrate on my study, are acknowledged. I greatly appreciate their friendship and assistance.

R.M.T. Raja Ismail

Sydney, Australia, 2015.

List of Publications

1. **R.M.T. Raja Ismail**, Nguyen D. That, Q.P. Ha (2015), *Modelling and robust trajectory following for offshore container crane systems*, "Automation in Construction" – accepted on 13 May 2015.

2. **R.M.T. Raja Ismail**, Nguyen D. That, and Q.P. Ha (2014), *Offshore container crane systems with robust optimal sliding mode control*, The 31st International Symposium on Automation and Robotics in Construction and Mining, Sydney, Australia, pp. 149-156.

3. **R.M.T. Raja Ismail**, Nguyen D. That, and Q.P. Ha (2013), *Adaptive fuzzy sliding mode control for uncertain nonlinear underactuated mechanical systems*, The 2nd International Conference on Control, Automation and Information Sciences, Nha Trang, Vietnam, pp. 212-217.

4. **R.M.T. Raja Ismail** and Q.P. Ha (2013), *Trajectory tracking and anti-sway control of three-dimensional offshore boom cranes using second-order sliding modes*, The 9th IEEE International Conference on Automation Science and Engineering, Wisconsin, Madison, USA, pp. 996-1001.

5. **R.M.T. Raja Ismail** and Q.P. Ha (2013), *Trajectory tracking control for offshore boom cranes using higherorder sliding modes*, The 30st International Symposium on Automation and Robotics in Construction and Mining, Montreal, Canada, pp. 894-904.

6. **R.M.T. Raja Ismail** and Q.P. Ha (2012), *Second-order sliding mode control for offshore container cranes*, The 22nd Australasian Conference on Robotics and Automation, Wellington, New Zealand, 7p.

7. **R.M.T. Raja Ismail**, Nguyen D. That, and Q.P. Ha (2012), *Observer-based trajectory tracking for a class of underactuated Lagrangian systems using higher-order sliding modes*, The 8th IEEE International Conference on Automation Science and Engineering, Seoul, Korea, pp. 1200-1205.

8. Nguyen D. That, Nguyen K. Quang, **R.M.T. Raja Ismail**, P.T. Nam and Q.P. Ha (2012), *Improved reachable set bounding for linear systems with discrete and distributed delays*, The 1st International Conference on Control, Automation and Information Sciences, Ho Chi Minh, Vietnam, pp. 137-141.

Contents

Certificate ii

Abstract iii

Acknowledgments v

List of Publications vi

List of Figures xii

List of Tables xvi

Notation xvii

1 Introduction 1

1.1 Background 1

1.2 Research objectives 7

1.3 Thesis organization 7

2 Literature Survey 9

2.1 Underactuated mechanical system 9

2.1.1 Equations of motion 11

2.1.2 Feedback linearisation 13

2.2 Crane dynamics and control 15

2.2.1 Crane dynamics 15

2.2.2 Crane control 16

2.3 Sliding mode control 24

2.3.1 Regular form of linear-time invariant system 25

2.3.2 First-order sliding mode control 27

2.3.3 Second-order sliding mode 35

2.4 Summary 40

3 Modelling of Offshore Crane Systems 42

3.1 Introduction 42

3.2 Euler-Lagrange equation for cranes 42

3.3 Modelling of offshore gantry cranes 44

3.3.1 2-D model 44

3.3.2 3-D model 49

3.4 Modelling of offshore boom cranes 52

3.4.1 2-D model 53

3.4.2 3-D model 57

3.5 Summary 63

4 Sliding Mode Control Approaches for Underactuated Mechanical Systems with Application to Cranes 64

4.1 Introduction 64

4.2 Problem formulation 64

4.3 First-order sliding mode control 66

4.4 Adaptive fuzzy sliding mode control 67

4.4.1 Fuzzy logic control 67

4.4.2 Adaptive fuzzy sliding mode controller 68

4.4.3 Stability analysis 70

4.4.4 Results and discussion 71

4.5 Second-order sliding mode control 76
4.5.1 Second-order sliding mode controller 78
4.5.2 Second-order sliding mode observer 79
4.5.3 Observer-based 2-SMC 81
4.5.4 Results and discussion 81
4.6 Summary 88

5 Development of First-order Sliding Mode Control for Offshore Crane Systems 90

5.1 Introduction 90
5.2 Problem statement 90
5.3 Control design for 2-D offshore gantry crane 92
5.3.1 Crane trajectory 92
5.3.2 Sliding surface design using LQR approach 95
5.3.3 Sliding mode control 97
5.3.4 Results and discussion 100
5.4 Control design for 2-D offshore boom crane 110
5.4.1 Sliding surface design using LMI approach 110
5.4.2 Sliding mode control 111
5.4.3 Results and discussion 114
5.5 Summary 119

6 Development of Second-order Sliding Mode Control for Offshore Crane Systems 120

6.1 Introduction 120
6.2 Second-order sliding mode control 120

6.2.1 The control algorithm 120
6.2.2 Stability analysis 123
6.3 Results and discussion 124
6.3.1 Offshore gantry crane 124
6.3.2 Offshore boom crane 129
6.4 Summary 130

7 Thesis Contributions and Conclusions 134

7.1 Thesis contributions 134
7.2 Conclusions 135
7.3 Future work 137

Bibliography 139

List of Figures

1.1 Panoramic view of Sydney Harbour. 2

1.2 Ships lightering operation [126]. 4

1.3 An offshore crane transferring containers between a ship and a vessel [135]. 4

1.4 Container gantry crane mounted on a vessel [113]. 5

1.5 Ship-mounted boom cranes near Port Botany, Sydney. 5

2.1 Architecture of feedback linearisation control. 14

3.1 Motion of the offshore crane during containers transfer operation. . . 45

3.2 Motion of the offshore crane during containers transfer operation. . . 50

3.3 Motion of the 2-D offshore boom crane. 53

3.4 An offshore boom crane. 58

3.5 Motion of the offshore boom crane. 58

4.1 Two-dimensional gantry crane system at UTS laboratory. 72

4.2 Motion of the gantry crane system. 72

4.3 (a) Trolley position; (b) Sway angle; and (c) Control effort; when $d_x = d_\phi = 0$. 75

4.4 (a) Trolley position; (b) Sway angle; and (c) Control effort; when $d_x \neq 0$ and $d_\phi \neq 0$. 76

4.5 (a) Trolley position; (b) Sway angle; (c) Control effort; and (d) Payload mass; when $d_x \neq 0$, $d_\phi \neq 0$, and the payload mass is varied. . 77

4.6 Motion of a 3D overhead gantry crane. 82

4.7 Schematic diagram of the observer-based control using second-order sliding modes for an underactuated mechanical system. 83

4.8 Sigmoid function trajectory. 84

4.9 (a) Cart position in X- and Y-directions; (b) Actual and reference trajectories. 85

4.10 Trajectory tracking error in (a) X-direction; and (b) Y-direction. . . 86

4.11 Swing angle projection to the (a) $Y_M Z_M$-plane; and (b) $X_M Z_M$-plane. 86

4.12 Real and estimated cart velocities in (a) X-direction; and (b) Y-direction. 87

4.13 Cart position with payload variation. 87

5.1 Cart position and velocity reference trajectories. 94

5.2 Hoisting rope length and velocity reference trajectories. 94

5.3 Wind drags due to (a) short burst; and (b) persistent wind disturbances. 100

5.4 Trajectory tracking responses of the (a) cart position; (b) rope length; and (c) swing angle subject to short burst wind disturbance. . 101

5.5 Tracking error responses of the (a) cart position; (b) rope length; and (c) swing angle subject to short burst wind disturbance. 102

5.6 (a) Cart velocity and (b) hoist velocity responses subject to short burst wind disturbance. 103

5.7 Sliding functions subject to short burst wind disturbance. 104

5.8 (a) Cart driving force; and (b) hoisting input force subject to short burst wind disturbance. 105

5.9 Trajectory tracking responses of the (a) cart position; (b) rope length; and (c) swing angle subject to persistent wind disturbance. . . 106

5.10 Switching functions subject to persistent wind disturbance. 107

5.11 (a) Cart driving force; and (b) hoisting input force subject to persistent wind disturbance. 108

5.12 Cart position responses with nominal values of system masses and with $\Delta m_p/m_p = 10\%$. 108

5.13 Rope length responses with nominal values of system masses and with $\Delta m_p/m_p = 10\%$. 109

5.14 Swing angle responses with nominal values of system masses and with $\Delta m_p/m_p = 10\%$. 109

5.15 Trajectory tracking responses of the (a) luff angle; (b) rope length; and (c) swing angle. 116

5.16 Tracking error responses of the (a) luff angle; (b) rope length; and (c) swing angle. 117

5.17 Sliding functions. 118

5.18 (a) Boom input torque; (b) hoisting input force. 118

6.1 Block diagram of the offshore crane control system 123

6.2 (a) Trolley position; (b) rope length; and (c) swing angles; when the mobile harbour is stationary, i.e. $\zeta = 0$ m and $\phi = \psi = 0$ rad. 126

6.3 (a) Trolley position; (b) rope length; and (c) swing angles; when $\zeta = 0.02 \sin 1.25t$ m, $\phi = 0.02 \sin 1.25t$ rad and $\psi = 0.01 \sin 1.25t$ rad. 127

6.4 (a) Trolley position and payload mass; (b) rope length; and (c) swing angles; when $\zeta = 0.02 \sin 1.25t$ m, $\phi = 0.02 \sin 1.25t$ rad, $\psi = 0.01 \sin 1.25t$ rad, and $\Delta m/m = 10\%$. 128

6.5 (a) Slew angle; (b) luff angle; (c) rope length; and (d) swing angles; when the vessel is stationary, i.e. $\zeta = 0$ m and $\phi = \psi = 0$ rad. 131

6.6 (a) Slew angle; (b) luff angle; (c) rope length; and (d) swing angles; when $\zeta = 0.02 \sin 1.25t$ m and $\phi = \psi = 0.01 \sin 1.25t$ rad. 132

6.7 (a) Slew angle; (b) luff angle; (c) rope length; and (d) swing angles; when $\zeta = 0.02 \sin 1.25t$ m, $\phi = \psi = 0.01 \sin 1.25t$ rad, and $\Delta m/m = 10\%$ 133

List of Tables

2.1 Summary of previous offshore crane models and control methods. . . 18

Nomenclature and Notation

Throughout the thesis, the following nomenclatures and notations are used:

- 1-SMC: First-order sliding mode control
- 2-SMC: Second-order sliding mode control
- 2-D: Two-dimensional
- 3-D: Three-dimensional
- AFSMC: Adaptive fuzzy sliding mode control
- DOF: Degree of freedom
- HOSM: Higher-order sliding modes
- LQR: Linear quadratic regulator
- LMI: Linear matrix inequality
- LTI: Linear time-invariant
- MIMO: Multi input multi output
- SISO Single input single output
- SMC: Sliding mode control
- SVD: Singular value decomposition
- UMS: Underactuated mechanical system
- VSC: Variable structure control
- $\mathbb{R}$: Field of real numbers
- $\mathbb{R}^n$: n-dimensional space
- $\mathbb{R}^{n\times m}$: Space of all matrices of $(n \times m)$-dimension
- A^T: Transpose of matrix A
- A^{-1}: Inverse of matrix A
- I_n: Identity matrix of $(n \times n)$-dimension
- $0_{n\times m}$: Zero matrix of $(n \times m)$-dimension
- C_θ: $\cos\theta$

- S_θ: $\sin\theta$
- $\lambda(A)$: Set of all eigenvalues of matrix A
- $\lambda_{\min}(A)$: Smallest eigenvalue of matrix A
- $\lambda_{\max}(A)$: Largest eigenvalue of matrix A
- $\text{diag}(\lambda_1, \cdots, \lambda_i, \cdots, \lambda_n)$: Diagonal matrix with diagonal entries λ_i, $i = 1, \cdots, n$
- $\text{rank}(A)$: Rank of matrix A
- $\text{sign}(\cdot)$: Signum function
- $||\cdot||$: Euclidean norm of a vector or spectral norm of a matrix
- $\forall$: For all

Chapter 1

Introduction

1.1 Background

Cranes are used for transportation of heavy loads such as containers and construction materials on land as well as at open sea. They are widely used in construction sites, warehouses and harbours (Figure 1.1) due to their ability to handle hefty objects.

In general, cranes can be regarded as underactuated Lagrangian system. Firstly, crane systems are underactuated because they have fewer independent control actuators than degrees of freedom (DOF) to be controlled. For example, in a 2-D gantry crane system, both cart position on the girder and payload sway are controlled by a single motor. Secondly, cranes are classified as Lagrangian systems because their equations of motion can be obtained based on the formulation of Lagrangian mechanics like robotic manipulators. Basically, a crane system consists of a support mechanism, which is a part of its structure, and a hoisting mechanism. The hoisting mechanism of a crane often exhibits an oscillatory behaviour due to the underactuation of the system. For this reason, it is important for a crane operation to meet stringent safety requirement.

A large number of studies on the development of control strategies to improve the efficiency and safety of crane operations has been seen over the past few decades. The hoisting mechanism that typically consists of cable, hook and payload assembly has high compliance. Hence, certain exogenous excitations at the suspension point can produce high amplitude of oscillations to the payload. The inertia forces due to

Figure 1.1 : Panoramic view of Sydney Harbour.

the motion of the crane can induce significant payload pendulations as well. This problem occurs because cranes are typically lightly damped. In other words, any transient oscillation response in crane systems takes a long time to dampen out.

As the research on conventional cranes becomes well established, researchers have explored a more complex problem, namely the offshore cranes. The growing usage of ocean facilities in many segments such as shipping of containers, oil and gas exploration, and offshore wind farm construction have necessitated certain operations occur in open sea conditions. These activities require the application of offshore cranes to transfer loads between vessels or to place loads from a vessel to an offshore site.

In general, offshore cranes operations can be categorised into two types, namely the stevedoring and the moonpool operations. Offshore stevedoring or lightering is the process of transferring containers between vessels, and moonpool operation is the activity of a payload placement underwater or on the seabed for the purpose of underwater installation. The advantage of offshore stevedoring operation is it can avoid marine traffic congestion in a port. The transfer of containers between two

vessels requires a crane equipment on one of the vessel (Figure 1.2) or a third vessel (Figure 1.3). The common types of offshore cranes used in this operation is gantry crane (Figure 1.4) and boom crane (Figure 1.5).

Port congestion has become a major issue over the last few years due to rapid developments of logistics industry causing a substantial increase in the trading volume [50, 74, 144]. Some ambitious plans of port expansion have been proposed to overcome this problem, but it is not a feasible solution due to land constraints. Consequently, a new method of transportation, namely, the ship-to-ship cargo transfer operation, is introduced [81]. This method, emerging to become a promising solution to improve ports' efficiency and productivity and reduce operational costs, could enable the ports to stay competitive.

Despite all the necessities and benefits of offshore transportation and installation, the presences of persistent disturbances in the crane operations due to harsh sea condition are inevitable. Ocean waves can induce motions to vessels or ships where cranes are located. These motions include roll, pitch, yaw, surge, sway and heave. Besides, wind drag or buoyancy of seawater can produce exogenous forces on the payload, whenever it is suspended in the air or submerged. For this reason, it is necessary to have an element of robustness in the offshore cranes control system to deal with the aforementioned disturbances.

In particular, motivated by a large amount of significant practical problems, the control of underactuated nonlinear systems has become an important subject of research. Intuitively, the control synthesis for underactuated systems is more complex than that for fully actuated systems. Control of underactuated systems is currently an active field of research due to their broad applications in robotics, land and aerospace vehicles, surface vessels and crane automation. Based on recent surveys, control of general underactuated systems is a major open problem. Since the

Figure 1.2 : Ships lightering operation [126].

Figure 1.3 : An offshore crane transferring containers between a ship and a vessel [135].

presence of uncertainties and parameter variations always aroused in underactuated nonlinear systems, the implementation of robust control approach on the systems is appealing.

Sliding mode control (SMC) is a well-known control methodology belonging to the variable structure systems which are characterised by their robustness with re-

Figure 1.4 : Container gantry crane mounted on a vessel [113].

Figure 1.5 : Ship-mounted boom cranes near Port Botany, Sydney.

spect to parameter variations and external disturbances. The basic idea of the sliding mode is to drive the system trajectories into a predetermined hyperplane or surface and maintain the trajectory on it for all subsequent time. During the ideal sliding motion, the system is completely insensitive to uncertainties or external disturbances. The dynamics and performance of the systems then depend on the selection of the sliding surface. In SMC design, a sliding surface is first constructed

to meet existence conditions of the sliding mode. Then, a discontinuous control law is synthesized to drive the system state to the sliding surface in a finite time and maintain it thereafter on that surface. However, the effects of the discontinuous nature of the control, known as the chattering phenomenon have originated a certain scepticism about such an approach. The common practice to overcome the chattering phenomena is by changing the system dynamics in a small vicinity of the discontinuity surface. This modification can avoid real discontinuity while preserving the main properties of the whole system. However, robustness of the sliding mode were partially lost.

The introduction of higher-order sliding modes (HOSM) can practically attenuate the chattering if properly designed. The chattering attenuation can be achieved because the HOSM acting on the higher order derivatives of the system deviation from the constraint (e.g., sliding function), instead of influencing the first deviation derivative that occurs in standard or first-order sliding modes. HOSM preserve the main advantages of the original approach, as well as totally remove the chattering effect. Besides, HOSM can provide higher accuracy in realization of the control system. Second-order sliding mode control (2-SMC) algorithms recently developed have produced satisfactory results for single-input systems. The extension of second-order sliding mode to multi-input systems, as in general, most of the underactuated systems are, is nontrivial.

Fuzzy logic control has been an active research topic in automation and control. The basic concept of fuzzy logic control is to utilize the qualitative knowledge of a system for designing a practical controller. Generally, fuzzy logic control is applicable to plants that are ill-modelled, but qualitative knowledge of an experienced operator is available. The principle of SMC has been introduced in designing fuzzy logic controllers. This combination which is known as adaptive fuzzy sliding mode control (AFSMC) provides the mechanism to design robust controllers for nonlin-

ear systems with uncertainty. Adaptive fuzzy has been either used to adjust the control gain of the sliding mode or approximate the system dynamics to construct the sliding function or the control law. The development of AFSMC for uncertain mechanical systems to tackle more generic problems have been an active research topic in recent years.

The motivation for this thesis is based on recent growing research interest in the derivation of dynamic models and development of control techniques for offshore cranes subject to exogenous disturbances and parameter variations. This research has been conducted in the analytical modelling and control design for offshore crane systems, for which new results represent its contributions.

1.2 Research objectives

The main objectives of this research are:

i. To develop dynamic models of 2-D and 3-D offshore cranes in the presence of system disturbances due to open-sea condition.

ii. To formulate the generalisation of sliding mode control for a class of nonlinear underactuated mechanical systems with bounded uncertainties.

iii. To construct the robust first-order and second-order sliding mode controllers for offshore crane systems subject to system disturbances.

1.3 Thesis organization

This thesis is organised as follows:

- *Chapter 2*: This chapter presents a survey of the underactuated mechanical systems, cranes dynamics and control, the recent development of offshore crane control systems, and sliding mode control approaches.

- *Chapter 3*: The dynamic models of offshore crane systems subject to disturbances and uncertainties based on the Euler-Lagrange formulation are derived in this chapter.

- *Chapter 4*: This chapter presents the sliding mode control designs for a generic form of underactuated mechanical systems. The proposed controllers have been implemented to conventional crane systems.

- *Chapter 5*: In this chapter, the problem of robust sliding mode control is investigated for trajectory tracking problem of offshore crane systems with bounded disturbances.

- *Chapter 6*: In this chapter, a second-order sliding mode control law is proposed for offshore gantry crane and boom crane, making use of its capability of chattering alleviation while achieving high tracking performance and preserving strong robustness.

- *Chapter 7*: A brief summary of the thesis contents and its contributions are given in the final chapter. Recommendation for future works is given as well.

Chapter 2

Literature Survey

In this chapter, a brief survey of underactuated mechanical systems, cranes dynamics and control, and sliding mode control including the general first- and the second-order control laws, is presented.

2.1 Underactuated mechanical system

Underactuated mechanical systems (UMS) are systems that have fewer independent control actuators than degrees of freedom (DOF) to be controlled. UMS arise in a broad range of real-life applications, and this class of systems have been the subject of active scientific research. In general, the control of UMS is a more challenging task as compared to the control of fully actuated systems because the former presents additional restrictions on the control design. Besides, it gives rise to complex theoretical problems that may not found in fully actuated systems, and that may not be solved using classical control techniques. The control of UMS has been studied for a long period in the control literature and has been attracting more attention in recent years due to the growing interests in new theories and applications. This section provides brief survey of the most recent studies on UMS from control point of view and focuses on its application to marine vehicles and crane systems. A more detail survey of crane control strategies is provided in Section 2.2.2.

Research on UMS can trace back to twenty years ago when control of nonholonomic mechanical systems were of great interest to researchers, e.g., [9, 21], and references therein. Studies on this class of systems have gained more attention years

after, and they have been widely used in robotics, aircrafts and marine vehicles. Various control strategies for UMS have been proposed in the literature, including intelligent control, backstepping, sliding mode, and many more. The most recent review paper on UMS has been reported by Liu and Yu [90], in which a comprehensive survey of UMS is presented from its history to the state-of-the-art research on modelling, classification, and control.

Numerous studies have attempted to give a classification and a generalisation of these systems with the aim of proposing a systematic control design method for UMS. Several researchers have formulated the stabilisation problems of UMS by using controlled Lagrangian methods [19, 20, 26], passivity-based control [106], equivalent-input-disturbance approach [123], and Lyapunov-based method [117]. Sliding mode control (SMC) is one of the most popular methods in the control designs for a generic form of UMS. These include studies on reachability [102], stabilisation [100], and sliding surface design techniques [91]. The works on generic SMC control design have been reported for two DOF UMS [94, 95] and also for UMS without any restriction on the number of DOF [8, 121, 140, 142]. Other control methods proposed for a generic form of UMS are hybrid control [55], adaptive control [27], and passivity-based control [31].

Marine vehicles and cranes are among UMS, which attracted many research interests as the topic of control problems. The challenge in the underactuated ship and surface vessel control systems is to solve the trajectory tracking problem in the presence of ocean waves disturbance. Among the control strategies that have been proposed for underactuated ships and surface vessels are state feedback control [82], backstepping method [38, 58, 59, 111], adaptive control [37, 39], Lyapunov's method [36, 42, 72], SMC [7, 49, 146], and cooperative control [41, 57]. Studies on underactuated gantry cranes, which have similar equations of motion with cart-pole systems, are also have been reported by many researchers. Most recent works on

underactuated crane motion control can be referred to [52, 130, 131, 147].

2.1.1 Equations of motion

The dynamics of UMS is formulated based on Lagrangian mechanics. In general, the equations of motion of UMS can be written in the form of Euler-Lagrange equation as follows [90, 91]:

$$\frac{d}{dt}\left(\frac{\partial \mathcal{L}}{\partial \dot{q}}\right) - \frac{\partial \mathcal{L}}{\partial q} = E(q)u, \tag{2.1}$$

where $\mathcal{L} = \mathcal{K}(q,\dot{q}) - \mathcal{P}(q)$ is the Lagrangian, $\mathcal{K}(q,\dot{q})$ is the total kinetic energy, $\mathcal{P}(q)$ is the total potential energy, $q \in \mathbb{R}^n$ is the vector of generalised coordinates, $u \in \mathbb{R}^m$ is the vector of actuator input, and $E(q) \in \mathbb{R}^{n\times m}$ is the matrix of external forces, with $1 \leq m < n$. The kinetic energy $\mathcal{K}(q,\dot{q})$ is a quadratic function of the vector $\dot{q}$ of the form

$$\mathcal{K}(q,\dot{q}) = \frac{1}{2}\sum_{i,j}^{n} m_{ij}(q)\dot{q}_i\dot{q}_j = \frac{1}{2}\dot{q}^T M(q)\dot{q},$$

where $M(q) \in \mathbb{R}^{n\times n}$ is the inertia matrix and $m_{ij}(q)$ is an element of the matrix. The Euler-Lagrange equation (2.1) can be written as [128]:

$$\sum_j m_{kj}(q)\ddot{q}_j + \sum_{i,j} c_{ijk}(q)\dot{q}_i\dot{q}_j + \frac{\partial \mathcal{P}(q)}{\partial q_k} = p_k^T E(q)u, \quad k = 1,\cdots,n, \tag{2.2}$$

where p_k is the kth standard basis in $\mathbb{R}^n$ and $c_{ijk}(q)$ are known as Christoffel symbols, defined as

$$c_{ijk}(q) = \frac{1}{2}\left(\frac{\partial m_{kj}(q)}{\partial q_i} + \frac{\partial m_{ki}(q)}{\partial q_j} - \frac{\partial m_{ij}(q)}{\partial q_k}\right).$$

Finally, by defining $G_k(q) = \partial \mathcal{P}(q)/\partial q_k$ or

$$G(q) = \frac{\partial \mathcal{P}(q)}{\partial q},$$

(2.2) can be expressed in matrix form as

$$M(q)\ddot{q} + C(q,\dot{q})\dot{q} + G(q) = E(q)u, \tag{2.3}$$

where $C(q,\dot{q}) \in \mathbb{R}^{n\times n}$ is the centrifugal-Coriolis matrix, $c_{kj} = \sum_{i=1}^{n} c_{ijk}(q)\dot{q}_i$ is an element of $C(q,\dot{q})$, and $G(q) \in \mathbb{R}^n$ is the vector of gravity. The dynamics (2.3) has some important properties that facilitate control analysis and design. Among these properties, the following are often used in control development [90]:

i. The inertia matrix $M(q)$ is positive definite, symmetric, and bounded such as for $M(q) \in \mathbb{R}^{n\times n}$,

$$k_1 I_n \leq M(q) = M^T(q) \leq k_2 I_n,$$

where $k_1, k_2 > 0$.

ii. A skew symmetric relationship exists between the inertia matrix $M(q)$ and the centrifugal-Coriolis matrix $C(q,\dot{q})$ such as for $M(q), C(q,\dot{q}) \in \mathbb{R}^{n\times n}$

$$\nu^T \left(\dot{M}(q) - 2C(q,\dot{q})\right)\nu = 0, \quad \forall \nu \in \mathbb{R}^n.$$

iii. Define the total energy of the system as

$$\mathcal{W}(q,\dot{q}) = \mathcal{K}(q,\dot{q}) + \mathcal{P}(q) = \frac{1}{2}\dot{q}^T M(q)\dot{q} + \mathcal{P}(q).$$

Then the time derivative of the total energy is

$$\dot{\mathcal{W}}(q,\dot{q}) = \frac{1}{2}\ddot{q}^T M(q)\dot{q} + \frac{1}{2}\dot{q}^T M(q)\ddot{q} + \frac{1}{2}\dot{q}^T \dot{M}(q)\dot{q} + \dot{q}^T \frac{\partial \mathcal{P}(q)}{\partial q}$$

Since $\ddot{q}^T M(q)\dot{q} = \dot{q}^T M^T(q)\ddot{q} = \dot{q}^T M(q)\ddot{q}$ (Property i) and $\dot{q}^T \dot{M}(q)\dot{q} = 2\dot{q}^T C(q,\dot{q})\dot{q}$ (Property ii), the above equation becomes

$$\begin{aligned}\dot{\mathcal{W}}(q,\dot{q}) =& \dot{q}^T M(q)\ddot{q} + \dot{q}^T C(q,\dot{q})\dot{q} + \dot{q}^T G(q) \\ =& \dot{q}^T \left(M(q)\ddot{q} + C(q,\dot{q})\dot{q} + G(q)\right) \\ =& \dot{q}^T E(q)u,\end{aligned}$$

which implies that the system is passive with respect to the input u and output $\dot{q}$. The passivity is an important character of UMS which shows that the system has a stable origin.

If the matrix $E(q)$ is assumed to be $E(q) = [I_m \ 0^T_{(n-m)\times m}]^T$, the vector of generalised coordinates can be partitioned as $q = [q_a^T, q_u^T]^T$. By letting $f(q,\dot{q}) = C(q,\dot{q})\dot{q} + G(q)$ and partitioning the vector as $f(q,\dot{q}) = [f_a^T(q,\dot{q}), f_u^T(q,\dot{q})]^T$, (2.3) can be expressed in the following form [8, 100, 102, 142]:

$$\begin{bmatrix} M_{aa}(q) & M_{au}(q) \\ M_{au}^T(q) & M_{uu}(q) \end{bmatrix} \begin{bmatrix} \ddot{q}_a \\ \ddot{q}_u \end{bmatrix} + \begin{bmatrix} f_a(q,\dot{q}) \\ f_u(q,\dot{q}) \end{bmatrix} = \begin{bmatrix} I_m \\ 0_{(n-m)\times m} \end{bmatrix} u, \tag{2.4}$$

where $q_a \in \mathbb{R}^m$, $q_u \in \mathbb{R}^{n-m}$, $M_{aa}(q) \in \mathbb{R}^{m\times m}$, $M_{au}(q) \in \mathbb{R}^{m\times(n-m)}$, $M_{uu}(q) \in \mathbb{R}^{(n-m)\times(n-m)}$, $f_a(q,\dot{q}) \in \mathbb{R}^m$, and $f_u(q,\dot{q}) \in \mathbb{R}^{n-m}$.

2.1.2 Feedback linearisation

The feedback linearisation approach generalised the concept of inverse dynamics of Lagrangian systems. The basic concept of feedback linearisation is to construct a nonlinear control law as an inner-loop control (see Figure 2.1). In ideal case, the inner-loop control exactly linearises the nonlinear system after a proper state space change of coordinates. One can then design a second stage or outer-loop control in the new coordinates to satisfy the control design specifications.

Consider the dynamics equation in the form of (2.4). The idea of inverse dynamics is to seek a nonlinear feedback control law

$$u = U(q,\dot{q})$$

which, when substituted into (2.4), results in a linear closed-loop system. If we choose the control u according to the equation

$$u = \begin{bmatrix} I_m & -M_{au}(q)M_{uu}^{-1}(q) \end{bmatrix} \begin{bmatrix} f_a(q,\dot{q}) \\ f_u(q,\dot{q}) \end{bmatrix} + \Big(M_{aa}(q) - M_{au}(q)M_{uu}^{-1}(q)M_{au}^T(q)\Big)v, \tag{2.5}$$

then, since the matrix $M(q)$ as well as its partitions $M_{aa}(q)$ and $M_{uu}(q)$ are invert-

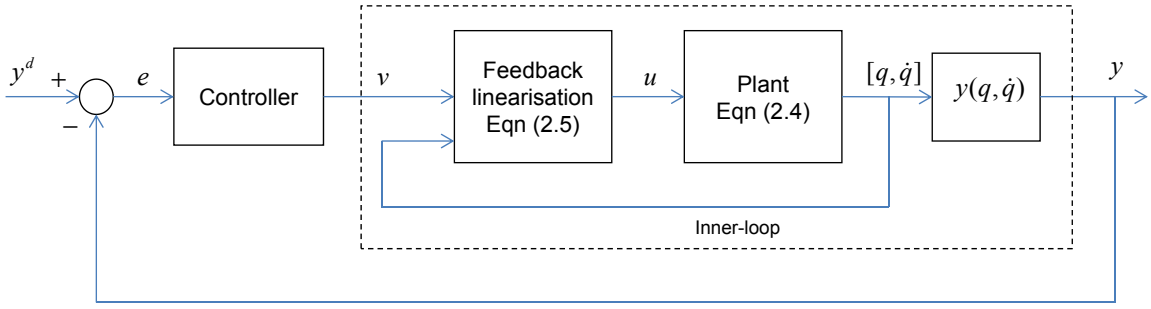

Figure 2.1 : Architecture of feedback linearisation control.

ible, the combined system (2.4) and (2.5) becomes

$$\begin{bmatrix} M_{aa}(q) & M_{au}(q) \\ M_{au}^T(q) & M_{uu}(q) \end{bmatrix} \begin{bmatrix} \ddot{q}_a \\ \ddot{q}_u \end{bmatrix} = \begin{bmatrix} I_m & -M_{au}(q)M_{uu}^{-1}(q) \\ 0_{(n-m)\times m} & 0_{(n-m)\times(n-m)} \end{bmatrix} \begin{bmatrix} f_a(q,\dot{q}) \\ f_u(q,\dot{q}) \end{bmatrix}$$
$$- \begin{bmatrix} f_a(q,\dot{q}) \\ f_u(q,\dot{q}) \end{bmatrix} + \begin{bmatrix} M_{aa}(q) - M_{au}(q)M_{uu}^{-1}(q)M_{au}^T(q) \\ 0_{(n-m)\times m} \end{bmatrix} v$$
$$= - \begin{bmatrix} M_{au}(q)M_{uu}^{-1}(q) \\ I_{n-m} \end{bmatrix} f_u(q,\dot{q})$$
$$+ \begin{bmatrix} M_{aa}(q) - M_{au}(q)M_{uu}^{-1}(q)M_{au}^T(q) \\ 0_{(n-m)\times m} \end{bmatrix} v.$$

Eventually, one can show that the last equation can be reduced to

$$\begin{bmatrix} \ddot{q}_a \\ \ddot{q}_u \end{bmatrix} = \begin{bmatrix} 0_{m\times 1} \\ -M_{uu}^{-1}(q)f_u(q,\dot{q}) \end{bmatrix} + \begin{bmatrix} I_m \\ -M_{uu}^{-1}(q)M_{au}^T(q) \end{bmatrix} v. \tag{2.6}$$

The term v represents a new input to the system which is yet to be chosen. However, practical implementation of the inverse dynamics control law (2.5) requires both that the parameters in the dynamic model of the system be known precisely and also that the complete equations of motion be computable in real time [128].

2.2 Crane dynamics and control

Cranes can be categorised based on the DOF the support mechanism offers the payload suspension point, e.g., gantry cranes (rectiliner translations in a horizontal plane); tower cranes (translation and rotation in a horizontal plane); and boom cranes (rotations around two orthogonal axes). From the control literature, cranes can be classified as UMS. The payload swing angles are considered as unactuated coordinates in cranes dynamics, e.g., longitudinal and lateral sways in a gantry crane system, and tangential and radial sways in a boom crane system. Abdel-Rahman et al. [1] have conducted a comprehensive literature review of crane modelling and control starting in 1961. In the following, we provide a survey of the most recent works on crane dynamics and control.

2.2.1 Crane dynamics

The most common crane modelling approaches are the lumped-mass and distributed-mass approaches. In the distributed-mass approach, the hoisting cable is modelled as a distributed-mass system and the hook and payload, lumped as a point mass, are applied as a boundary condition for this distributed-mass system [32, 114]. The lumped-mass approach is the most widely used method to crane modelling. The hoisting line is modelled as a massless rigid cable. The payload is lumped with the hook and modelled as a point mass.

The complexities of dealing with a nonlinear model of the crane systems drive many works on crane control to make-do with linearized approximations of the model. This simplification, however, may reduce controller robustness, in which linear controller may provide acceptable performance only within a small fixed operating range around the equilibrium point of the pendulation angles. As a result, there has been an increasing interest in the design of crane control strategies based on nonlinear crane models.

The general form of crane dynamics are presented in the extended form of underactuated mechanical systems (2.3) as follows:

$$M(q)\ddot{q} + C(q,\dot{q})\dot{q} + G(q) + d(t) = E(q)u, \tag{2.7}$$

where $d(t)$ can be regarded as the system uncertainty which may contains frictions and external disturbances. Conventional and offshore container crane dynamics are often presented in the form of (2.7), e.g., see [5, 53, 103]. Besides, in the case of offshore cranes, the matrices $M(q)$, $C(q,\dot{q})$ and $G(q)$ may contain the disturbance terms from the vessel's motion.

The offshore crane system in moonpool operation has a different form of dynamics as compared to (2.7), in which, the system is modelled as a fully-actuated system. In this case, the crane dynamics are modelled based on the vertical motion of the payload. Besides, most of the studies on offshore cranes in moonpool operation neglected the sway of the payload as well as the vessel's rolling motion [76, 97, 98, 120, 125]. However, the complexity of the model lies in the system disturbance, namely the hydrodynamic forces due to the effects of buoyancy and added mass. The crane dynamics in this working environment is represented in the following form [98, 125]:

$$m\ddot{z} + mg = f(t,z,\dot{z}) + u, \tag{2.8}$$

where $z \in \mathbb{R}$ is the payload position, m is the payload mass, $u \in \mathbb{R}$ is the cable force, and $f(t,z,\dot{z})$ is the hydrodynamic forces.

2.2.2 Crane control

In the following, we discuss the survey on crane control strategies. Due to some major differences between conventional and offshore cranes, each type is discussed separately.

Conventional crane control

A significant research effort has been devoted to the development of control strategies to improve the efficiency and safety of crane operations. From the crane control literature, the control techniques can be categorised into two types, namely, the open-loop and closed-loop control. In the conventional crane systems, the open-loop control methods for sway suppression are input-shaping [18, 56] and filtering techniques [68]. However, these methods are limited by the fact that they are sensitive to external disturbances. On the other hand, various closed-loop control methods have been proposed for trajectory tracking and sway suppression of conventional cranes. These methods include linear control [104], adaptive control [52, 143], fuzzy logic control [25], optimal control [132], delayed-feedback technique [67], and nonlinear control. The nonlinear control methods for conventional cranes can further be classified as Lyapunov's direct method [51, 131], first-order sliding mode control [5], and second-order sliding mode control [16]. In addition, many studies on crane trajectory planning have been reported, for example, [130, 147].

Offshore crane control

Over the past two decades, research on cranes' control and automation has focused on addressing challenges in their offshore operations. The synthesis of feedback control for offshore cranes remains a challenge because the systems involve the presence of parameter variations, e.g., changes of load during the process of loading/unloading, and the presence of disturbances, e.g., wave- and wind-induced motion. Besides, the presence of obstacles in the environment, such as harbour and vessel, must be taken into consideration for the path planning of load transfer.

Because of the facts as mentioned earlier, some researchers have proposed the modifications of offshore cranes' mechanical parts to change the properties of the systems. The new mechanical properties can avoid resonance in the system during

Table 2.1 : Summary of previous offshore crane models and control methods.

Author	**Modelling approach**	**Control method**	**Limitation**
Osinski & Wojciech (1998) [107]	– Boom crane – Euler-Lagrange formulation – Flexible boom	– Input shaping	– Only consider vessel's heave
Driscoll et al. (2000) [43]	– Underwater conveying – Finite-element lumped-mass model	– Passive heave compensation – Impedance control	– Only consider vessel's heave
Kimiaghalam et al. (2002) [75]	– Boom crane – Stevedoring operation – Use Maryland rigging – 2 DOF crane, 1 DOF vessel	– Feedforward control	– 2-D model – Only consider vessel's roll angle
Sagatun (2002) [120]	– Moonpool operation – Vertical motion – Consider hydrodynamics force	– Passive heave compensation – Impedance control	– Only consider vessel's heave

Author	**Modelling approach**	**Control method**	**Limitation**
Johansen et al. (2003) [73]	– Moonpool operation – Vertical motion – Consider hydrodynamics force	– Active heave compensation – Feedforward control	– Only consider vessel's heave
Masoud et al. (2004) [96]	– Boom crane – Stevedoring operation – 4 DOF crane, 3 DOF vessel	– Delayed-feedback control	– Fixed rope length – Vessel's motion is not included in the dynamics model
Skaare & Egeland (2006) [125]	– Moonpool operation – Vertical motion – Consider hydrodynamics force	– Active heave compensation – Parallel force/position control	– Only consider vessel's heave
Al-Sweiti & Söffker (2007) [4]	– Boom crane – Stevedoring operation – Use Maryland rigging	– Variable gain state-feedback control	– 2-D model – Only consider vessel's roll angle

Author	**Modelling approach**	**Control method**	**Limitation**
Hatleskog & Dunningan (2007) [66]	– Moonpool operation – Vertical motion	– Passive heave compensation – Impedance control	– 2-D model – Only consider vessel's heave
Parker et al. (2007) [110]	– Boom crane – Stevedoring operation – Use rider block tagline – Inverse kinematic	– Utilise the rider block tagline (no specific control method)	– 2-D model – Lack of analytic modeling in system dynamics
Do & Pan (2008) [40]	– Underwater conveying – Planar motion – Use electro-hydraulic system	– Active heave compensation – Lyapunov's direct method	– 2-D model – Only consider vessel's heave
Messineo et al. (2008) [97]	– Moonpool operation – Vertical motion	– Feedback compensator	– 2-D model – Only consider vessel's heave

Author	**Modelling approach**	**Control method**	**Limitation**
Schaub (2008) [122]	– Boom crane – Stevedoring operation – Velocity-based inverse kinematic – 3 DOF crane, 3 DOF vessel	– Rate-based control	– Ignore payload sway/oscillation
Messineo & Serrani (2009) [98]	– Moonpool operation – Vertical motion – Consider hydrodynamics force	– Heave compensation – Adaptive control	– Only consider vessel's heave
Küchler et al. (2011) [76]	– Underwater conveying – 2 DOF crane, 1 DOF vessel	– Prediction algorithm – Input/output linearisation	– Assume fully actuated system

Author	**Modelling approach**	**Control method**	**Limitation**
Ngo & Hong (2012) [103]	– Gantry (container) crane – Stevedoring operation – Euler-Lagrange formulation – 3 DOF crane, 3 DOF vessel	– Sliding mode control	– Assume fixed rope length
Fang et al. (2014) [53]	– Boom crane – Stevedoring operation – Euler-Lagrange formulation – 3 DOF crane, 2 DOF vessel	– Lyapunov method	– 2-D model

load transfer. For example, the rider block tagline system has been utilised to change the natural frequency of offshore crane's pendulation [110]. The Maryland rigging system was also proposed to change the properties of offshore crane systems, which can dissipate the payload sway with some additional control strategies, such as feedforward control [75] and state feedback control [4]. However, the introduction of the additional mechanism to crane systems leads to a higher complexity in the analysis of the crane dynamics.

Recently, the works on offshore crane systems have utilised their available control inputs rather than introducing additional mechanism. A common approach to deal

with the complexity and underactuation of offshore crane dynamics is to break up the system into several parts and then analyse only a part or a decoupled part of the system states. Some researchers have first separated payload motion in the vertical direction and then designed a controller to vary the cable length. For example, the application of input shaping to minimise the cable deformation during payload vertical motion has been reported in [107]. Later, researchers have introduced the heave compensation approach to assign the payload to move at a constant vertical velocity in an earth-fixed reference frame in order to reduce the variations of the cable tension. This approach can further be categorised into passive and active heave compensations. Passive heave compensations can be constructed using augmented impedance control laws by utilising the tension of the cable as the only control input [43, 66, 120]. Some active compensation approaches have been constructed by using various type of control strategies, for example, feedforward scheme [73], feedback scheme [97], parallel force/position control [125], adaptive control [98], and Lyapunov's direct method [40]. Besides, active heave compensation approach combined with prediction algorithm for vessel motion has been reported in [76].

On the other hand, research on offshore crane dynamics and control has been devoted to considering a higher number of DOF in the systems' model to achieve satisfactory control performance. In [96], a delayed-feedback controller has been proposed to place the payload by using a linearised offshore crane system. A rate-based control strategy by using the measurements from onboard sensors has been reported in [122]. The most recent work on the dynamics analysis and nonlinear control has been reported in [53]. In this work, a Lyapunov's based controller has been designed for a simplified two-dimensional offshore crane model.

In terms of control strategies, sliding mode control (SMC) has been recognised as a strong control methodology for Lagrangian systems. Most recent works on SMC for offshore cranes have been reported in [103], [115] and [116]. However, the

selections of SMC parameters to deal with the bounded disturbances were not fully addressed in [103, 115] while model uncertainties and practical scenarios were not adequately detailed in [116]. For this reason, the control designs for offshore crane systems remains an open problem. The previous study on offshore crane models and control methods are summarised in Table 2.1.

2.3 Sliding mode control

Research on variable structure control (VSC) systems has progressed from the pioneering work in Russia of Emel'yanov and Barbashin in the early 1960s. The idea of VSC only wide-spread outside of Russia during mid 1970s when a book by Itkis in 1976 and a survey paper by Utkin [137] in 1977 were published in English. VSC concepts have subsequently been utilised in the design of robust regulators, model-reference systems, adaptive schemes, tracking systems, state observers and fault detection schemes. The ideas have successfully been applied to problems as diverse as automatic flight control, control of electric motors, chemical processes, helicopter stability augmentation systems, space systems and robots [44]. One of the earliest survey paper on VSC was written by Hung et al. [69] that provides many references to the application of sliding mode ideas in various engineering problems. Years later, the generalisation of VSC for a class of uncertain systems have been developed, for example, in [29, 45]. The VSC approaches have been further distinguished to two types of controls, i.e., (i) VSCs that switch between different parameters and (ii) systematic further development of the methods which is known as soft variable structure controls (soft VSC) that continuously vary controllers' parameters or structures and achieve nearly time-optimal control performance. A survey paper on soft VSC has been reported in [3].

Sliding mode control (SMC) belonging to the VSC systems became popular because of its application to a broad class of systems containing discontinuous control

elements such as relays. Among the earliest works involving the use of SMC in mechanical systems is done by Young [145]. SMC has subsequently been applied and developed for underwater vehicles, robust regulators, adaptive control, electrical motors control, chemical processes, robotic manipulators, and in simulation of automatic flight control, helicopter stability and space systems [127]. A generic SMC for linear systems with bounded uncertainties has been proposed in [119]. This proposition has been extended in [129] to design output tracking control and in [10] to provide the sliding surface design procedure. Sliding mode control is inherently a nonlinear methodology, so its applications are not limited to linear systems. It offers a framework for controller design for a wide class of nonlinear systems. A controller can be expected to perform better if it is based on a nonlinear model rather than a linear approximation. Several works on generalisation of SMC have been reported in [17, 30, 65, 141]. Some recent survey papers on SMC have been reported, namely, the survey on SMC with application in mathematics [112] and the survey on SMC strategies for induction motors [109].

2.3.1 Regular form of linear-time invariant system

A convenient way to facilitate the sliding mode control design for a linear time invariant (LTI) system is to first transform the system into a suitable canonical form. Consider the following LTI system:

$$\dot{x}(t) = Ax(t) + Bu(t), \tag{2.9}$$

where $A \in \mathbb{R}^{n\times n}$ and $B \in \mathbb{R}^{n\times m}$ with $1 \leq m \leq n$. Without loss of generality it can be assumed that matrix B has full rank, i.e., $\text{rank}(B) = m$, and the pair of (A, B) is controllable. Since $\text{rank}(B) = m$, there exists an orthogonal matrix $T \in \mathbb{R}^{n\times n}$ such that [44]

$$TB = \begin{bmatrix} 0_{(n-m)\times m} \\ B_2 \end{bmatrix}, \tag{2.10}$$

where $B_2 \in \mathbb{R}^{m\times m}$ is nonsingular. This orthogonal matrix T can be obtained by using QR decomposition based on (2.10). By using the coordinate transformation $z(t) = Tx(t)$, (2.9) becomes

$$\dot{z}(t) = TAT^{-1}z(t) + TBu(t). \tag{2.11}$$

If the states $z(t)$ and the matrix TAT^{-1} in (2.11) are partitioned so that

$$z = \begin{bmatrix} z_1(t) \\ z_2(t) \end{bmatrix}, \qquad TAT^{-1} = \begin{bmatrix} A_{11} & A_{12} \\ A_{21} & A_{22} \end{bmatrix},$$

and by noting (2.10), (2.9) can be written as

$$\dot{z}_1(t) = A_{11}z_1(t) + A_{12}z_2(t), \tag{2.12}$$

$$\dot{z}_2(t) = A_{21}z_1(t) + A_{22}z_2(t) + B_2u(t). \tag{2.13}$$

The representation in (2.12) and (2.13) is referred to as regular form [44]. Let the sliding function $s(t)$ represented as

$$s(t) = Sz(t),$$

where $S \in \mathbb{R}^{m\times n}$ is full rank, and can be partitioned as

$$S = [S_1 \;\; S_2],$$

with $S_1 \in \mathbb{R}^{m\times(n-m)}$ and $S_2 \in \mathbb{R}^{m\times m}$. During ideal sliding, $s(t) = Sz(t) = 0$ or

$$\begin{aligned} S_1z_1(t) + S_2z_2(t) &= 0 \\ z_2(t) &= -S_2^{-1}S_1z_1(t) = -L_sz_1(t), \end{aligned}$$

where $L_s = S_2^{-1}S_1$. Substituting the expression of $z_2(t) = -L_sz_1(t)$ into the (2.12) gives

$$\dot{z}_1(t) = (A_{11} - A_{12}L_s)z_1(t). \tag{2.14}$$

Note that this is similar with the problem of finding the state feedback matrix L_s for the system in (2.12), where $z_2(t)$ has the role of a linear state feedback control

signal. Any classical state feedback control method can be used to compute L_s. Then the matrix S can be obtained as

$$S = S_2[L_s \ I_m].$$

The matrix S_2 acts only as scaling factor for the sliding function, so it has no effect on the dynamics of the sliding motion and can be chosen arbitrarily. Among the approaches to compute the matrix L_s and subsequently obtaining the matrix S are robust eigenstructure assignment, linear quadratic regulator, direct eigenstructure assignment, and linear matrix inequality (LMI) method.

2.3.2 First-order sliding mode control

1-SMC for linear time invariant system

The most convenient control structure for multivariable systems, from a sliding mode perspective, is the unit vector approach attributed to [119]. Consider an LTI system with matched uncertainty

$$\dot{x}(t) = Ax(t) + Bu(t) + d(t, x, u), \tag{2.15}$$

where $d(t, x, u)$ is in the range space of matrix B, and is assumed to be unknown but bounded and satisfies

$$\|d(t, x, u)\| \leq k\|u(t)\| + \alpha(t, x),$$

in which $k \geq 0$ and $\alpha(t, x)$ is a known function. Without loss of generality, it can be assumed that (2.15) is already in regular form as described in the previous section. Thus, (2.15) can be written as

$$\dot{x}_1(t) = A_{11}x_1(t) + A_{12}x_2(t), \tag{2.16}$$

$$\dot{x}_2(t) = A_{21}x_1(t) + A_{22}x_2(t) + B_2u(t) + \overline{d}(t, x, u), \tag{2.17}$$

where $\overline{d}(t,x,u)$ is a projection of $d(t,x,u)$ in the regular form coordinates. Therefore

$$\|\overline{d}(t,x,u)\| \leq k\|u(t)\| + \alpha(t,x), \tag{2.18}$$

since the Euclidean norm of $d(t,x,u)$ is preserved by the orthogonal transformation. In the notation of Section 2.3.1, the sliding function can be expressed as

$$s(t) = S_2 L_s x_1(t) + S_2 x_2(t), \tag{2.19}$$

and the derivative of the sliding function is

$$\dot{s}(t) = S_2 L_s \dot{x}_1(t) + S_2 \dot{x}_2(t), \tag{2.20}$$

where $L_s \in \mathbb{R}^{m\times(n-m)}$ has been chosen by some appropriate design procedure to stabilise the pair (A_{11}, A_{12}) of (2.16). Rearranging (2.19), we have

$$x_2(t) = S_2^{-1} s(t) - L_s x_1(t). \tag{2.21}$$

By substituting (2.21) into (2.16) and (2.17), and further substituting the obtained equations into (2.20), one can show that

$$\dot{x}_1(t) = \overline{A}_{11} x_1(t) + A_{12} S_2^{-1} s(t) \tag{2.22}$$

$$\dot{s}(t) = S_2 \overline{A}_{21} x_1(t) + S_2 \overline{A}_{22} S_2^{-1} s(t) + S_2 B_2 u(t) + S_2 \overline{d}(t,x,u), \tag{2.23}$$

where $\overline{A}_{11} = A_{11} - A_{12}L_s$, $\overline{A}_{21} = L_s\overline{A}_{11} + A_{21} - A_{22}L_s$ and $\overline{A}_{22} = L_s A_{12} + A_{22}$. The control law comprises linear and nonlinear components given by [44]

$$u(t) = u_E(t) + u_R(t), \tag{2.24}$$

where the linear component is given by

$$u_E(t) = (S_2 B_2)^{-1}\Big(- S_2 \overline{A}_{21} x_1(t) - (S_2 \overline{A}_{22} S_2^{-1} - \Phi) s(t)\Big) \tag{2.25}$$

and the nonlinear component is defined to be

$$u_R(t) = -\rho(t,x)\Lambda^{-1}\frac{Ps(t)}{\|Ps(t)\|}, \quad s(t) \neq 0, \tag{2.26}$$

where $\Lambda = S_2 B_2$. Matrix $\Phi \in \mathbb{R}^{m\times m}$ is any stable design matrix and $P \in \mathbb{R}^{m\times m}$ is a symmetric positive definite matrix satisfying the Lyapunov equation

$$P\Phi + \Phi^T P = -I_m.$$

The scalar function $\rho(t,x)$, which depends only on the magnitude of the uncertainty, is any function satisfying

$$\rho(t,x) \geq \frac{\|S_2\|\Big(k\|u_E(t)\| + \alpha(t,x)\Big) + \eta}{1 - k\|\Lambda^{-1}\|\|S_2\|}, \tag{2.27}$$

where η is a positive scalar and k must satisfy $k < \|B_2^{-1}\|^{-1}$. Substituting the control law (2.24) into (2.23) gives

$$\dot{s}(t) = \Phi s(t) - \rho(t,x)\frac{Ps(t)}{\|Ps(t)\|} + S_2\overline{d}(t,x,u). \tag{2.28}$$

To prove the stability of the control system, consider a Lyapunov function

$$V(s) = \frac{1}{2}s^T(t)Ps(t).$$

Differentiating the Lyapunov function and using (2.28) yields

$$\begin{aligned}
\dot{V}(s) =& \frac{1}{2}\dot{s}^T(t)Ps(t) + \frac{1}{2}s^T(t)P\dot{s}(t) \\
=& \frac{1}{2}\left(s^T(t)\Phi^T - \rho(t,x)\frac{s^T(t)P}{\|Ps(t)\|} + \big(S_2\overline{d}(t,x,u)\big)^T\right)Ps(t) \\
&+ \frac{1}{2}s^T(t)P\left(\Phi s(t) - \rho(t,x)\frac{Ps(t)}{\|Ps(t)\|} + S_2\overline{d}(t,x,u)\right) \\
=& -\frac{1}{2}\|s(t)\|^2 - \rho(t,x)\|Ps(t)\| + s^T(t)PS_2\overline{d}(t,x,u) \\
\leq& -\frac{1}{2}\|s(t)\|^2 - \|Ps(t)\|\Big(\rho(t,x) - \|S_2\|\|\overline{d}(t,x,u)\|\Big).
\end{aligned} \tag{2.29}$$

From (2.24), using triangular inequality and together with (2.26), it can be shown that

$$\|u(t)\| \leq \|u_E(t)\| + \|u_R(t)\| \leq \|u_E(t)\| + \rho(t,x)\|\Lambda^{-1}\|. \tag{2.30}$$

Rearranging (2.27), and using (2.30), one can show that

$$\begin{aligned}\rho(t,x) \geq & \|S_2\| \left[k \left(\|u_E(t)\| + \rho(t,x)\|\Lambda^{-1}\|\right) + \alpha(t,x)\right] + \eta \\ \geq & \|S_2\| \left[k\|u(t)\| + \alpha(t,x)\right] + \eta \\ \geq & \|S_2\|\|\overline{d}(t,x,u)\| + \eta. \end{aligned} \tag{2.31}$$

Finally, by using inequalities (2.31) and (2.29), it can be shown that

$$\dot{V}(s) \leq -\frac{1}{2}\|s(t)\|^2 - \eta\|Ps(t)\|,$$

which proves that the controller induces ideal sliding in the presence of matched uncertainty in finite time.

1-SMC for nonlinear system

Consider the state space equation

$$\dot{x}(t) = f(x) + g(x)u(t) + d(t), \tag{2.32}$$

where $x(t) \in \mathbb{R}$ and $u(t) \in \mathbb{R}$. Let $s(t) = 0$ be the sliding surface on which we want to drive the system state. For simplicity, let consider a stabilisation problem where $s(t) = x(t)$. Assume that there exist a constant $d_M > 0$ such that $|d(t)| < d_M$. Hence, the following 1-SMC law can drive the system trajectories of (2.32) onto sliding surface $s(t) = 0$ in finite time [112]:

$$u(t) = \frac{1}{g(x)}[-f(x) - K \operatorname{sign} s(t)], \tag{2.33}$$

where $K = d_M + \eta$, $\eta > 0$. To prove the stability of the system, choose the Lyapunov function candidate to be

$$V = \frac{1}{2}s(t)^T s(t).$$

Hence, the time derivative of V is

$$\begin{aligned}\dot{V} = & s(t)\dot{s}(t) \\ = & s(t)[-K \operatorname{sign} s(t) + d(t)] \\ \leq & |s(t)|\Big(- K + d(t)\Big) \leq -\eta\|s(t)\|,\end{aligned}$$

which shows that sliding surface is reached in finite time.

Next, we present a 1-SMC law for Lagrangian system in the form of

$$M(q)\ddot{q} + C(q,\dot{q})\dot{q} + G(q) = \tau, \tag{2.34}$$

where $q \in \mathbb{R}^n$ and $\tau \in \mathbb{R}^n$. The controller is assigned to drive the generalised coordinates to the desired trajectories $q^d \in \mathbb{R}^n$. Define the tracking error

$$e = q - q^d$$

and define the sliding surface

$$s = \dot{e} + \lambda e = \dot{q} - \dot{q}^d + \lambda e \tag{2.35}$$

where $\lambda = \text{diag}(\lambda_1, \cdots, \lambda_n)$, with $\lambda_i > 0$ for $i = 1, \cdots, n$. From (2.35), let

$$\begin{aligned}\dot{q}^r =& \dot{q} - s = \dot{q}^d - \lambda e,\\ \ddot{q}^r =& \ddot{q} - \dot{s} = \ddot{q}^d - \lambda \dot{e}.\end{aligned}$$

Using feedback linearisation, we obtain

$$\tau = \hat{M}(q)u + \hat{C}(q,\dot{q})\dot{q} + \hat{G}(q),$$

in which u is chosen as [61]

$$u = \ddot{q}^r - \hat{M}^{-1}(q)\left[\left(\hat{C}(q,\dot{q}) + \Phi\right)s + K\,\text{sign}\,s\right], \tag{2.36}$$

where $\Phi = \text{diag}(\Phi_1, \cdots, \Phi_n)$ and $K = \text{diag}(K_1, \cdots, K_n)$ are positive definite matrices with $\Phi_i, K_i > 0$ for $i = 1, \cdots, n$. The matrices $\hat{M}$, $\hat{C}$, and $\hat{G}$ are the estimations of M, C, and G, respectively. Let Δh express the bounded uncertainties as

$$\Delta h = \Delta M \ddot{q}^r + \Delta C \dot{q}^r + \Delta G, \tag{2.37}$$

where $\Delta M = \hat{M} - M$, $\Delta C = \hat{C} - C$, and $\Delta G = \hat{G} - G$. Furthermore, we assume that there exist $\Psi_i > 0$, for $i = 1, \cdots, n$ such as $|\Delta h_i| \leq \Psi_i$. We choose K such that

$$K_i \geq \Psi_i, \quad i = 1, \cdots, n. \tag{2.38}$$

To prove the stability of the system, we choose the Lyapunov function candidate to be

$$V = \frac{1}{2} s^T M(q) s.$$

Hence, the time derivative of V is

$$\begin{aligned}
\dot{V} =& \frac{1}{2}\left(\dot{s}^T M(q)s + s^T M(q)\dot{s} + s^T \dot{M}(q)s\right) \\
=& s^T M(q)\dot{s} + \frac{1}{2} s^T \dot{M}(q)s \\
=& s^T M(q)\dot{s} + s^T C(\dot{q}, q)s, \qquad (2.39)
\end{aligned}$$

in which (2.39) is obtained by using the first and the second property of matrix $M(q)$ as mentioned in Section 2.1.1. Substituting $s = \dot{q} - \dot{q}^r$ and $\dot{s} = \ddot{q} - \ddot{q}^r$ into (2.39) yields

$$\begin{aligned}
\dot{V} =& s^T \left[M(q)(\ddot{q} - \ddot{q}^r) + C(\dot{q}, q)(\dot{q} - \dot{q}^r)\right] \\
=& s^T \left[M(q)\ddot{q} + C(\dot{q}, q)\dot{q} - M(q)\ddot{q}^r - C(\dot{q}, q)\dot{q}^r\right]. \qquad (2.40)
\end{aligned}$$

Substituting $M(q)\ddot{q} + C(\dot{q}, q)\dot{q} = \tau - G(q)$ obtained from (2.34) into (2.40) yields

$$\begin{aligned}
\dot{V} =& s^T \left[\tau - G(q) - M(q)\ddot{q}^r - C(\dot{q}, q)\dot{q}^r\right] \\
=& s^T \left[\hat{M}(q)u + \hat{C}(q, \dot{q})\dot{q} + \hat{G}(q) - G(q) - M(q)\ddot{q}^r - C(\dot{q}, q)\dot{q}^r\right] \\
=& s^T \left[\hat{M}(q)\ddot{q}^r - \hat{C}(q, \dot{q})s + \Phi s - K \operatorname{sign} s + \hat{C}(q, \dot{q})\dot{q} + \hat{G}(q) - G(q) - M(q)\ddot{q}^r - C(\dot{q}, q)\dot{q}^r\right] \\
=& s^T \left[(\hat{M}(q) - M(q))\ddot{q}^r + (\hat{C}(q, \dot{q}) - C(q, \dot{q}))\dot{q}^r + (\hat{G}(q) - G(q)) - \Phi s - K \operatorname{sign} s\right] \\
=& s^T \left(\Delta M \ddot{q}^r + \Delta C \dot{q}^r + \Delta G - \Phi s - K \operatorname{sign} s\right) \\
=& s^T \left(\Delta h - \Phi s - K \operatorname{sign} s\right). \qquad (2.41)
\end{aligned}$$

It follows that

$$\begin{aligned}
\dot{V} =& \sum_{i=1}^{n} s_i(\Delta h_i - K_i \operatorname{sign} s_i) - s^T \Phi s \\
\leq& \sum_{i=1}^{n} |s_i|(|\Delta h_i| - K_i) - s^T \Phi s. \qquad (2.42)
\end{aligned}$$

Taking into account (2.38), it can be shown that (2.42) becomes

$$\dot{V} \leq -s^T \Phi s,$$

which implies that sliding on the surface $s(t) = 0$ takes place in finite time.

Application of fuzzy logic in sliding modes

An alternative approach to constructing the SMC laws is by applying fuzzy logic. It provides a method for formulating linguist rules from expert knowledge and is able to approximate any real continuous system to arbitrary accuracy. Thus, it provides a simple solution dealing with the broad range of the system parameters. In general, fuzzy SMC approaches can be divided into two different types. In the first type of fuzzy SMC, it is assumed that the model of the system is entirely unknown, and the fuzzy systems are used to estimate the system dynamics [24, 70, 118]. In the second type, it is assumed that the system model is partly known, and the fuzzy system efforts are contributed to the construction of the control gain [61, 79, 88].

Previous researchers have applied fuzzy SMC in various kinds of nonlinear systems such as robotic manipulators [2, 62, 87], robot arms [46, 63], and overhead cranes [89]. Some works have proposed the generalisation of fuzzy SMC [78, 80, 88, 101] and fuzzy terminal SMC [133] for a class of uncertain nonlinear systems. Also, an adaptive fuzzy hierarchical SMC has been proposed for a class of uncertain underactuated nonlinear systems [71]. The recently developed fuzzy second-order sliding mode control [93] has combined the flexibility and intelligence of fuzzy logic with the efficiency of the second-order SMC.

Usually, a fuzzy system has one or more inputs and a single output. A multiple-output system can be considered as a combination of several single-output systems. There are four basic parts of a fuzzy system. The fuzzification and defuzzification are the interfaces between the fuzzy systems and the crisp systems. The rule base

includes a set of "IF ... THEN ..." rules extracted from the human experience. Each rule describes a relation between the input space and the output space. For each rule, the inference engine maps the input fuzzy sets to an output fuzzy set according to the relation defined by the rule. It then combines the fuzzy sets of all the rules in the rule base into the output fuzzy set. This output fuzzy set is translated into a crisp value output by the defuzzification.

Let consider a system represented in the form of

$$\dot{x}(t) = f(x) + g(x)u + d(t, x), \tag{2.43}$$

where $x \in \mathbb{R}$, $u \in \mathbb{R}$, and $d(t, x)$ is the bounded disturbance. The terms $f(x)$ and $g(x)$ are unknown. Let $|d(t, x)| \leq d_M$ where $d_M > 0$ is known. The kth rule in the rule base are in the following format:

Rule k : IF v_1 is F_1^k AND $\cdots$ AND v_j is F_j^k AND $\cdots$ AND v_r is F_r^k, THEN y is θ_k,

where r is the number of input of the fuzzy controller, v_j is the fuzzy input, and F_j^k is the jth fuzzy set corresponding to the kth fuzzy rule. Hence, by using the centre of average defuzzification, the output of the fuzzy system can be written as

$$y = \frac{\sum_{k=1}^{l} \prod_{j=1}^{r} \mu_{F_j^k}(v_j)\theta_k}{\sum_{k=1}^{l} \prod_{j=1}^{r} \mu_{F_j^k}(v_j)}, \tag{2.44}$$

where $\mu_{F_j^k}$ is the membership function of the fuzzy set F_j^k, and θ_k is the centroid of the kth fuzzy set corresponding to the output y. For example, the fuzzification of control law (2.33) can be express as follows:

$$u(t) = \frac{1}{\hat{g}(x|\theta_g)}\Big[- \hat{f}(x|\theta_f) - K \operatorname{sign} s(t)\Big], \tag{2.45}$$

where $\hat{f}(x|\theta_f)$ and $\hat{g}(x|\theta_g)$ are the estimates of $f(x)$ and $g(x)$, respectively.

2.3.3 Second-order sliding mode

The discontinuous control of the sliding mode provides the robustness of the control system with respect to matched uncertainties. However, the drawback of the discontinuous control is chattering effect. A natural solution is to attempt to smooth the discontinuity in the signum function, by replacing it with saturation function to obtain an arbitrarily close but continuous approximation. Such continuous approximation enables sliding mode controller to be utilised in the situations where high-frequency chattering effects would be unacceptable. However, the continuous control action only drives the states to a neighbourhood of the switching surface, in which the ideal sliding no longer takes place. This situation can cause the ultimate accuracy and robustness of the sliding mode partially lost. Moreover, 1-SMC general application may be restricted, that is, for an output sliding function to be zeroed, the standard sliding mode may keep the sliding function equal to zero only if the outputs relative degree is one [86]. The equality of the relative degree to r means, that the control u first appears explicitly only in the rth total time derivative of the sliding function s. Higher-order sliding modes (HOSM) remove the relative degree restriction of 1-SMC.

Emel'yanov et al. in 1986 initially presented the idea of acting on the higher derivatives of the sliding variable and provided second-order sliding algorithms such as the twisting algorithm, and algorithm with a prescribed law of convergence [47]. Emel'yanov et al. have also proposed the real second-order drift algorithm and the super twisting algorithm, respectively in 1986 and 1990. According to Levant [83], the sliding accuracy in the second-order sliding mode is proportional to the square of the switching time delay that turns out to be another advantage of HOSM.

The implementation of HOSM requires the knowledge of a number of time derivatives of the sliding function, depending on the system relative degree. For exam-

ple, a second-order sliding mode controller (2-SMC) keeping $s = 0$ needs s and $\dot{s}$ to be available. The only exclusion is the super-twisting controller [83, 84] which requires only measurements of s. The use of differentiators to obtain the derivatives of a sliding function requires particular care in real implementation due to the measurement noise, whose adverse effects on the overall closed-loop performance dramatically increase with the number of differentiation stages. Some research have been devoted to developing differentiation algorithms based on second- and higher-order sliding modes that have shown an interesting trade-off between precision and noise-immunity [13, 84]. Later, a development of real-time differentiators that is less sensitive to the noise propagation, as well as control algorithms for nonlinear uncertain systems with relative degrees higher than one, has been reported [12].

On the other hand, an active research have been devoted to propose control algorithms belonging to the family of 2-SMC, i.e., algorithms in which the relative degree between the constraint output and the discontinuous control is two. The main challenge when dealing with 2-SMC for uncertain systems is due to the need to solve differential inequalities of order greater than one. 2-SMC has been successfully implemented in various types of mechanical systems over the last two decades that can be referred to survey papers [15] and [112]. Some efforts on the generalisation of 2-SMC for a class of uncertain systems have also been developed, for example, in [33, 54]. A formulation of nonlinear sliding surface based 2-SMC for uncertain linear systems has been proposed in [99]. Some most recent works on the implementation of 2-SMC for mechanical systems have been reported, which include the implementation on robotic manipulator [23], permanent magnet synchronous motor [35], pneumatic actuator [48], land vehicle [22], surface vessel [139], and underwater vehicle [14].

Like the first-order sliding mode, the stability of the second-order sliding mode can be ensured if the derivative of a Lyapunov function is negative definite. However,

it is difficult to find such a Lyapunov function [92]. In the literature, the finite-time stability proofs are based on geometrical ideas.

Consider an uncertain system of the form

$$\dot{x} = f(t,x) + g(t,x)u, \tag{2.46}$$

where $x \in \mathbb{R}^n$ and $u \in \mathbb{R}$. The key step in the procedure is to describe the second-order sliding dynamics of the system (2.46) with relative degree two in the form

$$\ddot{s}(t) = a(t,x) + b(t,x)u, \tag{2.47}$$

with assumption the conditions

$$|a(t,x)| \leq C, \quad 0 < K_m \leq b(t,x) \leq K_M,$$

holds globally for some $C, K_m, K_M > 0$. This implies the following differential inclusion [86]:

$$\ddot{s}(t) \in [-C, C] + [K_m, K_M]u. \tag{2.48}$$

The problem is to find such a feedback

$$u = U(s, \dot{s}),$$

that all the trajectories of (2.48) converge in finite time to the origin $s = \dot{s} = 0$ of the phase plane $(s, \dot{s})$.

The twisting controller

The twisting controller can be applied to relative degree two systems and implement a feedback switching logic derived from the time optimal control problem and based on the current and past values of the system output. The controller is defined by [83]:

$$u = -(r_1 \operatorname{sign} s(t) + r_2 \operatorname{sign} \dot{s}(t)), \tag{2.49}$$

with convergence conditions

$$(r_1 + r_2)K_m - C > (r_1 - r_2)K_M + C, \qquad (r_1 - r_2)K_m > C.$$

The sub-optimal controller

Like the twisting controller, the sub-optimal controller can also be applied to relative degree two systems, defined by the following formula [15, 86]:

$$u = -r_1 \operatorname{sign}\left(s(t) - \frac{s^*}{2}\right) + r_2 \operatorname{sign} s^*, \quad r_1 > r_2 > 0, \tag{2.50}$$

where s^* is the value of $s(t)$ detected at the closest time in the past when $\dot{s}(t)$ was zero. The convergence conditions for this controller are

$$2[(r_1 + r_2)K_m - C] > (r_1 - r_2)K_M + C, \qquad (r_1 - r_2)K_m > C.$$

The super twisting controller

The super twisting controller can be applied to relative degree one systems and is characterised by a dynamic controller that, using only the current value of the sliding variable, applies a continuous control to the system input while maintaining the discontinuity on the time derivative of the plant input. It is effective only for chattering attenuation purposes as far as relative degree one constraints are dealt with. For this case, (2.47) is replaced by [86]

$$\dot{s}(t) = a(t, x) + b(t, x)u. \tag{2.51}$$

Differentiating (2.51) yields

$$\ddot{s}(t) = \frac{\partial a(t,x)}{\partial t} + \frac{\partial a(t,x)}{\partial x}\dot{x} + \left(\frac{\partial b(t,x)}{\partial t} + \frac{\partial b(t,x)}{\partial x}\dot{x}\right)u + b(t,x)\dot{u}.$$

Substituting (2.46) into the above equation yields

$$\ddot{s}(t) = a'(t, x, u) + b(t, x)\dot{u}. \tag{2.52}$$

where

$$\begin{aligned} a'(t,x,u) =& \frac{\partial a(t,x)}{\partial t} + \frac{\partial a(t,x)}{\partial x}(f(t,x) + g(t,x)u) \\ &+ \left(\frac{\partial b(t,x)}{\partial t} + \frac{\partial b(t,x)}{\partial x}(f(t,x) + g(t,x)u)\right)u. \end{aligned}$$

Thus, the differential inclusion (2.48) is replaced by

$$\ddot{s}(t) \in [-C_1, C_1] + [K_m, K_M]\dot{u}, \tag{2.53}$$

with assumption $|a'(t, x, u)| \leq C_1$. The super twisting controller is defined by the following formula [85, 112]:

$$\begin{aligned} u(t) =& v(t) - \lambda |s(t)|^{1/2} \operatorname{sign} s(t) \\ \dot{v}(t) =& -\alpha \operatorname{sign} s(t), \end{aligned} \tag{2.54}$$

with convergence conditions

$$\alpha > \frac{C_1}{K_m}, \qquad \lambda^2 > \frac{2(\alpha K_M + C_1)}{K_m}.$$

Second-order sliding mode observer

In order to realise a sliding function, it requires the availability of error and derivative of error, which correspond to position and velocity, respectively. In many applications of multivariable control, it is economically beneficial to avoid the direct measurement of velocities, which can be estimated by a high-gain differentiator or state observer based on the information of positions [5, 146]. Parameter estimation using a high-gain differentiator [28] offers an exact derivative, but its gains tend to infinity. Thus, the drawback of the high-gain differentiator is its sensitivity to high-frequency noise, and it produces the so-called peaking effect [85]. Besides, these mentioned observers and differentiators neglected the presence of nonlinear friction terms. A new generation of observers based on the second-order sliding mode algorithms has been recently developed. In particular, the asymptotic observers for systems with Coulomb friction [6, 105] were designed based on the second-order sliding mode. These observers require the verification of the separation principle due to the asymptotic convergence of the estimated values to the actual ones. Davila et al. [34] proposed a second-order sliding mode observer (2-SMO) for systems with Coulomb friction. This 2-SMO design benefits from the *a priori* knowledge

of the mathematical model of the process while its implementation does not need the separation principle to be proven. It has been implemented for a fully actuated system with a single coordinate.

In the following we presents one of the basic examples of 2-SMO. Consider an n-dimensional observer proposed by Utkin [138]. Let the linear plant be the nth order dynamical system as follows:

$$\begin{cases} \dot{x}(t) = Ax(t) + Bu(t) \\ y(t) = Cx(t) \end{cases} \tag{2.55}$$

where $x \in \mathbb{R}^n$, $u \in \mathbb{R}$, and the pair (C, A) is assumed to be observable. The 2-SMO can be designed in the same form as the original system (2.55) with an additional control input that depends on the error between the output of the observer and the output of the plant:

$$\begin{cases} \dot{\hat{x}}(t) = A\hat{x}(t) + Bu(t) + Lw(t) \\ \hat{y}(t) = C\hat{x}(t) \end{cases} \tag{2.56}$$

where $\hat{x}$ and $\hat{y}$ are the estimates of the system state vector and system output, respectively, and $w \in \mathbb{R}$ is the output of the 2-SMO algorithm. To drive $\hat{y}$ to $y(t)$, let utilise the super twisting algorithm (2.54):

$$\begin{cases} w(t) = v(t) - \lambda |s(t)|^{1/2} \operatorname{sign} s(t) \\ \dot{v}(t) = \alpha \operatorname{sign} s(t) \\ s(t) = y(t) - \hat{y}(t), \end{cases} \tag{2.57}$$

where α and λ are design parameters, and $s(t)$ is the sliding function. It can be shown that if the elements of L are sufficiently large, the sliding function converges to zero in finite time.

2.4 Summary

The survey on underactuated mechanical systems (UMS), crane dynamics and control, and sliding mode control (SMC) have been presented. The equations of

motion of UMS and the notion of feedback linearisation have been introduced. The dynamics model and control approaches of conventional and offshore crane systems have been reviewed. The last section has listed some basic SMC algorithms including the first-order SMC, the second-order SMC and the second-order sliding mode observer.

Chapter 3

Modelling of Offshore Crane Systems

3.1 Introduction

The chapter begins with the generalisation of cranes dynamics by using the Lagrangian mechanics as the preliminary to the model derivations. From the Euler-Lagrange formulation, the dynamic models of offshore gantry crane and boom crane are derived by considering the vessels' motion. For each crane types, 2-D and 3-D models are developed with full system dynamics with respect to system dimensions. To facilitate the first-order sliding mode control designs in the latter chapter, we provide the linearised forms of 2-D offshore crane models.

3.2 Euler-Lagrange equation for cranes

In this section, we provide the generalisation of offshore crane dynamics based on Lagrangian mechanics. The offshore crane models are derived based on the following assumptions:

i. The payload is considered as a point mass.

ii. The crane's support mechanism (girder or boom) has even mass distribution.

iii. The rope or cable is massless and there always exists strain in the rope so that the rope will not bend under the motion of vessel or crane.

Consider a crane system consisting of r links and suppose the mass of link k is m_k. Let center of mass m_k has position vector $p_k \in \mathbb{R}^3$. Thus, the kinetic energy of the

system is

$$\mathcal{K} = \frac{1}{2}\sum_{k=1}^{r} m_k \|\dot{p}_k\|^2$$

and the potential energy of the system is

$$\mathcal{P} = \sum_{k=1}^{r} m_k [0 \;\; 0 \;\; g] p_k$$

where g is the gravitational acceleration. It follows that, the Lagrangian of the system can be obtained as

$$\mathcal{L} = \mathcal{K} - \mathcal{P}.$$

Let $q \in \mathbb{R}^n$ be the vector of generalised coordinates and $\tau \in \mathbb{R}^n$ be the corresponding generalised forces. By applying the Euler-Lagrange formulation

$$\frac{d}{dt}\left(\frac{\partial \mathcal{L}}{\partial \dot{q}}\right) - \frac{\partial \mathcal{L}}{\partial q} = \tau, \tag{3.1}$$

the equation of motion of the system can be expressed in the following form:

$$M(q)\ddot{q} + C(q,\dot{q})\dot{q} + G(q) + d(t) = \tau, \tag{3.2}$$

where $M(q) \in \mathbb{R}^{n\times n}$ is the inertia matrix, $C(q,\dot{q}) \in \mathbb{R}^{n\times n}$ is the centrifugal-Coriolis matrix and $G(q) \in \mathbb{R}^n$ is the vector of gravity. Vector $d(t) \in \mathbb{R}^n$ may consist of frictions, uncertainty and disturbance terms. For simplicity, (3.2) can also be written as

$$M(q)\ddot{q} + f(q,\dot{q}) = \tau, \tag{3.3}$$

where $f(q,\dot{q}) = C(q,\dot{q})\dot{q} + G(q) + d(t)$.

Now consider an underactuated mechanical system with m number of inputs such that $1 \leq m < n$. By partitioning vector of generalised coordinates as $q = [q_a^T \;\; q_u^T]^T$ and vector of generalised forces as $\tau = [\tau_a^T \;\; 0_{1\times(n-m)}]^T$, (3.3) can be expressed in the following form:

$$\begin{bmatrix} M_{aa}(q) & M_{au}(q) \\ M_{au}^T(q) & M_{uu}(q) \end{bmatrix} \begin{bmatrix} \ddot{q}_a \\ \ddot{q}_u \end{bmatrix} + \begin{bmatrix} f_a(q,\dot{q}) \\ f_u(q,\dot{q}) \end{bmatrix} = \begin{bmatrix} \tau_a \\ 0_{(n-m)\times 1} \end{bmatrix}, \tag{3.4}$$

where $q_a \in \mathbb{R}^m$, $q_u \in \mathbb{R}^{n-m}$, $\tau_a \in \mathbb{R}^m$, $M_{aa}(q) \in \mathbb{R}^{m\times m}$, $M_{au}(q) \in \mathbb{R}^{m\times(n-m)}$, $M_{uu}(q) \in \mathbb{R}^{(n-m)\times(n-m)}$, $f_a(q,\dot{q}) \in \mathbb{R}^m$, and $f_u(q,\dot{q}) \in \mathbb{R}^{n-m}$. It follows from the second row of (3.4) that

$$\ddot{q}_u = M_{uu}^{-1}(q)[-M_{au}^T(q)\ddot{q}_a - f_u(q,\dot{q})]. \tag{3.5}$$

Substituting (3.5) into the first row of (3.4) yields

$$\ddot{q}_a = (M_{aa}(q) - M_{au}(q)M_{uu}^{-1}(q)M_{au}^T(q))^{-1} \times \big[- f_a(q,\dot{q}) + M_{au}(q)M_{uu}^{-1}(q)(f_u(q,\dot{q})) + \tau_a\big]. \tag{3.6}$$

3.3 Modelling of offshore gantry cranes

In this section, we present the models of two-dimensional (2-D) and three-dimensional (3-D) offshore gantry cranes. The 2-D model is presented in the form of uncertain LTI system, and the 3-D model is presented as the extended model of [103] with full DOF in the crane coordinates.

3.3.1 2-D model

The offshore crane system considered in this study consists of a gantry crane mounted on a ship vessel as visualize in Figure 3.1, where $\{O_G x_G y_G z_G\}$, $\{O_B x_B y_B z_B\}$ and $\{O_N x_N y_N z_N\}$ are the coordinate frames of the ground, the container ship, and the cart's starting point, respectively. The offshore crane system motion is represented by three generalized coordinates, i.e., the position of the cart, y, the length of the rope measured from the cart to the payload, l, and the sway angle induced by the motion of the cart, θ. Let h_t denote the vertical position of the cart from O_B, and d_y denote the distance of the cart's starting point from z_B-axis. The masses of the cart and payload are denoted by m_c and m_p, respectively. Let $\zeta(t)$ be the heaving and $\phi(t)$ be the rolling angular displacement of the vessel. Thus, the position vectors of the cart and the payload with respect to the ground coordinate

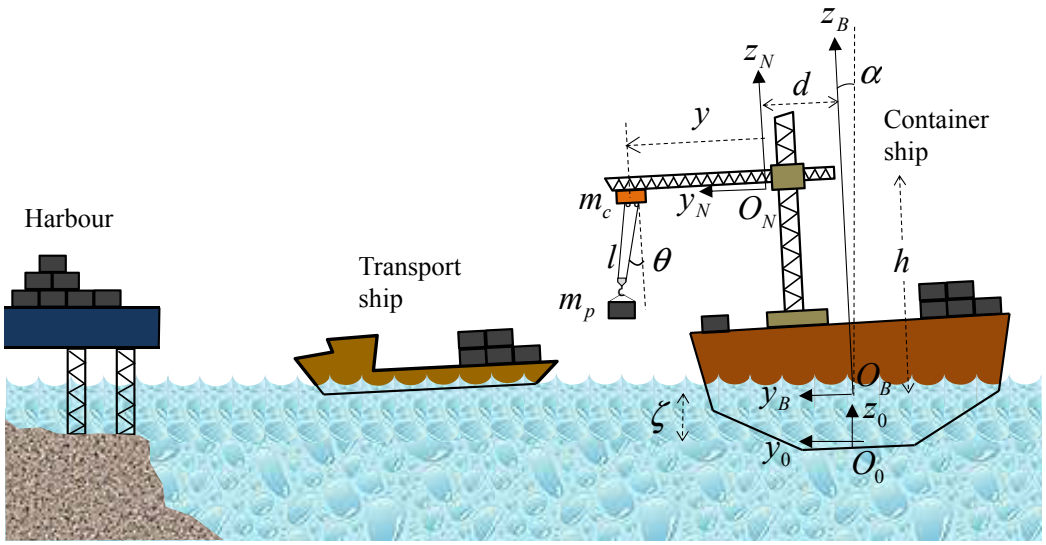

Figure 3.1 : Motion of the offshore crane during containers transfer operation.

frame $\{O_G x_G y_G z_G\}$ are obtained as

$$p_G^c = \begin{bmatrix} (y+d_y)C_\phi + h_t S_\phi \\ -(y+d_y)S_\phi + h_t C_\phi + \zeta \end{bmatrix},$$

$$p_G^m = \begin{bmatrix} (y+d_y)C_\phi + lS_{\theta-\phi} + h_t S_\phi \\ -(y+d_y)S_\phi - lC_{\theta-\phi} + h_t C_\phi + \zeta \end{bmatrix}.$$

It follows that, the kinetic energy, potential energy and Lagrangian of the crane system can be respectively obtained as,

$$\begin{aligned} \mathcal{K} =& \frac{1}{2} m_c \|\dot{p}_G^c\|^2 + \frac{1}{2} m_p \|\dot{p}_G^m\|^2, \\ \mathcal{P} =& m_c [0, g] p_G^c + m_p [0, g] p_G^m, \\ \mathcal{L} =& \mathcal{K} - \mathcal{P}. \end{aligned}$$

By applying the Euler-Lagrange formulation (3.1) with $q = [y \ l \ \theta]^T$ and $\tau = [F_y \ F_l \ 0]^T$, the equation of motion of the offshore crane system can be expressed in the following form:

$$M(q)\ddot{q} + f(t, q, \dot{q}) = \tau(t) - \omega_d(t), \tag{3.7}$$

where

$$f(t,q,\dot{q}) = h(q,\dot{q}) + \Delta h(t,q,\dot{q}),$$

in which $h(q,\dot{q}) = C(q,\dot{q}) + K\dot{q} + P(\dot{q}) + G(q)$ and $\Delta h(\cdot)$ contains the information of the vessel's rolling angle, velocity and acceleration, and heaving acceleration. The matrices and vectors in (3.7) are listed as follows:

$$\begin{aligned}
M(q) &= \begin{bmatrix} m_c + m_p & m_p S_\theta & m_p l C_\theta \\ m_p S_\theta & m_p & 0 \\ m_p l C_\theta & 0 & m_p l^2 \end{bmatrix}, \\
C(q,\dot{q}) &= \begin{bmatrix} 0 & m_p C_\theta \dot{\theta} & m_p(\dot{l} C_\theta - l S_\theta \dot{\theta}) \\ 0 & 0 & -m_p l \dot{\theta} \\ 0 & m_p l \dot{\theta} & m_p \dot{l} \end{bmatrix}, \\
G(q) &= \begin{bmatrix} 0, & -m_p g C_\theta, & m_p g l S_\theta \end{bmatrix}^T, \\
K &= \mathrm{diag}(K_{cy}, K_{cl}, K_{c\theta}), \\
P(\dot{q}) &= \begin{bmatrix} P_{cy} \operatorname{sign} \dot{y}, & P_{cl} \operatorname{sign} \dot{l}, & P_{c\theta} \operatorname{sign} \dot{\theta} \end{bmatrix}^T, \\
\Delta h(t,q,\dot{q}) &= \begin{bmatrix} \Delta h_1, \Delta h_2, \Delta h_3 \end{bmatrix}^T, \\
\omega_d(t) &= \begin{bmatrix} \omega_{d1}(t), & \omega_{d2}(t), & \omega_{d3}(t) \end{bmatrix}^T,
\end{aligned}$$

where

$$\begin{aligned}
\Delta h_1 =& (m_c + m_p)\left(-y\dot{\phi}^2 + h_t\ddot{\phi} - (g + \ddot{\zeta})S_\phi\right) + 2m_p(l\dot{\theta}\dot{\phi}S_\theta - \dot{l}\dot{\phi}C_\theta) \\
& - m_p l\left(S_\theta\dot{\phi}^2 + C_\theta\ddot{\phi}\right), \\
\Delta h_2 =& m_p\Big[(yC_\theta + h_t S_\theta)\ddot{\phi} + 2\dot{y}\dot{\phi}C_\theta + 2l\dot{\theta}\dot{\phi} - (yS_\theta - h_t C_\theta + l)\dot{\phi}^2 \\
& + gC_\theta - (g + \ddot{\zeta})C_{\theta-\phi}\Big], \\
\Delta h_3 =& m_p\Big[-2l\dot{l}\dot{\phi} - 2\dot{y}\dot{\phi}lS_\theta - (ylS_\theta - h_t l C_\theta - l^2)\ddot{\phi} - glS_\theta \\
& + l(yC_\theta + h_t S_\theta)\dot{\phi}^2 + (g + \ddot{\zeta})lS_{\theta-\phi}\Big],
\end{aligned}$$

in which K_{cy}, K_{cl} and $K_{c\theta}$ are the viscous friction coefficients and P_{cy}, P_{cl} and $P_{c\theta}$ are the Coulomb friction coefficients. By letting $q_1 = q$, $q_2 = \dot{q}$ and introducing a state variable vector $x_a = [q_1^T \ q_2^T]^T \in \mathbb{R}^6$, system (3.7) can be expressed in state space as,

$$\dot{x}_a = F(t, x_a) + G_a(x_a)u_a(t) + H(x_a)\omega(t), \tag{3.8}$$

where

$$F(t, x_a) = \begin{bmatrix} q_2 \\ -M^{-1}(q)f(t, q, \dot{q}) \end{bmatrix}, \qquad G_a(x_a) = -H(x_a)E_0,$$

$$H(x_a) = \begin{bmatrix} 0_{3\times 3} \\ -M^{-1}(q) \end{bmatrix}, \qquad E_0 = \begin{bmatrix} 1 & 0 & 0 \\ 0 & 1 & 0 \end{bmatrix}^T,$$

$$u_a(t) = [u_1, u_2]^T = [F_y, F_l]^T.$$

The linearization of system (3.8) about an operating point (x_{a0}, u_{a0}) can be obtained in the following form:

$$\dot{x}(t) = (A + \Delta A(t))x(t) + Bu(t) + D\omega(t), \tag{3.9}$$

where $x(t) = x_a(t) - x_{a0}$ and $u(t) = u_a(t) - u_{a0}$. Since $l \neq 0$, we choose $x_{a0} = [0 \ L \ 0 \ 0 \ 0 \ 0]^T$, where $L > 0$ is the median length of the rope. It follows that $x(t) = [y \ \Delta l \ \theta \ \dot{y} \ \dot{l} \ \dot{\theta}]^T$, where $\Delta l = l - L$. Thus, the system matrix, the input matrix, and the disturbance matrices are respectively obtained as follows:

$$A + \Delta A(t) = \frac{\partial F(t, x_a)}{\partial x_a} + \sum_{j=1}^{2} \frac{\partial G_{a_j}(x_a)}{\partial x_a} u_{a_j} \Bigg|_{\substack{x_a = x_{a0} \\ u_a = u_{a0}}},$$

$$B = G_a(x_{a0}),$$

$$D = H(x_{a0}),$$

where $G_{a_j}(\cdot)$, $j = 1, 2$, denotes the jth column of matrix $G_a(\cdot)$. The wind-induced motion, on the other hand provides an exogenous disturbance to system (3.7). Since the wind drag mainly affects the motion of suspended container during transfer

operation, we assume that the exogenous force has a direct influence on the payload sway dynamics only, such that $\omega_{d1}(t) = \omega_{d2}(t) = 0$. Besides, the nonlinear Coulomb friction terms $P(\dot{q})$ can be combined with vector $\omega_d(t)$, such as

$$\omega(t) = P(\dot{q}) + \omega_d(t) = \begin{bmatrix} P_{cy} \operatorname{sign} \dot{y} \\ P_{cl} \operatorname{sign} \dot{l} \\ \tau_{wd}(t) + P_{c\theta} \operatorname{sign} \dot{\theta} \end{bmatrix}.$$

The term $\tau_{wd}(t)$ represents the torque produced by the wind drag $F_{wd}(t)$ on the payload such that $\tau_{wd}(t) = F_{wd}(t) l C_{\theta-\phi}$. The magnitude of the wind drag can be estimated by [77]:

$$F_{wd}(t) = \frac{1}{2} \rho_w v_w(t) |v_w(t)| c_d S_p, \tag{3.10}$$

where ρ_w is the density of air, c_d is the drag coefficient, $v_w(t)$ is the wind velocity and S_p is the effective surface area of the payload. Finally, by taking into account all of the disturbance and uncertainty terms, (3.9) can be rewritten as,

$$\dot{x}(t) = (A + \Delta A(t))x(t) + Bu(t) + D\omega(t). \tag{3.11}$$

After some mathematical manipulations, the details of system matrix, input matrix and disturbance matrices in (3.11) are obtained as follows:

$$A = \begin{bmatrix} 0_{3\times3} & I_3 \\ A_3 & A_4 \end{bmatrix}, \qquad B = \begin{bmatrix} 0_{3\times2} \\ \underline{B}_2 \end{bmatrix},$$

$$\Delta A(t) = \begin{bmatrix} 0_{3\times3} & 0_{3\times3} \\ \Delta A_3 & \Delta A_4 \end{bmatrix}, \qquad D = \begin{bmatrix} 0_{3\times3} \\ D_2 \end{bmatrix},$$

$$A_3 = \begin{bmatrix} 0 & 0 & \frac{m_p g}{m_c} \\ 0 & 0 & 0 \\ 0 & 0 & -\frac{(m_c+m_p)g}{m_c L} \end{bmatrix}, \qquad A_4 = \begin{bmatrix} -\frac{K_{cy}}{m_p} & 0 & \frac{K_{c\theta}}{m_c L} \\ 0 & -\frac{K_{cl}}{m_p} & 0 \\ \frac{K_{cy}}{m_c L} & 0 & -\frac{(m_c+m_p)K_{c\theta}}{m_c m_p L^2} \end{bmatrix},$$

$$\underline{B}_2 = \begin{bmatrix} \frac{1}{m_c} & 0 \\ 0 & \frac{1}{m_p} \\ -\frac{1}{m_c L} & 0 \end{bmatrix}, \qquad D_2 = \begin{bmatrix} -\frac{1}{m_c} & 0 & \frac{1}{m_c L} \\ 0 & -\frac{1}{m_p} & 0 \\ \frac{1}{m_c L} & 0 & -\frac{m_c+m_p}{m_c m_p L^2} \end{bmatrix},$$

$$\Delta A_3 = \begin{bmatrix} \left(1+\frac{2m_p}{m_c}\right)\dot{\phi}^2 & -\frac{m_p}{m_c L}(g+\ddot{\zeta})S_\phi & \Psi_{43} \\ -\ddot{\phi} & \dot{\phi}^2 & \Psi_{53} \\ -\frac{2}{L}\left(1+\frac{m_p}{m_c}\right)\dot{\phi}^2 & \Psi_{62} & \Psi_{63} \end{bmatrix},$$

$$\Delta A_4 = \begin{bmatrix} \frac{2m_p}{m_c}\dot{\phi} & 0 & 0 \\ -2\dot{\phi} & 0 & 0 \\ -\frac{2}{L}\left(1+\frac{m_p}{m_c}\right)\dot{\phi} & 0 & 0 \end{bmatrix},$$

$$\Psi_{43} = \frac{m_p}{m_c}\left[(L+h_t)\dot{\phi}^2 - d_y\ddot{\phi} + (g+\ddot{\zeta})C_\phi - g\right],$$

$$\Psi_{53} = -h_t\ddot{\phi} + d_y\dot{\phi}^2 - (g+\ddot{\zeta})S_\phi,$$

$$\Psi_{62} = \frac{1}{L^2}\left(1+\frac{m_p}{m_c}\right)(g+\ddot{\zeta})S_\phi,$$

$$\Psi_{63} = -\frac{1}{L}\left(1+\frac{m_p}{m_c}\right)\left[h_t\dot{\phi}^2 - d_y\ddot{\phi} + (g+\ddot{\zeta})C_\phi - g\right] - \frac{m_p}{m_c}\dot{\phi}^2.$$

3.3.2 3-D model

The coordinates system of the offshore crane is shown in Figure 3.2 where $\{O_G x_G y_G z_G\}$, $\{O_B x_B y_B z_B\}$, and $\{O_C x_C y_C z_C\}$ respectively represent the coordinate frames of the ground, the vessel, and the cart. The masses of the cart and the payload are denoted as m_c and m_p, respectively. Let x and y respectively denote the position of the girder and the cart, h_t denote the crane height, l denote the rope length. The longitudinal and the lateral sway angles of the load are denoted as θ and δ, respectively. Let F_y and F_l denote the control forces applied at the cart and hoist, respectively. Since F_y can only control the longitudinal sway, a control torque τ_δ is applied to the rope to control the lateral sway. Let ζ, ϕ, ψ denote the heave, roll, and yaw of the vessel, respectively. Based on Figure 3.2, the position vectors of the cart and and the payload with respect to $\{O_G x_G y_G z_G\}$ can be obtained as

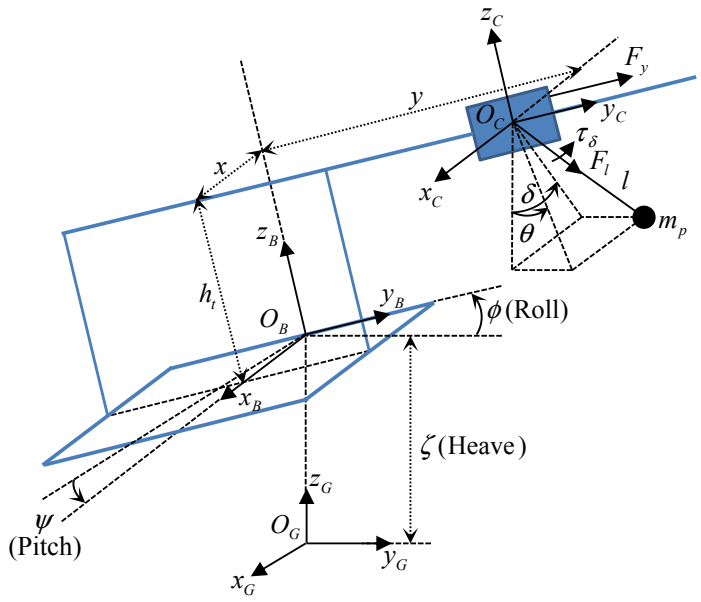

Figure 3.2 : Motion of the offshore crane during containers transfer operation.

$$p_G^c = \begin{bmatrix} xC_\psi + yS_\psi S_\phi + h_t S_\psi C_\phi \\ yC_\phi - h_t S_\phi \\ \zeta - xS_\psi + yC_\psi S_\phi + h_t C_\psi C_\phi \end{bmatrix},$$

$$p_G^m = \begin{bmatrix} xC_\psi + yS_\psi S_\phi + h_t S_\psi C_\phi - lC_\theta S_\delta \\ yC_\phi - h_t S_\phi + lS_\theta \\ \zeta - xS_\psi + yC_\psi S_\phi + h_t C_\psi C_\phi - lC_\theta C_\delta \end{bmatrix}.$$

By applying the Euler-Lagrange formulation with $q = [y\ l\ \delta\ \theta]^T$ and $\tau = [F_y\ F_l\ \tau_\delta\ 0]^T$, the dynamic model of the offshore crane system can be cast in the form of

$$M(q)\ddot{q} + f(q, \dot{q}) = \tau, \tag{3.12}$$

where

$$M(q) = \begin{bmatrix} m_c + m_p & m_p(-S_\phi C_\theta C_{\delta-\psi} + C_\phi S_\theta) & m_p l S_\phi C_\theta S_{\delta-\psi} \\ m_p(-S_\phi C_\theta C_{\delta-\psi} + C_\phi S_\theta) & m_p & 0 \\ m_p l S_\phi C_\theta S_{\delta-\psi} & 0 & m_p l^2 C_\theta^2 \\ m_p l(S_\phi S_\theta C_{\delta-\psi} + C_\phi C_\theta) & 0 & 0 \end{bmatrix}$$

$$\begin{matrix} m_p l(S_\phi S_\theta C_{\delta-\psi} + C_\phi C_\theta) \\ 0 \\ 0 \\ m_p l^2 \end{matrix} \Bigg],$$

$$f(q,\dot{q}) = [f_1 \;\; f_2 \;\; f_3 \;\; f_4]^T,$$

$$\begin{aligned}
f_1 =& (m_c + m_p)\left[-x\ddot{\psi}S_\phi - h_t\ddot{\phi} - h_t\dot{\psi}^2 S_\phi C_\phi + (g+\ddot{\zeta})C_\psi S_\phi - \left(\dot{\psi}^2 S_\phi^2 + \dot{\phi}^2\right) y\right] \\
&+ m_p\left[2\dot{l}\dot{\delta}S_\phi C_\theta S_{\delta-\psi} + 2\dot{l}\dot{\theta}S_\phi S_\theta C_{\delta-\psi} + 2\dot{l}\dot{\theta}C_\phi C_\theta + l\left(\ddot{\theta}^2 + \dot{\delta}^2\right) S_\phi C_\theta C_{\delta-\psi}\right. \\
&\left. - l\dot{\theta}^2 C_\phi S_\theta - 2l\dot{\theta}\dot{\delta}S_\phi S_\theta S_{\delta-\psi}\right], \\
f_2 =& m_p\left[-2\dot{l}\dot{\theta}C_\theta S_\theta - l\left(\dot{\theta}^2 + \dot{\delta}^2\right) C_\theta^2 - 2\dot{y}\dot{\phi}C_\phi C_\theta C_{\delta-\psi} - 2\dot{y}\dot{\psi}S_\phi C_\theta S_{\delta-\psi}\right. \\
&- y\ddot{\psi}S_\phi C_\theta S_{\delta-\psi} - y\ddot{\phi}C_\phi C_\theta C_{\delta-\psi} + y\left(\dot{\psi}^2 + \dot{\phi}^2\right) S_\phi C_\theta C_{\delta-\psi} - 2y\dot{\psi}\dot{\phi}C_\phi C_\theta S_{\delta-\psi} \\
&- h_t\ddot{\psi}C_\phi C_\theta S_{\delta-\psi} + h_t\ddot{\phi}S_\phi C_\theta C_{\delta-\psi} + h_t\left(\dot{\psi}^2 + \dot{\phi}^2\right) C_\phi C_\theta C_{\delta-\psi} + 2h_t\dot{\psi}\dot{\phi}S_\phi C_\theta S_{\delta-\psi} \\
&\left. + x\ddot{\psi}C_\theta C_{\delta-\psi} + x\dot{\psi}^2 C_\theta S_{\delta-\psi} - (g+\ddot{\zeta})C_\theta C_\delta\right], \\
f_3 =& m_p l\left[-2l\dot{\delta}\dot{\theta}S_\theta C_\theta + 2\dot{l}\dot{\delta}C_\theta^2 + 2\dot{y}\dot{\phi}C_\phi C_\theta S_{\delta-\psi} - 2\dot{y}\dot{\psi}S_\phi C_\theta C_{\delta-\psi} - y\ddot{\psi}S_\phi C_\theta C_{\delta-\psi}\right. \\
&+ y\ddot{\phi}C_\phi C_\theta S_{\delta-\psi} - y\left(\dot{\psi}^2 + \dot{\phi}^2\right) S_\phi C_\theta S_{\delta-\psi} - 2y\dot{\psi}\dot{\phi}C_\phi C_\theta C_{\delta-\psi} - h_t\ddot{\psi}C_\phi C_\theta C_{\delta-\psi} \\
&- h_t\ddot{\phi}S_\phi C_\theta S_{\delta-\psi} - h_t\left(\dot{\psi}^2 + \dot{\phi}^2\right) C_\phi C_\theta S_{\delta-\psi} + 2h_t\dot{\psi}\dot{\phi}S_\phi C_\theta C_{\delta-\psi} - x\ddot{\psi}C_\theta S_{\delta-\psi} \\
&\left. + x\dot{\psi}^2 C_\theta C_{\delta-\psi} + (g+\ddot{\zeta})C_\theta S_\delta\right],
\end{aligned}$$

$$
\begin{aligned}
f_4 =& m_p l \Big[2\dot{l}\dot{\theta} + 2\dot{y}\dot{\psi} S_\phi S_\theta S_{\delta-\psi} + 2\dot{y}\dot{\phi} C_\phi S_\theta C_{\delta-\psi} - 2\dot{y}\dot{\phi} S_\phi C_\theta + 2y\dot{\psi}\dot{\phi} C_\phi S_\theta S_{\delta-\psi} \\
& - y\dot{\phi}^2 C_\phi C_\theta - y\left(\dot{\psi}^2 + \dot{\phi}^2\right) S_\phi S_\theta C_{\delta-\psi} - y\ddot{\phi} S_\phi C_\theta + h_t \dot{\phi}^2 S_\phi C_\theta + y\ddot{\psi} S_\phi S_\theta S_{\delta-\psi} \\
& - h_t \ddot{\phi} C_\phi C_\theta + y\ddot{\phi} C_\phi S_\theta C_{\delta-\psi} - x\dot{\psi}^2 S_\theta S_{\delta-\psi} - x\ddot{\psi} S_\theta C_{\delta-\psi} + l\dot{\delta}^2 S_\theta C_\theta \\
& - 2h_t \dot{\psi}\dot{\phi} S_\phi S_\theta S_{\delta-\psi} - h_t \left(\dot{\psi}^2 + \dot{\phi}^2\right) C_\phi S_\theta C_{\delta-\psi} + h_t \ddot{\psi} C_\phi S_\theta S_{\delta-\psi} \\
& - h_t \ddot{\phi} S_\phi S_\theta C_{\delta-\psi} + (g + \ddot{\zeta}) S_\theta C_\delta \Big].
\end{aligned}
$$

The control torque τ_δ is produced by adjusting the tensions in the additional ropes such that

$$\tau_\delta = (d_1 - d_2)F_{\delta 0} + (d_1 + d_2)F_\delta$$

where $F_{\delta 0}$ is the initial tension in each additional rope and d_1 and d_2 are the distances from the cart centre to the additional ropes, which are defined as follows:

$$
\begin{aligned}
d_1 &= \frac{blC_{\psi-\delta}}{\sqrt{(b-a)^2 + l^2 + 2l(b-a)S_{\psi-\delta}}} \\
d_2 &= \frac{blC_{\psi-\delta}}{\sqrt{(b-a)^2 + l^2 - 2l(b-a)S_{\psi-\delta}}}
\end{aligned}
$$

in which a and b are the specific distances between spreader centres and pulleys [103]. Then (3.12) can be rewritten as

$$M(q)\ddot{q} + \overline{f}(q, \dot{q}) = \overline{\tau}, \tag{3.13}$$

where

$$
\begin{aligned}
\overline{f}(q, \dot{q}) &= \left[f_1 \quad f_2 \quad f_3 \quad \frac{f_4 - (d_1 - d_2)F_{\delta 0}}{d_1 + d_2} \right]^T, \\
\overline{\tau} &= [F_y \;\; F_l \;\; F_\delta \;\; 0]^T.
\end{aligned}
$$

3.4 Modelling of offshore boom cranes

In this section, we derive the dynamics models of 2-D and 3-D offshore boom cranes. In a similar fashion of Section 3.3, we present an uncertain LTI model for the 2-D crane and a nonlinear model for the 3-D crane.

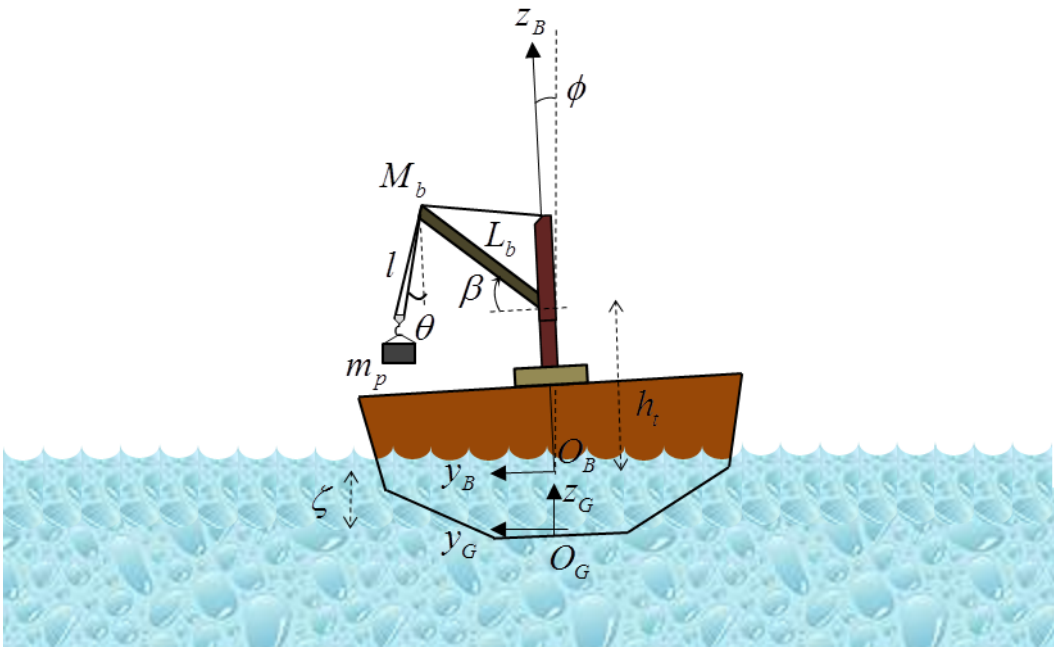

Figure 3.3 : Motion of the 2-D offshore boom crane.

3.4.1 2-D model

The offshore boom crane motion is represented by three generalised coordinates, i.e., the luff angle, β, the rope length measured from the boom tip to the payload, l, and the sway angle, θ. Let L_b denote the boom length and h_t denote the height from O_B to the joint of tower and boom. Let M_b and m_p denote the masses of the boom and the payload, respectively. Let introduce L as the length from the joint of tower and boom to a point b in the boom. Thus, the position vectors of the point b, p_G^b and the payload, p_G^m, with respect to the ground coordinate frame $\{O_G x_G y_G z_G\}$ are respectively obtained as

$$p_G^b = \begin{bmatrix} LC_{\beta-\phi} + h_t S_\phi \\ LS_{\beta-\phi} + h_t C_\phi + \zeta \end{bmatrix},$$

$$p_G^m = \begin{bmatrix} L_b C_{\beta-\phi} + lS_{\theta-\phi} + h_t S_\phi \\ L_b S_{\beta-\phi} - lC_{\theta-\phi} + h_t C_\phi + \zeta \end{bmatrix}.$$

Thus, the kinetic energy, $\mathcal{K}$, potential energy, $\mathcal{P}$ and Lagrangian, $\mathcal{L}$ of the system can be respectively obtained as,

$$\begin{aligned}
\mathcal{K} =& \frac{1}{2}\frac{M_b}{L_b}\int_0^{L_b} \|\dot{p}_G^b\|^2 dL + \frac{1}{2}m_p\|\dot{p}_G^m\|^2,\\
\mathcal{P} =& \frac{M_b}{L_b}\int_0^{L_b} [0,g]p_G^b dL + m_p[0,g]p_G^m,\\
\mathcal{L} =& \mathcal{K} - \mathcal{P}.
\end{aligned}$$

Hence, by using the Euler-Lagrange formulation with $q = [\beta, l, \theta]^T$ and $\tau = [\tau_\beta, F_l, 0]^T$, the dynamics of the offshore boom crane can be represented as

$$M(q)\ddot{q} + f(t,q,\dot{q}) = \tau(t) - \omega_d(t), \tag{3.14}$$

where

$$M(q) = \begin{bmatrix} J_b + m_p L_b^2 & -m_p L_b C_{\beta-\theta} & -m_p L_b l S_{\beta-\theta} \\ -m_p L_b C_{\beta-\theta} & m_p & 0 \\ -m_p L_b l S_{\beta-\theta} & 0 & m_p l^2 \end{bmatrix},$$

$$\begin{aligned}
f(t,q,\dot{q}) =& [f_1,\ f_2,\ f_3]^T,\\
f_1 =& \frac{3J_b}{2L_b}\left[(g+\ddot{\zeta})C_{\beta-\phi} - h_t(S_\beta\ddot{\phi} + C_\beta\dot{\phi}^2)\right] - J_b\ddot{\phi}\\
&+ m_p L_b\left[lS_{\beta-\theta}\ddot{\phi} - 2\dot{l}S_{\beta-\theta}(\dot{\theta}-\dot{\phi}) + lC_{\beta-\theta}(\dot{\theta}-\dot{\phi})^2 - L_b\ddot{\phi} + (g+\ddot{\zeta})C_{\beta-\phi}\right.\\
&\left.- h_t(S_\beta\ddot{\phi} + C_\beta\dot{\phi}^2)\right] + K_{c\beta}\dot{\beta} + P_{c\beta}\,\mathrm{sign}\,\dot{\beta},\\
f_2 =& m_p\left[L_b C_{\beta-\theta}\ddot{\phi} - l(\dot{\theta}-\dot{\phi})^2 + L_b S_{\beta-\theta}(\dot{\beta}-\dot{\phi})^2 - (g+\ddot{\zeta})C_{\theta-\phi}\right.\\
&\left.+ h_t(S_\theta\ddot{\phi} + C_\theta\dot{\phi}^2)\right] + K_{cl}\dot{l} + P_{cl}\,\mathrm{sign}\,\dot{l},\\
f_3 =& m_p\left[L_b l S_{\beta-\theta}\ddot{\phi} + 2l\dot{l}(\dot{\theta}-\dot{\phi}) - L_b l C_{\beta-\theta}(\dot{\beta}-\dot{\phi})^2 - l^2\ddot{\phi} + (g+\ddot{\zeta})lS_{\theta-\phi}\right.\\
&\left.+ h_t l(C_\theta\ddot{\phi} - S_\theta\dot{\phi}^2)\right] + K_{c\theta}\dot{\theta} + P_{c\theta}\,\mathrm{sign}\,\dot{\theta},\\
\omega_d(t) =& [0\ \ 0\ \ \tau_{wd}(t)]^T.
\end{aligned}$$

in which $K_{c\beta}$, K_{cl} and $K_{c\theta}$ are the viscous friction coefficients and $P_{c\beta}$, P_{cl} and $P_{c\theta}$ are the Coulomb friction coefficients. Using the same notation in Section 3.3.1,

$\tau_{wd}(t)$ represents the torque produced by the wind drag $F_{wd}(t)$ on the payload such that $\tau_{wd}(t) = F_{wd}(t)lC_{\theta-\phi}$, in which, the magnitude of the wind drag is estimated by (3.10).

By letting $q_1 = q$, $q_2 = \dot{q}$ and introducing a state variable vector $x = [q_1^T \;\; q_2^T]^T$, the system (3.14) can be represented in state space as

$$\dot{x}(t) = F(t,x) + G(x)u(t) + H(x)\omega(t), \tag{3.15}$$

where

$$F(t,x) = \begin{bmatrix} q_2 \\ -M^{-1}(q)h(t,q,\dot{q}) \end{bmatrix}, \qquad G(x) = -H(x)E_0,$$

$$H(x) = \begin{bmatrix} 0_{3\times 3} \\ -M^{-1}(q) \end{bmatrix}, \qquad E_0 = \begin{bmatrix} 1 & 0 & 0 \\ 0 & 1 & 0 \end{bmatrix}^T,$$

$$u(t) = [u_1 \;\; u_2]^T = [\tau_\beta \;\; F_l]^T, \qquad \omega(t) = \begin{bmatrix} P_{c\beta}\operatorname{sign}\dot{\beta} \\ P_{cl}\operatorname{sign}\dot{l} \\ \tau_{wd}(t) + P_{c\theta}\operatorname{sign}\dot{\theta} \end{bmatrix}.$$

To facilitate the control design, system (3.15) is linearised about an operating point $x_0 = [\beta_e \; l_e \; 0 \; 0 \; 0 \; 0]^T$. The selection of the operating point x_0 with $\beta_e \neq 0$, $l_e \neq 0$ does not guarantee the existence of u_0 such that $F(t,x_0) + G(x_0)u_0 = 0$. In other words, x_0 is not an equilibrium state of (3.15). Therefore, we construct a linear model in x and u that approximates the behaviour of (3.15) in the vicinity of the operating state x_0, that is, we wish to find constant matrices A and B such that in a neighbourhood of x_0,

$$F(t,x) + G(x)u \approx Ax + Bu.$$

By following the approximation method in [134], the linearisation of (3.15) in the vicinity of $x_0 = [\pi/4 \; 1 \; 0 \; 0 \; 0 \; 0]^T$ is obtained as

$$\dot{x}(t) = (A + \Delta A(t))x(t) + Bu(t) + D\omega(t), \tag{3.16}$$

where

$$A + \Delta A(t) = \left.\frac{\partial F(t,x)}{\partial x}\right|_{x=x_0} + \left(F(t,x_0) - \left.\frac{\partial F(t,x)}{\partial x}\right|_{x=x_0} x_0\right)\frac{x_0^T}{\|x_0\|^2},$$

$$B = G(x_0),$$

$$D = H(x_0).$$

The matrices A, B, $\Delta A(t)$ and D are obtained as follows:

$$A = \begin{bmatrix} 0_{3\times3} & I_3 \\ A_3 & A_4 \end{bmatrix}, \qquad B = \begin{bmatrix} 0_{3\times2} \\ \underline{B}_2 \end{bmatrix},$$

$$\Delta A(t) = \begin{bmatrix} 0_{3\times3} & 0_{3\times3} \\ \Delta A_3 & \Delta A_4 \end{bmatrix}, \qquad D = \begin{bmatrix} 0_{3\times3} \\ D_2 \end{bmatrix},$$

$$A_3 = \begin{bmatrix} -\frac{3\sqrt{2}(\pi-4)g}{(\pi^2+16)L_b} & -\frac{3\sqrt{2}(\pi+4)g}{(\pi^2+16)L_b} & 0 \\ \frac{(\pi+24)g}{\pi^2+16} & -\frac{2(3\pi-2)g}{\pi^2+16} & -\frac{3g}{4} \\ -\frac{6\pi g}{\pi^2+16} & \frac{3(\pi^2-16)g}{4(\pi^2+16)} & -\frac{g}{4} \end{bmatrix},$$

$$A_4 = \begin{bmatrix} -\frac{3K_{c\beta}}{M_bL_b^2} & -\frac{3\sqrt{2}K_{cl}}{2M_bL_b} & -\frac{3\sqrt{2}K_{c\theta}}{2M_bL_b} \\ -\frac{3\sqrt{2}K_{c\beta}}{2M_bL_b} & -\frac{(2M_b+3m_p)K_{cl}}{2M_bm_p} & -\frac{3K_{c\theta}}{2M_b} \\ -\frac{3\sqrt{2}K_{c\beta}}{2M_bL_b} & -\frac{3K_{cl}}{2M_b} & -\frac{(2M_b+3m_p)K_{c\theta}}{2M_bm_p} \end{bmatrix},$$

$$\underline{B}_2 = \begin{bmatrix} \frac{3}{M_bL_b^2} & \frac{3\sqrt{2}}{2M_bL_b} \\ \frac{3\sqrt{2}}{2M_bL_b} & \frac{2M_b+3m_p}{2M_bm_p} \\ \frac{3\sqrt{2}}{2M_bL_b} & \frac{3}{2M_b} \end{bmatrix}, \qquad D_2 = \begin{bmatrix} -\frac{3}{M_bL_b^2} & -\frac{3\sqrt{2}}{2M_bL_b} & -\frac{3\sqrt{2}}{2M_bL_b} \\ -\frac{3\sqrt{2}}{2M_bL_b} & -\frac{2M_b+3m_p}{2M_bm_p} & -\frac{3}{2M_b} \\ -\frac{3\sqrt{2}}{2M_bL_b} & -\frac{3}{2M_b} & -\frac{2M_b+3m_p}{2M_bm_p} \end{bmatrix},$$

$$\Delta A_3 = \begin{bmatrix} \Psi_{41} & \Psi_{42} & 0 \\ \Psi_{51} & \Psi_{52} & \Psi_{53} \\ \Psi_{61} & \Psi_{62} & \Psi_{63} \end{bmatrix}, \qquad \Delta A_4 = \begin{bmatrix} 0 & 0 & 0 \\ \sqrt{2}L_b\dot{\phi} & 0 & -2\dot{\phi} \\ -\sqrt{2}L_b\dot{\phi} & 2\dot{\phi} & 0 \end{bmatrix},$$

$$\Psi_{41} = -\frac{1}{(\pi^2+16)L_b}\Big(24(g+\ddot{\zeta})S_{\phi-\frac{\pi}{4}} + 6\pi(g+\ddot{\zeta})C_{\phi-\frac{\pi}{4}} + (12-3\pi)\sqrt{2}h_t\dot{\phi}^2 - (4\pi L_b + (12+3\pi)\sqrt{2}h_t)\ddot{\phi} + (12-3\pi)\sqrt{2}g\Big),$$

$$\Psi_{42} = \frac{1}{(\pi^2+16)L_b}\Big(-24(g+\ddot{\zeta})C_{\phi-\frac{\pi}{4}} + 6\pi(g+\ddot{\zeta})S_{\phi-\frac{\pi}{4}} + (12+3\pi)\sqrt{2}h_t\dot{\phi}^2 + (16L_b + (12-3\pi)\sqrt{2}h_t)\ddot{\phi} + (12+3\pi)\sqrt{2}g\Big),$$

$$\Psi_{51} = -\frac{1}{\pi^2+16}\Big(-(24+\pi)(g+\ddot{\zeta})C_{\phi} + 3\pi(g+\ddot{\zeta})S_{\phi} + ((8+2\pi)\sqrt{2}L_b + (24+\pi)h_t)\dot{\phi}^2 - 3\pi h_t\ddot{\phi} + (24+\pi)g\Big),$$

$$\Psi_{52} = \frac{1}{\pi^2+16}\Big((4-6\pi)(g+\ddot{\zeta})C_{\phi} - 12(g+\ddot{\zeta})S_{\phi} + ((-8+2\pi)\sqrt{2}L_b + (-4+6\pi)h_t + \pi^2 + 16)\dot{\phi}^2 + 12h_t\ddot{\phi} + (-4+6\pi)g\Big),$$

$$\Psi_{53} = -\frac{3}{4}(g+\ddot{\zeta})C_{\phi} + \frac{1}{4}(g+\ddot{\zeta})S_{\phi} + \frac{1}{4}(2\sqrt{2}L_b + 3h_t)\dot{\phi}^2 - \frac{1}{4}h_t\ddot{\phi} + \frac{3}{4}g,$$

$$\Psi_{61} = \frac{1}{\pi^2+16}\Big(-6\pi(g+\ddot{\zeta})C_{\phi} + (-24+2\pi)(g+\ddot{\zeta})S_{\phi} + ((-8+4\pi)\sqrt{2}L_b + 6\pi h_t)\dot{\phi}^2 + ((24-2\pi)h_t + 4\pi)\ddot{\phi} + 6\pi g\Big),$$

$$\Psi_{62} = \frac{1}{4(\pi^2+16)}\Big((-48+3\pi^2)(g+\ddot{\zeta})C_{\phi} + (16+24\pi-\pi^2)(g+\ddot{\zeta})S_{\phi} + ((32+8\pi-2\pi^2)\sqrt{2}L_b + (48-3\pi^2)h_t)\dot{\phi}^2 + ((-16-24\pi+\pi^2)h_t + 64)\ddot{\phi} + (48-3\pi^2)g\Big),$$

$$\Psi_{63} = -\frac{1}{4}(g+\ddot{\zeta})C_{\phi} + \frac{3}{4}(g+\ddot{\zeta})S_{\phi} + \frac{1}{4}(2\sqrt{2}L_b + h_t)\dot{\phi}^2 - \frac{3}{4}h_t\ddot{\phi} + \frac{1}{4}g,$$

3.4.2 3-D model

The offshore crane system considered in this study consists of a boom crane mounted on a ship vessel as visualize in Figure 3.4. The coordinates system of the offshore crane is shown in Figure 3.5, where $\{O_G x_G y_G z_G\}$ and $\{O_B x_B y_B z_B\}$ respectively represent the coordinate frames of the ground and the vessel. The crane system motion is represented by five generalized coordinates; in which, α is the slew angle of the tower, β is the luff angle of the boom, l is the length of the rope, θ_1 is the tangential pendulation due to the motion of the tower and θ_2 is the radial sway due to the motion of the boom. The values of the boom length, L_b, and the tower height, h_t (measured from crane base $\{0\}$ to joint $\{1\}$), are considered

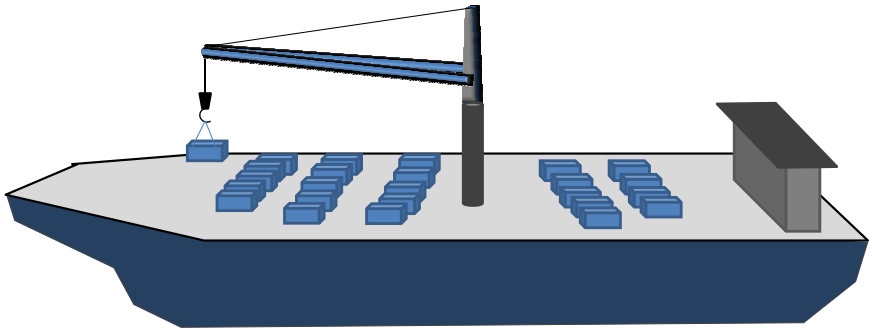

Figure 3.4 : An offshore boom crane.

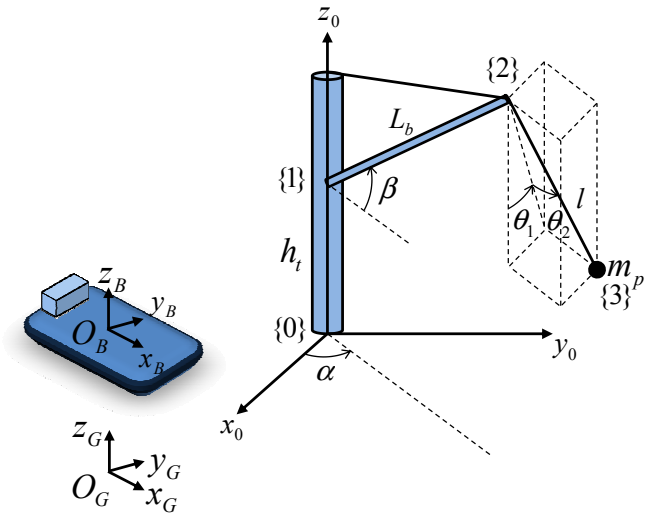

Figure 3.5 : Motion of the offshore boom crane.

as constants. By referring to Figure 3.5, the position vectors of the links {1} and {2}, and payload (point {3}) with respect to the frame $\{O_0x_0y_0z_0\}$ are respectively obtained as

$$\mathbf{p}_0^1 = [0 \;\; 0 \;\; h_t]^T,$$

$$\mathbf{p}_0^2 = [L_bC_\alpha C_\beta \;\; L_bS_\alpha C_\beta \;\; h_t + L_bS_\beta]^T,$$

$$\mathbf{p}_0^3 = \begin{bmatrix} L_bC_\alpha C_\beta - lS_\alpha S_{\theta_1} C_{\theta_2} + lC_\alpha S_{\theta_2} \\ L_bS_\alpha C_\beta + lC_\alpha S_{\theta_1} C_{\theta_2} + lS_\alpha S_{\theta_2} \\ h_t + L_bS_\beta - lC_{\theta_1} C_{\theta_2} \end{bmatrix}.$$

Let define the position vector of the crane base with respect to the frame $\{O_B x_B y_B z_B\}$ as

$$\mathbf{p}_B^0 = [p_{bx} \;\; p_{by} \;\; p_{bz}]^T.$$

The homogeneous transformation matrix from coordinates frame $\{O_B x_B y_B z_B\}$ to frame $\{O_G x_G y_G z_G\}$ and from frame $\{O_0 x_0 y_0 z_0\}$ to frame $\{O_B x_B y_B z_B\}$ are respectively given by

$$T_G^B = \begin{bmatrix} C_\psi & S_\psi S_\phi & S_\psi C_\phi & 0 \\ 0 & C_\phi & -S_\phi & 0 \\ -S_\psi & C_\psi S_\phi & C_\psi C_\phi & \zeta \\ 0 & 0 & 0 & 1 \end{bmatrix},$$

$$T_B^0 = \begin{bmatrix} I_3 & \mathbf{p}_B^0 \\ 0_{1\times 3} & 1 \end{bmatrix},$$

where ϕ and ψ are the rolling and pitching angular displacements of the vessel, respectively, and ζ is the heaving of the vessel. Therefore, the homogeneous transformation matrix from coordinates frame $\{O_0 x_0 y_0 z_0\}$ to frame $\{O_G x_G y_G z_G\}$ can be obtained as

$$T_G^0 = T_G^B T_B^0.$$

The dynamic model of the offshore crane system can be cast in the form of

$$M(q)\ddot{q} + C(q,\dot{q})\dot{q} + B\dot{q} + G(q) = \tau, \tag{3.17}$$

where $M(q)$ is the inertia, $C(q,\dot{q})$ is the centrifugal-Coriolis, B is the friction, and $G(q)$ is the gravity matrices. The system matrices are obtained as follows:

$$M(q) = \begin{bmatrix} m_{11} & m_{12} & m_{13} & m_{14} & m_{15} \\ m_{21} & m_{22} & m_{23} & m_{24} & m_{25} \\ m_{31} & m_{32} & m_{33} & 0 & 0 \\ m_{41} & m_{42} & 0 & m_{44} & 0 \\ m_{51} & m_{52} & 0 & 0 & m_{55} \end{bmatrix},$$

$$C(q,\dot{q}) = \begin{bmatrix} c_{11} & c_{12} & c_{13} & c_{14} & c_{15} \\ c_{21} & 0 & c_{23} & c_{24} & c_{25} \\ c_{31} & c_{32} & 0 & c_{34} & c_{35} \\ c_{41} & c_{42} & c_{43} & c_{44} & c_{45} \\ c_{51} & c_{52} & c_{53} & c_{54} & c_{55} \end{bmatrix},$$

$$B = \mathrm{diag}(b_1,\ b_2,\ b_3,\ b_4,\ b_5),$$

$$G(q) = m_p g \begin{bmatrix} 0 & L_b C_\beta & -C_{\theta_1} C_{\theta_2} & l S_{\theta_1} C_{\theta_2} & l C_{\theta_1} S_{\theta_2} \end{bmatrix}^T,$$

where

$$m_{11} = J_\alpha + m_p l^2 + m_p L_b^2 C_\beta^2 + 2 m_p L_b l C_\beta S_{\theta_2} - m_p l^2 C_{\theta_1}^2 C_{\theta_2}^2,$$

$$m_{12} = m_{21} = m_p L_b l S_\beta S_{\theta_1} C_{\theta_2},$$

$$m_{13} = m_{31} = m_p L_b C_\beta S_{\theta_1} C_{\theta_2},$$

$$m_{14} = m_{41} = m_p (L_b l C_\beta + l^2 S_{\theta_2}) C_{\theta_1} C_{\theta_2},$$

$$m_{15} = m_{51} = -m_p (L_b l C_\beta S_{\theta_2} + l^2) S_{\theta_1},$$

$$m_{22} = J_\beta + m_p L_b^2,$$

$$m_{23} = m_{32} = -m_p L_b (S_\beta S_{\theta_2} + C_\beta C_{\theta_1} C_{\theta_2}),$$

$$m_{24} = m_{42} = m_p L_b l C_\beta S_{\theta_1} C_{\theta_2},$$

$$m_{25} = m_{52} = m_p L_b l (-S_\beta C_{\theta_2} + C_\beta C \theta_1 C_{\theta_2}),$$

$$m_{33} = m_p,$$

$$m_{44} = m_p l^2 C_{\theta_2}^2,$$

$$m_{55} = m_p l^2,$$

$$\begin{aligned} c_{11} =& m_p l \dot{l} (1 - C_{\theta_1}^2 C_{\theta_2}^2) + m_p L_b \dot{l} C_\beta S_{\theta_2} + m_p (l^2 C_{\theta_1}^2 S_{\theta_2} + L_b l C_\beta) C_{\theta_2} \dot{\theta}_2 + m_p l^2 S_{\theta_1} C_{\theta_1} C_{\theta_2}^2 \dot{\theta}_1 \\ & - m_p (L_b^2 C_\beta + L_b l S_{\theta_2}) S_\beta \dot{\beta}, \end{aligned}$$

$$c_{12} = m_p L_b l C_\beta S_{\theta_1} C_{\theta_2} \dot{\beta} - m_p S_\beta \dot{\alpha} (L_b^2 C_\beta + L_b l S_{\theta_2}),$$

$$
\begin{aligned}
c_{13} =& m_p l C_{\theta_1} C_{\theta_2} S_{\theta_2} \dot{\theta}_1 + m_p L_b C_\beta (S_{\theta_2} \dot{\alpha} + C_{\theta_1} C_{\theta_2} \dot{\theta}_1 - S_{\theta_1} S_{\theta_2} \dot{\theta}_2) + m_p l \dot{\alpha} (1 - C_{\theta_1}^2 C_{\theta_2}^2) \\
& - m_p l S_{\theta_1} \dot{\theta}_2, \\
c_{14} =& m_p l^2 S_{\theta_1} C_{\theta_1} C_{\theta_2}^2 \dot{\alpha} + m_p \dot{l} C_{\theta_1} C_{\theta_2} (L_b C_\beta + l S_{\theta_2}) - m_p (L_b l C_\beta + l^2 S_{\theta_2}) S_{\theta_1} C_{\theta_2} \dot{\theta}_1 \\
& - m_p (L_b l C_\beta S_{\theta_2} + l^2 S_{\theta_2}^2) C_{\theta_1} \dot{\theta}_2, \\
c_{15} =& m_p (L_b l C_\beta + l^2 C_{\theta_1}^2 S_{\theta_2}) C_{\theta_2} \dot{\alpha} - m_p \dot{l} S_{\theta_1} (l + L_b C_\beta S_{\theta_2}) - m_p L_b l C_\beta S_{\theta_1} C_{\theta_2} \dot{\theta}_2 \\
& - m_p (L_b l C_\beta S_{\theta_2} + l^2 S_{\theta_2}^2) C_{\theta_1} \dot{\theta}_1, \\
c_{21} =& m_p S_\beta (L_b^2 C_\beta \dot{\alpha} + L_b l S_{\theta_2} \dot{\alpha} + L_b \dot{l} S_{\theta_1} C_{\theta_2} + L_b l C_{\theta_1} C_{\theta_2} \dot{\theta}_1 - L_b l S_{\theta_1} S_{\theta_2} \dot{\theta}_2), \\
c_{23} =& m_p L_b S_{\theta_1} C_{\theta_2} (S_\beta \dot{\alpha} + C_\beta \dot{\theta}_1) + m_p L_b (C_\beta S_{\theta_1} C_{\theta_2} \dot{\theta}_1 - S_\beta C_{\theta_2} \dot{\theta}_2 + C_\beta C_{\theta_1} S_{\theta_2} \dot{\theta}_2), \\
c_{24} =& m_p L_b l C_{\theta_1} C_{\theta_2} (S_\beta \dot{\alpha} + C_\beta \dot{\theta}_1) + m_p L_b C_\beta S_{\theta_1} (\dot{l} C_{\theta_2} - l S_{\theta_2} \dot{\theta}_2), \\
c_{25} =& - m_p L_b l S_\beta S_{\theta_1} S_{\theta_2} \dot{\alpha} - m_p L_b \dot{l} (S_\beta C_{\theta_2} + C_\beta C_{\theta_1} S_{\theta_2}) - m_p L_b l C_\beta S_{\theta_1} S_{\theta_2} \dot{\theta}_1 \\
& + m_p L_b l \dot{\theta}_2 (S_\beta S_{\theta_2} + C_\beta C_{\theta_1} S_{\theta_2}), \\
c_{31} =& m_p \dot{\alpha} (-l + l C_{\theta_1}^2 C_{\theta_2}^2 - L_b C_\beta S_{\theta_2}) - m_p L_b S_\beta S_{\theta_1} C_{\theta_2} \dot{\beta} - m_p l C_{\theta_1} S_{\theta_2} C_{\theta_2} \dot{\theta}_1 + m_p l S_{\theta_1} \dot{\theta}_2, \\
c_{32} =& m_p L_b (S_\beta C_{\theta_1} C_{\theta_2} \dot{\beta} - S_\beta S_{\theta_1} C_{\theta_2} \dot{\alpha} - C_\beta S_{\theta_2} \dot{\beta}), \\
c_{34} =& - m_p l (C_{\theta_2}^2 \dot{\theta}_1 + C_{\theta_1} S_{\theta_2} C_{\theta_2} \dot{\alpha}), \\
c_{35} =& m_p l (S_{\theta_1} \dot{\alpha} - \dot{\theta}_2), \\
c_{41} =& m_p C_{\theta_1} C_{\theta_2} (-l^2 S_{\theta_1} C_{\theta_2} \dot{\alpha} - L_b l S_\beta \dot{\beta} + l \dot{l} S_{\theta_2} + l^2 C_{\theta_2} \dot{\theta}_2), \\
c_{42} =& - m_p L_b l S_\beta C_{\theta_2} (C_{\theta_1} \dot{\alpha} + S_{\theta_1} \dot{\beta}), \\
c_{43} =& m_p l (C_{\theta_1} S_{\theta_2} C_{\theta_2} \dot{\alpha} + C_{\theta_2}^2 \dot{\theta}_1), \\
c_{44} =& m_p l \dot{l} C_{\theta_2}^2 - m_p l^2 S_{\theta_2} C_{\theta_2} \dot{\theta}_2, \\
c_{45} =& m_p l^2 (C_{\theta_1} C_{\theta_2}^2 \dot{\alpha} - S_{\theta_2} C_{\theta_2} \dot{\theta}_1), \\
c_{51} =& - m_p C_{\theta_2} \dot{\alpha} (L_b l C_\beta + l^2 C_{\theta_1}^2 S_{\theta_2}) + m_p S_{\theta_1} (L_b l S_\beta S_{\theta_2} \dot{\beta} - l \dot{l}) - m_p l^2 C_{\theta_1} C_{\theta_2}^2 \dot{\theta}_1, \\
c_{52} =& m_p L_b l (S_\beta S_{\theta_1} S_{\theta_2} \dot{\alpha} - C_\beta C_{\theta_2} \dot{\beta} - S_\beta C_{\theta_1} S_{\theta_2} \dot{\beta}), \\
c_{53} =& m_p l (-S_{\theta_1} \dot{\alpha} + \dot{\theta}_2), \\
c_{54} =& m_p l^2 (-C_{\theta_1} C_{\theta_2}^2 \dot{\alpha} + S_{\theta_2} C_{\theta_2} \dot{\theta}_1), \\
c_{55} =& m_p l \dot{l},
\end{aligned}
$$

in which m_p is the payload mass, and J_α and J_β are the inertias of the tower and the boom, respectively. The vector of generalized coordinates q and the input vector τ are respectively defined as $q = [\alpha\ \beta\ l\ \theta_1\ \theta_2]^T$ and $\tau = [\tau_\alpha\ \tau_\beta\ F_l\ 0\ 0]^T$.

In order to find the payload swing angle with respect to the earth coordinates frame, we express all the position vectors of the links and payload with respect to the frame $\{O_G x_G y_G z_G\}$, such that

$$\tilde{\mathbf{p}}_G^i = T_G^0 \tilde{\mathbf{p}}_0^i, \quad i = 1, 2, 3,$$

where $\tilde{\mathbf{p}}_G^i$ and $\tilde{\mathbf{p}}_0^i$ are the augmented vectors of homogeneous representation, i.e., $\tilde{\mathbf{p}}_G^i = [(\mathbf{p}_G^i)^T\ \ 1]^T$ and $\tilde{\mathbf{p}}_0^i = [(\mathbf{p}_0^i)^T\ \ 1]^T$. Then, we introduce the function of vector projection to the $x_N y_N$-plane as

$$\rho(\mathbf{p}_G^i) = [\mathbf{p}_G^i \cdot \hat{\mathbf{x}}_G \quad \mathbf{p}_G^i \cdot \hat{\mathbf{y}}_G \quad 0]^T,$$

where $\hat{\mathbf{x}}_G$ and $\hat{\mathbf{y}}_G$ are the unit vectors along x_G- and y_G-axes, respectively. Therefore, the projections of unit vectors in the radial and tangential directions of the boom motion to the $x_G y_G$-plane are respectively obtained as

$$\begin{aligned} \hat{\mathbf{r}} &= \frac{\rho(\mathbf{p}_G^2) - \rho(\mathbf{p}_G^1)}{\|\rho(\mathbf{p}_G^2) - \rho(\mathbf{p}_G^1)\|}, \\ \hat{\mathbf{t}} &= \hat{\mathbf{z}}_G \times \hat{\mathbf{r}}, \end{aligned}$$

where $\hat{\mathbf{z}}_G$ is the unit vectors along z_G-axis. Hence, the tangential pendulation and radial sway with respect to the earth coordinate frame $\{O_G x_G y_G z_G\}$ are respectively obtained as

$$\begin{cases} \delta_1 = \arctan \dfrac{(\mathbf{p}_G^3 - \mathbf{p}_G^2) \cdot \hat{\mathbf{t}}}{(\mathbf{p}_G^3 - \mathbf{p}_G^2) \cdot \hat{\mathbf{z}}_G}, \\ \delta_2 = \arcsin \dfrac{(\mathbf{p}_G^3 - \mathbf{p}_G^2) \cdot \hat{\mathbf{r}}}{l}. \end{cases} \tag{3.18}$$

We denote $\delta(q) = [\delta_1\ \delta_2]^T$ for the purpose of synthesizing the control algorithm.

3.5 Summary

The derivations of offshore gantry cranes and offshore boom cranes model have been presented. Based on the generalisation of system dynamics by using the Euler-Lagrange formulation, the offshore cranes model have been derived with full-scale system states with respect to the dimension of the systems. The linearisation of 2-D offshore gantry crane model has also been presented.

Chapter 4

Sliding Mode Control Approaches for Underactuated Mechanical Systems with Application to Cranes

4.1 Introduction

In this chapter, generic forms of sliding mode controllers for a class of underactuated mechanical systems (UMS) are proposed. Initially, the problem formulation which includes the trajectory tracking problem is presented. The basic formulation of the sliding mode control for UMS is introduced, by defining the sliding function as a linear combination of the actuated and unactuated position and velocity tracking errors. Firstly, an adaptive fuzzy sliding mode control law is proposed to deal with model uncertainties in the UMS. Secondly, a second-order sliding mode controller for UMS is designed in which an observer is utilised to estimate the system velocities. The performances of the proposed control laws are illustrated using gantry crane systems.

4.2 Problem formulation

Consider the Euler-Lagrange equation for UMS (2.3) with uncertainties in the following form:

$$M(q)\ddot{q} + \varphi(q,\dot{q}) + h(q,\dot{q}) = Eu, \tag{4.1}$$

with $q \in \mathbb{R}^n$, $u \in \mathbb{R}^m$, $M(q) \in \mathbb{R}^{n\times n}$, $\varphi(q,\dot{q}) = C(q,\dot{q}) + G(q) \in \mathbb{R}^n$, and $E = [I_m \ 0^T_{(n-m)\times m}]^T \in \mathbb{R}^{n\times m}$. The term $h(q,\dot{q}) \in \mathbb{R}^n$ is the vector of uncertainties in the system. Similarly, after partitioning the vector of generalized coordinates into

actuated and unactuated vectors, i.e. $q = [q_a^T \; q_u^T]^T$ with $q_a \in \mathbb{R}^m$ and $q_u \in \mathbb{R}^{n-m}$, (4.1) can be written as

$$M_{aa}(q)\ddot{q}_a + M_{au}(q)\ddot{q}_u + \varphi_a(\dot{q}, q) + h_a(\dot{q}, q) = u, \tag{4.2}$$

$$M_{au}^T(q)\ddot{q}_a + M_{uu}(q)\ddot{q}_u + \varphi_u(\dot{q}, q) + h_u(\dot{q}, q) = 0. \tag{4.3}$$

By substituting $\ddot{q}_u = -M_{uu}^{-1}(q)(M_{au}^T(q)\ddot{q}_a + \varphi_u(q, \dot{q}) + h_u(q, \dot{q}))$ obtained from (4.3) into (4.2), we get

$$\ddot{q}_a = \overline{\varphi}_a(q, \dot{q}) + \overline{h}_a(q, \dot{q}) + D_a(q)u, \tag{4.4}$$

where

$$\begin{aligned}
\overline{\varphi}_a(q, \dot{q}) &= -D_a^{-1}(q)\left(\varphi_a(q, \dot{q}) - M_{au}(q)M_{uu}^{-1}(q)\varphi_u(q, \dot{q})\right), \\
\overline{h}_a(q, \dot{q}) &= -D_a^{-1}(q)\left(h_a(q, \dot{q}) - M_{au}(q)M_{uu}^{-1}(q)h_u(q, \dot{q})\right), \\
D_a(q) &= \left(M_{aa}(q) - M_{au}(q)M_{uu}^{-1}(q)M_{au}^T(q)\right)^{-1}.
\end{aligned}$$

Consequently, it follows that

$$\ddot{q}_u = \overline{\varphi}_u(q, \dot{q}) + \overline{h}_u(q, \dot{q}) + D_u(q)u, \tag{4.5}$$

where

$$\begin{aligned}
\overline{\varphi}_u(q, \dot{q}) &= -M_{uu}^{-1}(q)\left(M_{au}^T(q)\overline{\varphi}_a(q, \dot{q}) + \varphi_u(q, \dot{q})\right), \\
\overline{h}_u(q, \dot{q}) &= -M_{uu}^{-1}(q)\left(M_{au}^T(q)\overline{h}_a(q, \dot{q}) + h_u(q, \dot{q})\right), \\
D_u(q) &= -M_{uu}^{-1}(q)M_{au}^T(q)D_a(q).
\end{aligned}$$

Let q^d denote the desired trajectory vector, with $q^d = [(q_a^d)^T \; (q_u^d)^T]^T$. Hence, the vector of trajectory tracking error is

$$e(t) = q - q^d = \begin{bmatrix} q_a - q_a^d \\ q_u - q_u^d \end{bmatrix} = \begin{bmatrix} e_a \\ e_u \end{bmatrix}. \tag{4.6}$$

The problem is to find suitable control strategies to drive the tracking error to zero subject to nonlinearity and uncertainty of the system.

4.3 First-order sliding mode control

The sliding functions can be defined as a weighted combination of position tracking error and velocity tracking error such that

$$s(t) = \Gamma\dot{e}(t) + \Lambda e(t) = \Gamma_a\dot{e}_a + \Gamma_u\dot{e}_u + \Lambda_a e_a + \Lambda_u e_u, \tag{4.7}$$

where $\Gamma = [\Gamma_a\ \Gamma_u]$ and $\Lambda = [\Lambda_a\ \Lambda_u]$, with $\Gamma_a, \Lambda_a \in \mathbb{R}^{m\times m}$ and $\Gamma_u, \Lambda_u \in \mathbb{R}^{m\times(n-m)}$. From (4.6), (4.7) can be written as

$$s(t) = \Gamma_a\dot{q}_a + \Gamma_u\dot{q}_u - \dot{q}^r, \tag{4.8}$$

where $\dot{q}^r = \Gamma_a\dot{q}_a^d + \Gamma_u\dot{q}_u^d - \Lambda_a e_a - \Lambda_u e_u$. Then the derivative of the sliding function is

$$\dot{s}(t) = \Gamma_a\ddot{q}_a + \Gamma_u\ddot{q}_u - \ddot{q}^r. \tag{4.9}$$

Substituting (4.4) and (4.5) into (4.9) yields

$$\dot{s}(t) = f(q,\dot{q}) + g(q)u - \ddot{q}^r + \overline{h}(q,\dot{q}), \tag{4.10}$$

where

$$\begin{aligned} f(q,\dot{q}) =& \Gamma_a\overline{\varphi}_a(q,\dot{q}) + \Gamma_u\overline{\varphi}_u(q,\dot{q}), \\ g(q) =& \Gamma_a D_a(q) + \Gamma_u D_u(q), \\ \overline{h}(q,\dot{q}) =& \Gamma_a\overline{h}_a(q,\dot{q}) + \Gamma_u\overline{h}_u(q,\dot{q}). \end{aligned}$$

We assume there exist a known positive scalar h_M such that $\|\overline{h}(q,\dot{q})\| \le h_M$. Thus, the 1-SMC law is proposed as

$$u = g^{-1}(q)\left[-f(q,\dot{q}) + \ddot{q}^r - \Phi s - (h_M + \eta)\,\mathrm{sign}\, s\right], \tag{4.11}$$

where $\Phi, \eta > 0$. To prove the stability of the system, choose the Lyapunov function candidate to be

$$V = \frac{1}{2}s(t)^T s(t).$$

Hence, the time derivative of V is

$$\begin{aligned}\dot{V} =& s^T(t)\dot{s}(t)\\ =& s^T(t)\left[f(q,\dot{q}) + g(q)u - \ddot{q}^r + \overline{h}(q,\dot{q})\right]\\ =& s^T(t)\left[\overline{h}(q,\dot{q}) - (h_M + \eta)\,\mathrm{sign}\, s - \Phi s\right]\\ \leq& - s^T\Phi s - \eta\|s(t)\|,\end{aligned}$$

which shows that sliding on the surface $s(t) = 0$ is attained in finite time.

4.4 Adaptive fuzzy sliding mode control

In this section, an adaptive fuzzy logic sliding mode control (AFSMC) is proposed for underactuated mechanical systems described in Section 4.2. The system dynamics subject to nonlinear frictions and disturbances are approximated with fuzzy logic. Based on the approximated functions of the system dynamics, the derivative of a sliding function in the form of (4.10) is composed and a fuzzy adaptive law for sliding mode controller is proposed. The adaptive law is designed based on the Lyapunov method. Besides, the stability of the closed-loop system is presented in the Lyapunov sense. The robust performance of the AFSMC is illustrated using a gantry crane system.

4.4.1 Fuzzy logic control

For a fuzzy logic controller with p inputs, $v_1, \ldots, v_j, \ldots, v_p$, and using the center of average defuzzification, it can be represented as

$$u = \frac{\sum_{k=1}^{l}\prod_{j=1}^{p}\mu_{F_j^k}(v_j)\theta_k}{\sum_{k=1}^{l}\prod_{j=1}^{p}\mu_{F_j^k}(v_j)}, \tag{4.12}$$

where l is the number of fuzzy rules, F_j^k is the jth fuzzy set corresponding to the kth fuzzy rule, and θ_k is the centroid of the kth fuzzy set corresponding to the

controller's output, u. By introducing regressor of kth fuzzy rule as

$$\zeta_k = \frac{\prod_{j=1}^{r} \mu_{F_j^k}(v_j)}{\sum_{k=1}^{l} \prod_{j=1}^{r} \mu_{F_j^k}(v_j)},$$

(4.12) can be written as

$$y = \sum_{k=1}^{l} \zeta_k \theta_k = \theta^T \zeta, \tag{4.13}$$

where $\theta = [\theta_1, \cdots, \theta_k, \cdots, \theta_l]^T$ and $\zeta = [\zeta_1, \cdots, \zeta_k, \cdots, \zeta_l]^T$. Now we consider the vector of the centroid of fuzzy sets as a function of time, that is,

$$\theta(t) = [\theta_1(t), \ldots, \theta_k(t), \ldots, \theta_l(t)]^T,$$

where $\dot{\theta}_k(t) = \omega_k(t)$, $k = 1, \ldots, l$. The function $\theta(t)$ can be ensured to lie between its lower bound $\underline{\theta}_k$ and upper bound $\overline{\theta}_k$, that is, $\underline{\theta}_k \leq \theta_k \leq \overline{\theta}_k$ by defining the following projection function:

$$\dot{\theta}_k(t) = \underset{\theta_k}{\text{proj}}(\omega_k) = \begin{cases} 0 & \text{if } \theta_k = \underline{\theta}_k \text{ and } \omega_k(t) < 0 \\ 0 & \text{if } \theta_k = \overline{\theta}_k \text{ and } \omega_k(t) > 0 \\ \omega_k(t) & \text{otherwise} \end{cases} \tag{4.14}$$

In the following, an AFSMC is proposed by using the notion introduced in this section.

4.4.2 Adaptive fuzzy sliding mode controller

Suppose that for $i = 1, \ldots, m$, the derivative of the sliding function (4.10) can be expressed as

$$\dot{s}_i = f_i(q, \dot{q}) + g_i(q, \dot{q}) u_i - \ddot{q}_i^r + \overline{h}_i(q, \dot{q}). \tag{4.15}$$

Here, we assume that $|\overline{h}_i(q, \dot{q})| \leq h_{M_i}$, $\forall i = 1, \ldots, m$, where $h_{M_i} > 0$ is known. It follows that, the sliding mode control (4.11) can be modified as

$$u_i = \frac{1}{g_i(\boldsymbol{x})}[-f_i(\boldsymbol{x}) - \Phi_i s_i + \ddot{q}_i^r] - K_i \operatorname{sign} s_i, \tag{4.16}$$

where $\boldsymbol{x} = [q^T \ \dot{q}^T]^T$. The first term on the right-hand side of (4.16) is the equivalent control which maintains the sliding motion on the sliding surface, and the second term is the switching control which forces the system trajectories towards the sliding surface. We now consider that the functions $f_i(\boldsymbol{x})$ and $g_i(\boldsymbol{x})$ are uncertain. Hence, we approximate $f_i(\boldsymbol{x})$ and $g_i(\boldsymbol{x})$ with fuzzy logic systems $\theta_{f_i}^T \xi_{f_i}$ and $\theta_{g_i}^T \xi_{g_i}$, respectively.

Let $\theta_{f_i}^*$ and $\theta_{g_i}^*$ be optimal vectors such that

$$\begin{cases} \theta_{f_i}^* = \underset{\theta_{f_i}}{\operatorname{argmin}} \sup_{\boldsymbol{x} \in \Omega} |f_i(\boldsymbol{x}) - \theta_{f_i}^T \xi_{f_i}(\boldsymbol{x})|, \\ \theta_{g_i}^* = \underset{\theta_{g_i}}{\operatorname{argmin}} \sup_{\boldsymbol{x} \in \Omega} |g_i(\boldsymbol{x}) - \theta_{g_i}^T \xi_{g_i}(\boldsymbol{x})|, \end{cases} \tag{4.17}$$

where $\Omega \subseteq \mathbb{R}^{2n}$ is a region to which the state $\boldsymbol{x}$ is constrained. We assume that

$$\begin{cases} |f_i(\boldsymbol{x}) - {\theta_{f_i}^*}^T \xi_{f_i}(\boldsymbol{x})| \leq d_{f_i}, \\ |g_i(\boldsymbol{x}) - {\theta_{g_i}^*}^T \xi_{g_i}(\boldsymbol{x})| \leq d_{g_i}, \end{cases} \quad \forall \boldsymbol{x} \in \Omega, \tag{4.18}$$

where $d_{f_i} > 0$ and $d_{g_i} > 0$, and each kth element of $\theta_{f_i}^*$ and $\theta_{g_i}^*$ is constant and bounded as follows:

$$\begin{cases} \underline{\theta}_{f_{i_k}} \leq \theta_{f_{i_k}}^* \leq \overline{\theta}_{f_{i_k}}, \\ \underline{\theta}_{g_{i_k}} \leq \theta_{g_{i_k}}^* \leq \overline{\theta}_{g_{i_k}}, \end{cases} \quad \forall k = 1, \ldots, l. \tag{4.19}$$

For the purpose of designing the sliding mode control, we choose the following adaptation laws:

$$\begin{cases} \dot{\theta}_{f_i} = \underset{\theta_{f_i}}{\operatorname{proj}}(\gamma_{f_i} s_i \xi_{f_i}), \\ \dot{\theta}_{g_i} = \underset{\theta_{g_i}}{\operatorname{proj}}(\gamma_{g_i} s_i \xi_{g_i} w_i), \end{cases} \tag{4.20}$$

where $\gamma_{f_i} > 0$ and $\gamma_{g_i} > 0$ are design parameters and

$$w_i = \frac{1}{\theta_{g_i}^T \xi_{g_i}} (-\theta_{f_i}^T \xi_{f_i} + \ddot{q}_i^r). \tag{4.21}$$

Then, we define the adaptation parameter errors δ_{f_i} and δ_{g_i} respectively as

$$\begin{cases} \delta_{f_i} = \theta_{f_i} - \theta_{f_i}^*, \\ \delta_{g_i} = \theta_{g_i} - \theta_{g_i}^*. \end{cases} \tag{4.22}$$

Since $\theta_{f_i}^*$ and $\theta_{g_i}^*$ are constants, and from (4.20), the time derivatives of the adaptation parameter errors are obtained as

$$\begin{cases} \dot{\delta}_{f_i} = \dot{\theta}_{f_i} = \underset{\theta_{f_i}}{\text{proj}}(\gamma_{f_i} s_i \xi_{f_i}), \\ \dot{\delta}_{g_i} = \dot{\theta}_{g_i} = \underset{\theta_{g_i}}{\text{proj}}(\gamma_{g_i} s_i \xi_{g_i} w_i). \end{cases} \tag{4.23}$$

Finally, by assuming that $g_i(q, \dot{q})$ has a positive lower bound, i.e., there exists a constant $\underline{g}_i$ such that $g_i(q, \dot{q}) \geq \underline{g}_i > 0$, $\forall i = 1, \ldots, m$, we propose the AFSMC as follows:

$$\begin{aligned} u_i &= w_i - \frac{1}{\underline{g}_i}\Phi_i s_i - K_i \operatorname{sign} s_i \\ &= \frac{1}{\theta_{g_i}^T \xi_{g_i}}(-\theta_{f_i}^T \xi_{f_i} + \ddot{q}_i^r) - \frac{1}{\underline{g}_i}\Phi_i s_i - K_i \operatorname{sign} s_i. \end{aligned} \tag{4.24}$$

4.4.3 Stability analysis

To prove the stability by means of control algorithm (4.24), we choose the following Lyapunov function candidate:

$$V = \frac{1}{2}\sum_{i=1}^{m}\left(s_i^2 + \frac{1}{\gamma_{f_i}}\delta_{f_i}^T\delta_{f_i} + \frac{1}{\gamma_{g_i}}\delta_{g_i}^T\delta_{g_i}\right).$$

Then, its time derivative is

$$\begin{aligned} \dot{V} &= \sum_{i=1}^{m}\left(s_i\dot{s}_i + \frac{1}{\gamma_{f_i}}\delta_{f_i}^T\dot{\delta}_{f_i} + \frac{1}{\gamma_{g_i}}\delta_{g_i}^T\dot{\delta}_{g_i}\right) \\ &= \sum_{i=1}^{m}\left(s_i(f_i + g_i u_i - \ddot{q}_i^r) + \frac{1}{\gamma_{f_i}}\delta_{f_i}^T\dot{\delta}_{f_i} + \frac{1}{\gamma_{g_i}}\delta_{g_i}^T\dot{\delta}_{g_i}\right). \end{aligned} \tag{4.25}$$

From (4.21), we have $\ddot{q}_i^r = \theta_{f_i}^T\xi_{f_i} + \theta_{g_i}^T\xi_{g_i}w_i$. Substituting this equation together with (4.23) and (4.24) into (4.25) yields

$$\begin{aligned} \dot{V} = \sum_{i=1}^{m}\Bigg[s_i\left(-\frac{g_i}{\underline{g}_i}\Phi_i s_i + (f_i - \theta_{f_i}^T\xi_{f_i}) + (g_i - \theta_{g_i}^T\xi_{g_i})w_i - g_i K_i \operatorname{sign} s_i\right) \\ + \frac{1}{\gamma_{f_i}}\delta_{f_i}^T \underset{\theta_{f_i}}{\text{proj}}(\gamma_{f_i} s_i \xi_{f_i}) + \frac{1}{\gamma_{g_i}}\delta_{g_i}^T \underset{\theta_{g_i}}{\text{proj}}(\gamma_{g_i} s_i \xi_{g_i} w_i)\Bigg]. \end{aligned} \tag{4.26}$$

From (4.18) and (4.22), (4.26) becomes

$$\begin{aligned}\dot{V} \leq \sum_{i=1}^{m} \Bigg[s_i \Bigg(-\frac{g_i}{\underline{g}_i}\Phi_i s_i - \delta_{f_i}^T \xi_{f_i} - \delta_{g_i}^T \xi_{g_i} w_i - g_i K_i \operatorname{sign} s_i \Bigg) \\ + \frac{1}{\gamma_{f_i}} \delta_{f_i}^T \operatorname*{proj}_{\theta_{f_i}} (\gamma_{f_i} s_i \xi_{f_i}) + \frac{1}{\gamma_{g_i}} \delta_{g_i}^T \operatorname*{proj}_{\theta_{g_i}} (\gamma_{g_i} s_i \xi_{g_i} w_i) \Bigg] \\ = \sum_{i=1}^{m} \Bigg[-\frac{g_i}{\underline{g}_i}\Phi_i s_i^2 - g_i K_i |s_i| + \delta_{f_i}^T \Bigg(\frac{1}{\gamma_{f_i}} \operatorname*{proj}_{\theta_{f_i}} (\gamma_{f_i} s_i \xi_{f_i}) - s_i \xi_{f_i} \Bigg) \\ + \delta_{g_i}^T \Bigg(\frac{1}{\gamma_{g_i}} \operatorname*{proj}_{\theta_{g_i}} (\gamma_{g_i} s_i \xi_{g_i} w_i) - s_i \xi_{g_i} w_i \Bigg) \Bigg]. \end{aligned} \tag{4.27}$$

From the definition of projection function (4.14), one can verify that

$$\begin{cases} \delta_{f_i}^T \left(\dfrac{1}{\gamma_{f_i}} \operatorname*{proj}_{\theta_{f_i}} (\gamma_{f_i} s_i \xi_{f_i}) - s_i \xi_{f_i} \right) \leq 0, \\ \delta_{g_i}^T \left(\dfrac{1}{\gamma_{g_i}} \operatorname*{proj}_{\theta_{g_i}} (\gamma_{g_i} s_i \xi_{g_i} w_i) - s_i \xi_{g_i} w_i \right) \leq 0, \end{cases}$$

By applying the above inequalities to (4.27), it gives

$$\begin{aligned} \dot{V} &\leq \sum_{i=1}^{m} \left(-\frac{g_i}{\underline{g}_i}\Phi_i s_i^2 - g_i K_i |s_i| \right) \\ &\leq \sum_{i=1}^{m} \left(-\frac{g_i}{\underline{g}_i}\Phi_i s_i^2 \right) \\ &\leq \sum_{i=1}^{m} (-\Phi_i s_i^2), \end{aligned}$$

since $g_i \geq \underline{g}_i$. Thus, it implies that the surface $s = 0$ is globally reached in a finite time.

4.4.4 Results and discussion

In this example, the adaptive fuzzy sliding mode control is applied to the two-dimensional gantry crane system as shown in Figure 4.1. The motion of the crane system is described in Figure 4.2, where x is the trolley position, ϕ is the swing angle of the hoisting rope, l is the rope length, M and m are the masses of the trolley and payload, respectively, and F_x is the trolley driving force. The crane dynamics is described by the following equation:

Figure 4.1 : Two-dimensional gantry crane system at UTS laboratory.

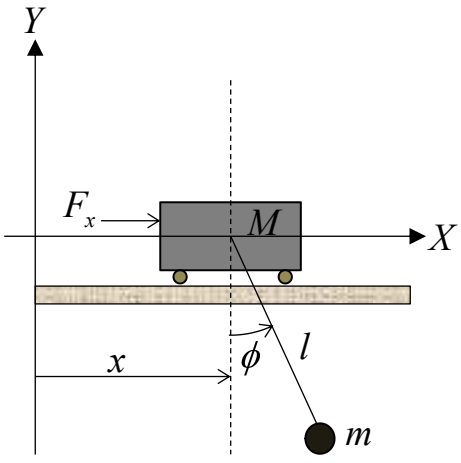

Figure 4.2 : Motion of the gantry crane system.

$$\begin{bmatrix} M+m & mlC_\phi \\ mlC_\phi & ml^2 \end{bmatrix} \begin{bmatrix} \ddot{x} \\ \ddot{\phi} \end{bmatrix} + \begin{bmatrix} -mlS_\phi \dot{x}\dot{\phi} + B_x\dot{x} + P_x \operatorname{sign}\dot{x} \\ mg_0 lS_\phi + B_\phi\dot{\phi} + P_\phi \operatorname{sign}\dot{\phi} \end{bmatrix} + \begin{bmatrix} d_x(t) \\ d_\phi(t) \end{bmatrix} = \begin{bmatrix} u \\ 0 \end{bmatrix}, \quad (4.28)$$

in which the vector of generalized coordinates is defined as $q = [q_a \; q_u]^T = [x \; \phi]^T$. In (4.28), g_0 is the gravitational acceleration, B_x and B_ϕ denote the viscous friction

coefficients, and P_x and P_ϕ denote the Coulomb friction coefficients associated with the trolley and rope sway motions, respectively.

The trajectory tracking problem consists of the positional control of the trolley while the sway angle must be suppressed to zero. Thus, the desired trajectory vector is defined as $q^d(t) = [q_a^d \;\; q_u^d]^T = [x^d(t)\; 0]^T$. Therefore, from (4.8), the sliding function is determined as

$$s(t) = \Gamma_a \dot{x} + \Gamma_u \dot{\phi} - \dot{q}^r(x, \phi)$$

where $\dot{q}^r(x, \phi) = (\Gamma_a \dot{x}^d(t) - \Lambda_a(x - x^d(t)) - \Lambda_u \phi)$. Then time derivative of the sliding function is

$$\dot{s}(t) = \Gamma_a \ddot{x} + \Gamma_u \ddot{\phi} - \ddot{q}^r(x, \phi)$$

which can be expressed in the form of

$$\dot{s}(t) = f(x, \phi, \dot{x}, \dot{\phi}) + g(x, \phi)u - \ddot{q}^r(x, \phi) + d(x, \phi, \dot{x}, \dot{\phi}).$$

By assuming that the functions $f(x, \phi, \dot{x}, \dot{\phi})$ and $g(x, \phi)$ are unknown apart from their bounds, we can propose the AFSMC, in which the control signal $u = F_x$ is defined as follows:

$$u = \frac{1}{\theta_g^T \xi_g}(-\theta_f^T \xi_f + \ddot{q}^r) - \frac{1}{\underline{g}} \Phi s - K \operatorname{sign} s, \tag{4.29}$$

where θ_f and θ_g are the vectors of the centroid of the membership functions and ξ_f and ξ_g are the corresponding regressor vectors, $\underline{g}$ is the known positive lower bound of $g(x, \phi)$, Φ is the positive design parameter, and K is the control gain.

In this work, we use adaptive fuzzy rules of the following form:

$$\text{Rule } k\text{: IF } s \text{ is } A^k \text{ AND } \dot{s} \text{ is } B^k, \text{ THEN } y = \theta_k$$

for $k = 1, \ldots, 12$, where $A^k = \{\mathrm{N}, \mathrm{P}\}$ and $B^k = \{\mathrm{LN}, \mathrm{N}, \mathrm{SN}, \mathrm{SP}, \mathrm{P}, \mathrm{LP}\}$ are the

linguistic variables. The membership functions are described as follows:

$$\mu_{\mathrm{P,N}}(s) = \min\left(1, \max\left(0, \frac{2 \pm s}{4}\right)\right),$$
$$\mu_{\mathrm{LP,LN}}(\dot{s}) = \min\left(1, \max\left(0, \frac{-1.5 \pm \dot{s}}{18.5}\right)\right),$$
$$\mu_{\mathrm{P,N}}(\dot{s}) = \min(0.5, \max(-0.5, -1 \pm \dot{s})) + \min\left(0.5, \max\left(-0.5, \frac{10.75 \pm \dot{s}}{18.5}\right)\right),$$
$$\mu_{\mathrm{SP,SN}}(\dot{s}) = \max(0, 1 - |\dot{s} \mp 0.5|).$$

The nominal values of the crane parameters are listed as $M = 2.70$ kg, $m = 2.24$ kg, $l = 0.795$ m, $g_0 = 9.8065$ m-s^{-2}, $B_x = 0.17$ N/m-s^{-1}, $B_\phi = 0.04$ N-m/rad-s^{-1}, $P_x = 0.90$ N, $P_\phi = 0.45$ N-m and the disturbances, are assumed bounded such that $|d_x(t)| \leq 10$ N and $|d_\phi(t)| \leq 20$ N-m. The controller parameters used are $\Gamma_a = 1$, $\Gamma_u = 0.5$, $\Lambda_a = 40$, $\Lambda_u = -10$, $\gamma_f = 5000$, $\gamma_g = 1000$, $\underline{g} = 1/(M + m)$, $\Phi = 250$, and $K = 100$. The bounds on the adaptation parameters are chosen as $\underline{\theta}_f = -200$, $\overline{\theta}_f = 200$, $\underline{\theta}_g = 50$, and $\overline{\theta}_g = 150$. The initial cart position is $(x_0, \phi_0) = (0 \text{ m}, 0.2 \text{ rad})$.

Figures 4.3(a) and (b) show the trolley position and sway angle responses without the presence of external disturbance. Figure 4.3(a) shows a good trajectory tracking, and Figure 4.3(b) shows the sway angle of the hoisting rope is suppressed from an initial value. The control effort for this corresponding case is shown in Figure 4.3(c).

Figure 4.4 shows the system responses and control effort with the presence of external disturbances. As can be seen in Figures 4.4(a) and 4.4(b), the proposed control system appears to be insensitive to the presence of the disturbances. However, higher control effort is required as shown in Figure 4.4(c).

The payload of the crane system consists of two steel blocks with 1.00 kg weight each and a carrier of 0.25 kg weight as shown in Figure 4.1. To demonstrate the robustness of the controller, the payload is varied between 1.00 kg to 2.25 kg, which

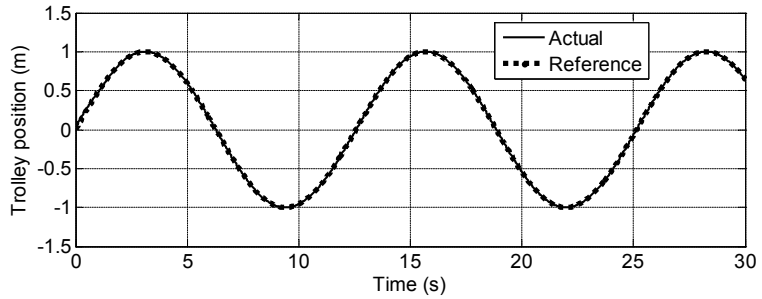

(a)

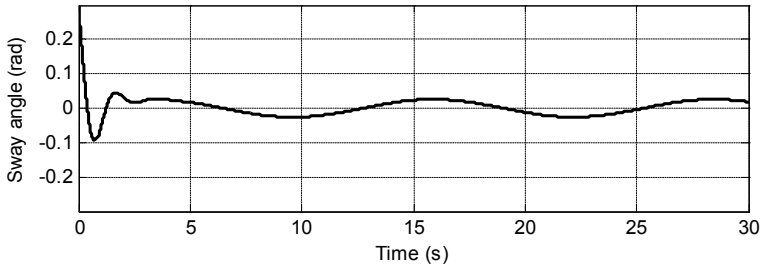

(b)

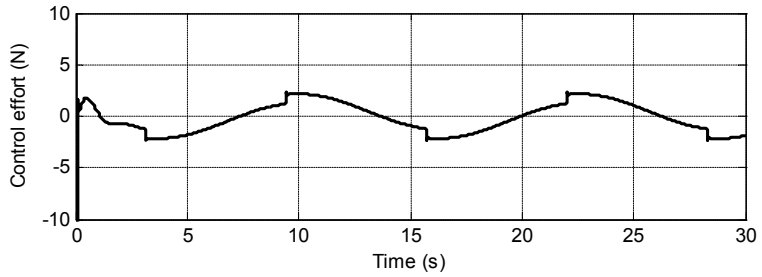

(c)

Figure 4.3 : (a) Trolley position; (b) Sway angle; and (c) Control effort; when $d_x = d_\phi = 0$.

reflects the process of loading/unloading of the gantry crane. From Figures 4.5(a) and 4.5(b), it is shown that the trajectory tracking of the trolley position and the sway angle of the hoisting rope are unperturbed by payload variations.

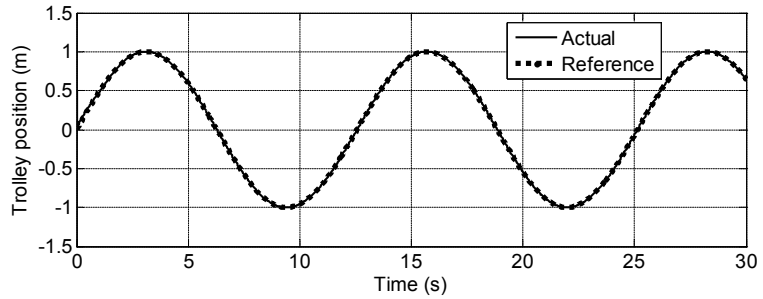

(a)

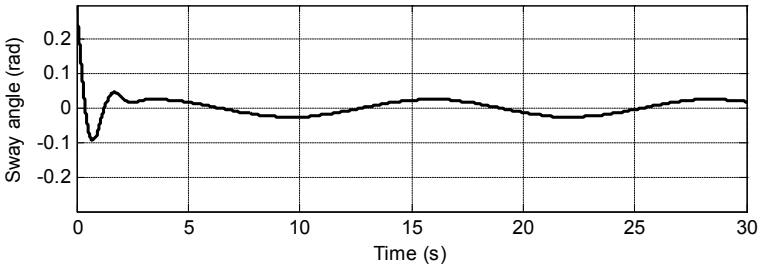

(b)

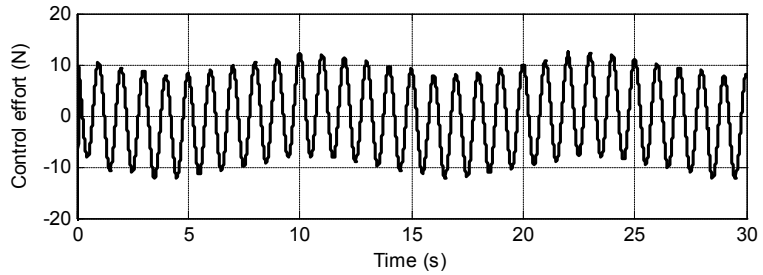

(c)

Figure 4.4 : (a) Trolley position; (b) Sway angle; and (c) Control effort; when $d_x \neq 0$ and $d_\phi \neq 0$.

4.5 Second-order sliding mode control

In this section, an observer-based control scheme based on the second-order sliding modes is proposed for underactuated systems described in Section 4.2, subject to modelling uncertainties, nonlinear frictions and disturbances. To remove the chattering effect, we consider higher-order sliding modes. Here, at first, a second-

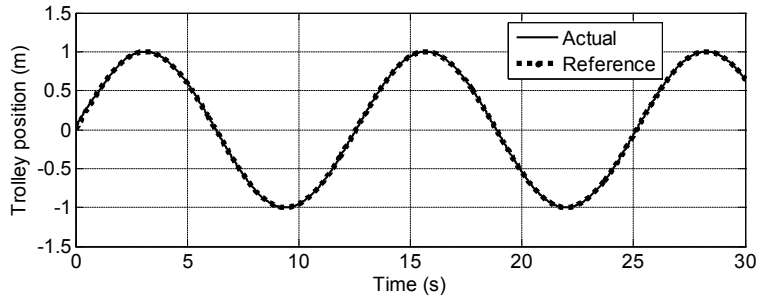

(a)

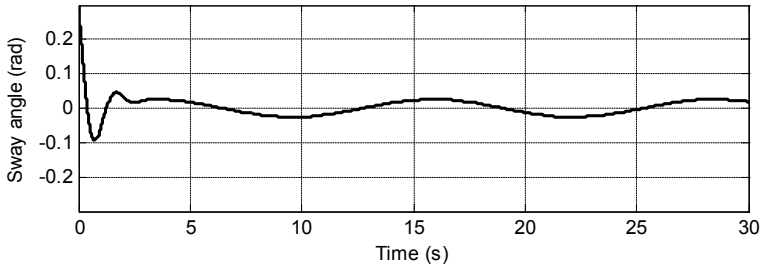

(b)

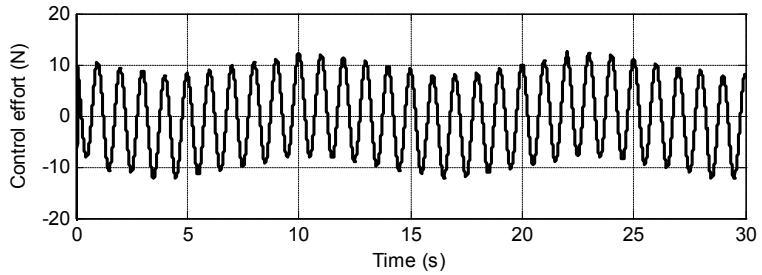

(c)

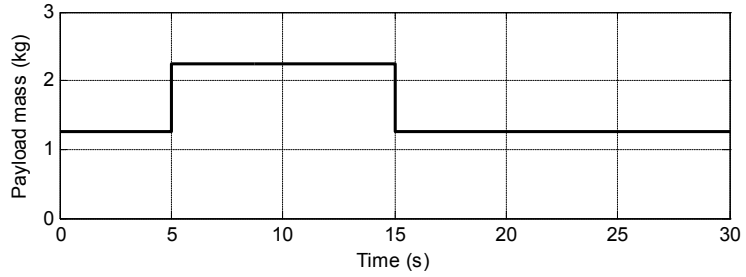

(d)

Figure 4.5 : (a) Trolley position; (b) Sway angle; (c) Control effort; and (d) Payload mass; when $d_x \neq 0$, $d_\phi \neq 0$, and the payload mass is varied.

order sliding mode observer is designed as the extension of [34] to estimate the velocities which are part of generalized vector coordinates of the system. Based on the measured outputs and estimated state variables, a 2-SMC is then proposed for trajectory tracking. The proposed observer-based controller is illustrated by using a 3-D gantry in the presence of Coulomb friction and high-frequency external disturbance.

4.5.1 Second-order sliding mode controller

Suppose that for $i = 1, \ldots, m$, the derivative of the sliding function in (4.10) can be expressed as

$$\dot{s}_i(t) = a_i(t, \boldsymbol{x}) + b_i(t, \boldsymbol{x})u_i, \tag{4.30}$$

where $\boldsymbol{x} = [q^T \ \dot{q}^T]^T$, $a_i(t, \boldsymbol{x}) = f_i(q, \dot{q}) - \ddot{q}_i^r + \overline{h}_i(q, \dot{q})$, and $b_i(t, \boldsymbol{x}) = g_i(q, \dot{q})$. It follows that, the second derivative of the sliding function is obtained in the form of

$$\ddot{s}_i(t) = a_i'(t, \boldsymbol{x}, u_i) + b(t, \boldsymbol{x})\dot{u}_i \tag{4.31}$$

where $a_i'(t, \boldsymbol{x}, u_i) = \dot{a}_i(t, \boldsymbol{x}) + \dot{b}_i(t, \boldsymbol{x})u_i$. Suppose that the following conditions

$$0 < K_{m_i} \leq b_i(t, \boldsymbol{x}) \leq K_{M_i}, \quad |a_{1i}(t, \boldsymbol{x}, u_i)| \leq C_{M_i} \tag{4.32}$$

hold globally for some K_{m_i}, K_{M_i}, $C_{M_i} > 0$. Let the super-twisting controller defined as [18, 19]

$$\begin{aligned} u_i(t) &= v_i(t) - \rho_i |s_i|^{\frac{1}{2}} \operatorname{sign} s_i, \\ \dot{v}_i(t) &= -\mu_i \operatorname{sign} s_i \end{aligned} \tag{4.33}$$

subject to the following sufficient condition

$$\mu_i > \frac{C_{M_i}}{K_{m_i}}, \quad \rho_i^2 > 2\frac{\mu_i K_{M_i} + C_{M_i}}{K_{m_i}}$$

can guarantee the finite time stability of the sliding manifold $\mathcal{S} = \{\boldsymbol{x} : \dot{s}(\boldsymbol{x}) = s(\boldsymbol{x}) = 0\}$. Then (4.31) and (4.33) imply the differential inclusion [112]

$$\ddot{s}_i(t) \in -[\mu_i K_{m_i} - C_{M_i}, \ \mu_i K_{M_i} + C_{M_i}] \operatorname{sign} s_i - \frac{\rho_i}{2}[K_{m_i}, K_{M_i}] \frac{\dot{s}_i}{|s_i|^{\frac{1}{2}}}.$$

4.5.2 Second-order sliding mode observer

Here, we use the same form of the sliding function in Section 4.3. For convenience, let renumber equations (4.7)-(4.10) as follows:

$$\begin{aligned} s(t) =& \Gamma_a \dot{e}_a + \Gamma_u \dot{e}_u + \Lambda_a e_a + \Lambda_u e_u && (4.34)\\ =& \Gamma_a \dot{q}_a + \Gamma_u \dot{q}_u - \dot{q}^r, && (4.35)\\ \dot{s}(t) =& \Gamma_a \ddot{q}_a + \Gamma_u \ddot{q}_u - \ddot{q}^r && (4.36)\\ =& f(q,\dot{q}) + g(q)u - \ddot{q}^r + \overline{h}(q,\dot{q}). && (4.37) \end{aligned}$$

To realise the sliding function in the form of (4.35), we require the availability of position and velocity. Here, we design a second-order sliding mode observer for system (4.1) subject to Coulomb frictions terms and uncertainties. Let us represent the system (4.1) in the following form:

$$M(q)\ddot{q} + C(q,\dot{q})\dot{q} + D\dot{q} + P(\dot{q}) + G(q) + d(t) = \tau, \tag{4.38}$$

where $D \in \mathbb{R}^{n\times n}$ is the matrix of viscous frictions, $P(\dot{q})$ is the vector of Coulomb frictions, and $d(t)$ is the vector of uncertainties. By letting $\boldsymbol{x} = [x_1^T \ x_2^T]^T$, where $x_1 = q$, $x_2 = \dot{q}$, (4.38) can be written in the state space form as follows:

$$\begin{aligned} \dot{x}_1 &= x_2 \\ \dot{x}_2 &= f(t,x_1,x_2,u) + \xi(t,x_1,x_2,u), \quad u = U(t,x_1,x_2), \end{aligned} \tag{4.39}$$

where the nominal part of the system dynamics is represented by the function

$$f(t,x_1,x_2,u) = -\hat{M}^{-1}(x_1)[\hat{C}(x_1,x_2)x_2 + \hat{D}x_2 + \hat{P}(x_2) + \hat{G}(x_1) - u],$$

containing the known nominal functions $\hat{M}$, $\hat{C}$, $\hat{D}$, $\hat{P}$ and $\hat{G}$. The uncertainties are lumped in the term $\xi(t,x_1,x_2,u)$. Thus, the super-twisting observer has the form of

$$\begin{aligned} \dot{\hat{x}}_1 &= \hat{x}_2 + w_1 \\ \dot{\hat{x}}_2 &= f(t,x_1,\hat{x}_2,u) + w_2, \end{aligned} \tag{4.40}$$

where $\hat{x}_1$ and $\hat{x}_2$ are the state estimates. The correction terms w_1 and w_2 are output injections of the form

$$\begin{aligned} w_1 &= \text{diag}\{\gamma_i\}\,\text{diag}\{|x_{1i} - \hat{x}_{1i}|^{\frac{1}{2}}\}\,\text{sign}(x_1 - \hat{x}_1) \\ w_2 &= \text{diag}\{\kappa_i\}\,\text{sign}(x_1 - \hat{x}_1), \end{aligned} \tag{4.41}$$

where $\kappa_i > 0$ and $\gamma_i > 0$, $i = 1, \ldots, n$. By taking $\tilde{x}_1 = x_1 - \hat{x}_1$ and $\tilde{x}_2 = x_2 - \hat{x}_2$, we obtain the error equations

$$\begin{aligned} \dot{\tilde{x}}_1 &= \tilde{x}_2 - \text{diag}\{\gamma_i\}\,\text{diag}\{|\tilde{x}_{1i}|^{\frac{1}{2}}\}\,\text{sign}\,\tilde{x}_1 \\ \dot{\tilde{x}}_2 &= \Psi(t, x_1, x_2, \hat{x}_2) - \text{diag}\{\kappa_i\}\tilde{x}_1, \end{aligned} \tag{4.42}$$

where

$$\begin{aligned} \Psi(t, x_1, x_2, \hat{x}_2) =& f(t, x_1, x_2, U(t, x_1, x_2)) - f(t, x_1, \hat{x}_2, U(t, x_1, x_2)) \\ &+ \xi(t, x_1, x_2, U(t, x_1, x_2)). \end{aligned}$$

Suppose that the system states are bounded, then the convergence of observer error system (4.42) is ensured if there exists constant $\Psi_{M_i} > 0$ such that the inequality

$$|\Psi_i(t, x_1, x_2, \hat{x}_2)| < \Psi_{M_i}$$

holds for any possible t, x_1, x_2 and $|\hat{x}_2| \leq 2\sup|x_2|$ [85]. Thus the proposed velocity observer has the form

$$\begin{aligned} \dot{\hat{x}}_1 =& \hat{x}_2 + \text{diag}\{\gamma_i\}\,\text{diag}\{|x_{1i} - \hat{x}_{1i}|^{\frac{1}{2}}\}\,\text{sign}(x_1 - \hat{x}_1) \\ \dot{\hat{x}}_2 =& -\hat{M}^{-1}(x_1)\left[\hat{C}(x_1, \hat{x}_2)\hat{x}_2 + \hat{D}\hat{x}_2 + \hat{G}(x_1) - \tau\right] \\ &+ \text{diag}\{\kappa_i\}\,\text{sign}(x_1 - \hat{x}_1). \end{aligned} \tag{4.43}$$

According to [84], the values of the constants are chosen as $\gamma_i = 1.5(\Psi_{M_i})^{\frac{1}{2}}$ and $\kappa_i = 1.1\Psi_{M_i}$, $\forall i = 1, \ldots, n$. Finally, estimates of the state vector and state vector error are respectively obtained by

$$\hat{\boldsymbol{x}} = \begin{bmatrix} x_1 \\ \hat{x}_2 \end{bmatrix} \quad \text{and} \quad \hat{\boldsymbol{e}} = \hat{\boldsymbol{x}} - \boldsymbol{x}^d = \begin{bmatrix} e_1 \\ \hat{e}_2 \end{bmatrix},$$

The measured and estimated state vector error can be partitioned further into actuated and unactuated parts as

$$e_1 = \begin{bmatrix} e_{1a} \\ e_{1u} \end{bmatrix}, \quad \hat{e}_2 = \begin{bmatrix} \hat{e}_{2a} \\ \hat{e}_{2u} \end{bmatrix}.$$

4.5.3 Observer-based 2-SMC

The control objective is to drive the vector $q(t)$ to the desired position $q^d(t)$. Based on the observer (4.43) and the sliding function (4.34), an observer-based sliding function is proposed as follows:

$$\hat{s}(t) = \Gamma_a \hat{e}_{2a}(t) + \Gamma_u \hat{e}_{2u}(t) + \Lambda_a e_{1a}(t) + \Lambda_u e_{1u}(t). \tag{4.44}$$

Hence, the super-twisting controller (4.33) becomes as proposed:

$$\begin{aligned} \hat{u}(t) &= \hat{v}(t) - \operatorname{diag}\{\rho_j\} \operatorname{diag}\{|\hat{s}_j|^{\frac{1}{2}}\} \operatorname{sign} \hat{s}(t), \\ \dot{\hat{v}}(t) &= - \operatorname{diag}\{\mu_j\} \operatorname{sign} \hat{s}(t) \end{aligned} \tag{4.45}$$

where $j = 1, \ldots, m$, and the sliding estimate $\hat{s}$ is used in lieu of s.

4.5.4 Results and discussion

In this example, the observer-based 2-SMC is applied to the bidirectional gantry crane as shown in Figure 4.6. In order to implement a control strategy to a crane system, position and velocity measurements must be available. In the case of a gantry crane, velocity sensors may not be ready because of the cost, volume and weight of the sensors [5, 60]. In practice, for the 3D overhead crane with a constant rope length, the motion is driven by two dc motors such that both rail and cart are capable of positioning horizontally in the X-direction while the cart is capable of positioning horizontally along the rail in the Y-direction. Thus, there are four incremental encoders measuring four state variables, i.e., the cart's x and y coordinates on the horizontal plane, and two deviation angles θ_x and θ_y of the payload

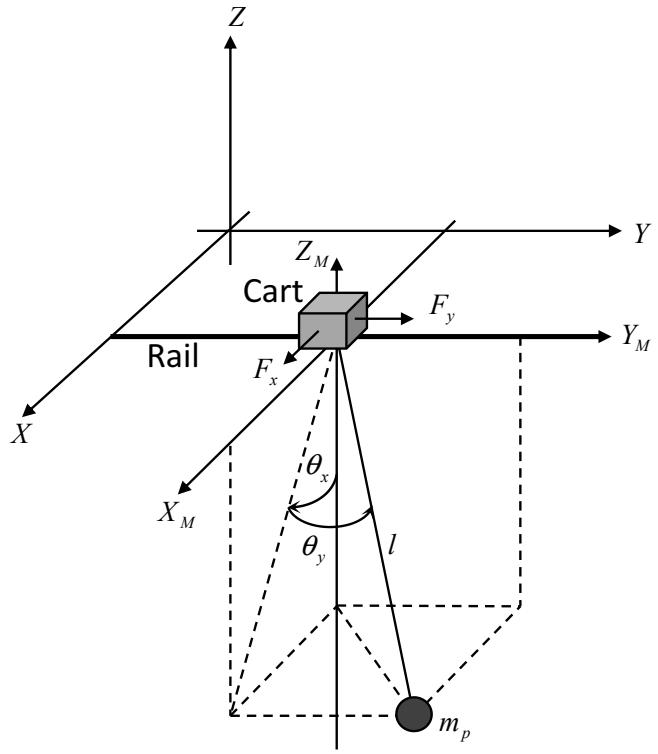

Figure 4.6 : Motion of a 3D overhead gantry crane.

(refer Figure 4.6). Based on the available position measurements, we implement the second-order sliding mode velocity observer. The block diagram, shown in Figure 4.7, indicates the relationship between the second-order sliding mode observer (2-SMO) and the second-order sliding mode controller (2-SMC) using the estimated sliding function $\hat{s} = \sigma(e_1, \hat{e}_2)$.

For the 3D overhead gantry crane system of Figure 4.6, where $n = 4$, $m = 2$, the matrices $M(q)$, $C(q, \dot{q})$, $G(q)$, $P(\dot{q})$ and D are:

$$M(q) = \begin{bmatrix} M_x + m_p & 0 & m_p l C_{\theta_x} C_{\theta_y} & -m_p l S_{\theta_x} S_{\theta_y} \\ 0 & M_y + m_p & 0 & m_p l C_{\theta_y} \\ m_p l C_{\theta_x} C_{\theta_y} & 0 & m_p l^2 C_{\theta_y}^2 & 0 \\ -m_p l S_{\theta_x} S_{\theta_y} & m_p l C_{\theta_y} & 0 & m_p l^2 \end{bmatrix},$$

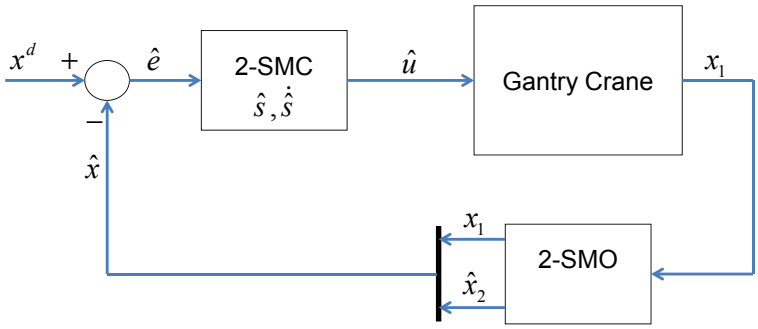

Figure 4.7 : Schematic diagram of the observer-based control using second-order sliding modes for an underactuated mechanical system.

$$C(q,\dot{q}) = \begin{bmatrix} 0 & 0 & -m_p l S_{\theta_x} C_{\theta_y} \dot{\theta}_x & -m_p l (C_{\theta_x} S_{\theta_y} \dot{\theta}_x + S_{\theta_x} C_{\theta_y} \dot{\theta}_y) \\ 0 & 0 & 0 & -m_p l S_{\theta_y} \dot{\theta}_y \\ 0 & 0 & -m_p l^2 S_{\theta_y} C_{\theta_y} \dot{\theta}_y & -m_p l^2 S_{\theta_y} C_{\theta_y} \dot{\theta}_x \\ 0 & 0 & m_p l^2 S_{\theta_y} C_{\theta_y} \dot{\theta}_x & 0 \end{bmatrix},$$

$$G(q) = m_p g l [0 \;\; 0 \;\; S_{\theta_x} C_{\theta_y} \;\; C_{\theta_x} S_{\theta_y}]^T,$$

$$D = \mathrm{diag}(D_x, D_y, 0, 0),$$

$$P(\dot{q}) = [P_x \,\mathrm{sign}\, \dot{x} \;\; P_y \,\mathrm{sign}\, \dot{y} \;\; 0 \;\; 0]^T,$$

where x and y are the cart position respectively in X- and Y-directions, θ_x and θ_y are the swing angle projection respectively onto the $Y_M Z_M$- and $X_M Z_M$-planes, M_x, M_y and m_p are the X- and Y-component masses of the crane and payload, respectively, l is the rope length, F_x and F_y are the cart's driving force respectively in X- and Y-directions, and g is the gravitational acceleration. D_x and D_y denote the viscous friction coefficients and P_x and P_y denote the Coulomb friction coefficients associated with the X- and Y-directions of motion, respectively. The state vector $q = [q_a^T \; q_u^T]^T$ and the control vector τ, are respectively defined as

$$q(t) = [x \;\; y \;\; \theta_x \;\; \theta_y]^T, \quad \tau = [F_x \;\; F_y \;\; 0 \;\; 0]^T,$$

where the actuated and unactuated state vectors from partitioning $q(t)$ are respec-

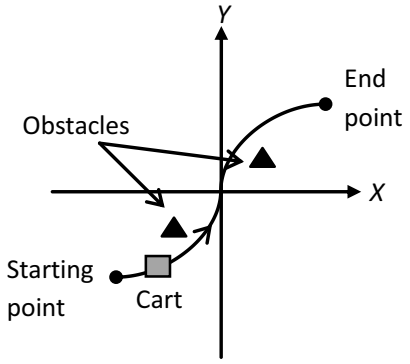

Figure 4.8 : Sigmoid function trajectory.

tively $q_a = [x\ y]^T$ and $q_u = [\theta_x\ \theta_y]^T$. Since the cart position is required to track a specific trajectory, let the vectors of desired position and swing angle respectively be

$$q_a^d(t) = [x^d(t)\ y^d(t)]^T, \quad q_u^d(t) = [0\ 0]^T,$$

such that $q^d(t) = [q_a^d(t)^T\ q_u^d(t)^T]^T$. Hence, from (4.6), the tracking errors of the cart position and rope swing angle respectively become

$$e_a(t) = q_a(t) - q_a^d(t), \quad e_u(t) = q_u(t).$$

Let the pre-specified trajectory shown in Figure 4.8 be defined as

$$x^d(t) = \frac{1}{3}t - 1,\ y^d(t) = \tanh(3x^d(t)), \quad 0 \le t \le 6. \tag{4.46}$$

We also denote

$$\boldsymbol{x}_1 = [x_1\ y_1\ \theta_{x1}\ \theta_{y1}]^T,\ \boldsymbol{x}_2 = [x_2\ y_2\ \theta_{x2}\ \theta_{y2}]^T,$$

where subscript 1 is used for the positions or angles and subscript 2 for the prismatic velocities or angular velocities. This trajectory tracking problem is to ensure the cart to track the specific path described by (4.46), for example, to avoid obstacles in a real situation. In this study the values of the crane parameters are listed as $M_x = 7.46$

kg, $M_y = 6.4$ kg, $m_p = 0.73$ kg, $l = 0.7$ m, and $g = 9.8065$ m-s^{-2}, $D_x = 0.17$ N/m-s^{-1}, $D_y = 0.04$ N/m-s^{-1}, $P_x = 0.90$ N, $P_y = 0.45$ N and the uncertain external perturbation, designated as high frequency noise, is assumed bounded such that $|d_i(t)| \leq 10$ N, $i = 1, \ldots, 4$. The controller parameters used in the simulations are $\text{diag}(\mu_1, \mu_2) = \text{diag}(30, 30)$, $\text{diag}(\rho_1, \rho_2) = \text{diag}(15, 15)$, $\Gamma_a = I_2$, $\Gamma_u = \text{diag}(0.1, 0.1)$, $\Lambda_a = \text{diag}(10, 10)$, and $\Lambda_u = \text{diag}(-1, -1)$. The nominal parameters for observer are $\hat{M}_x = 7$ kg, $\hat{M}_y = 6$ kg, $\hat{m}_p = 1$ kg, $\hat{l} = 0.75$ m, $\hat{D}_x = 0.15$ N/m-s^{-1}, $\hat{D}_y = 0.05$ N/m-s^{-1}, $\hat{P}_x = 0.1$ N, and $\hat{P}_y = 0.5$ N, where it is assumed that the real parameters differ from the nominal values by not more than 10%. Here, $\Psi_{M_i} = 60$, $\forall i = 1, \ldots, 4$. The initial cart position is $(x_0, y_0) = (-1, -1)$.

Figure 4.9(a) shows the cart position respectively in X- and Y-directions, and Figure 4.9(b) shows the actual and desired trajectories. Figure 4.10 shows the tracking errors of cart position, in which, it is exhibited that the magnitude and frequency of sway angles are greatly suppressed during the motion and at the mo-

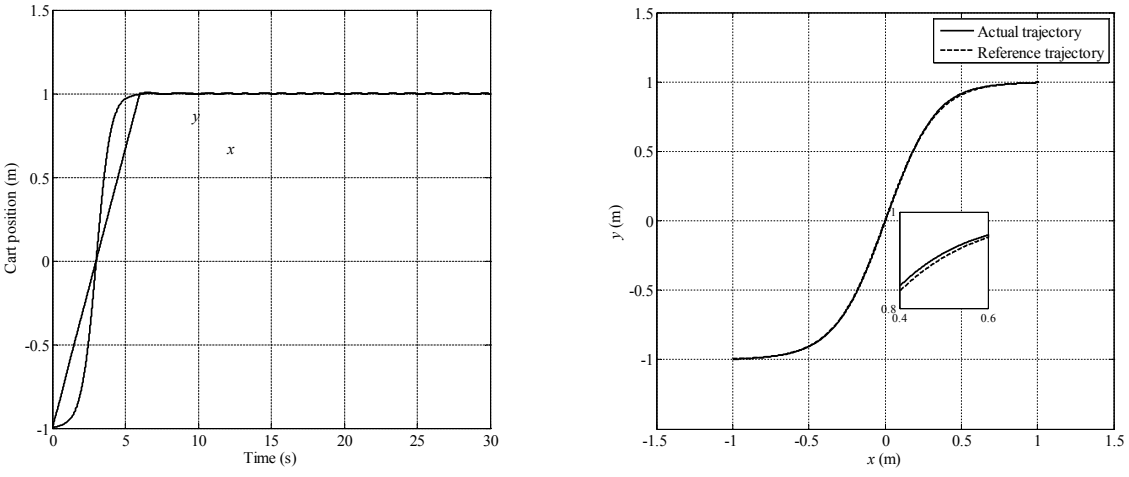

(a) (b)

Figure 4.9 : (a) Cart position in X- and Y-directions; (b) Actual and reference trajectories.

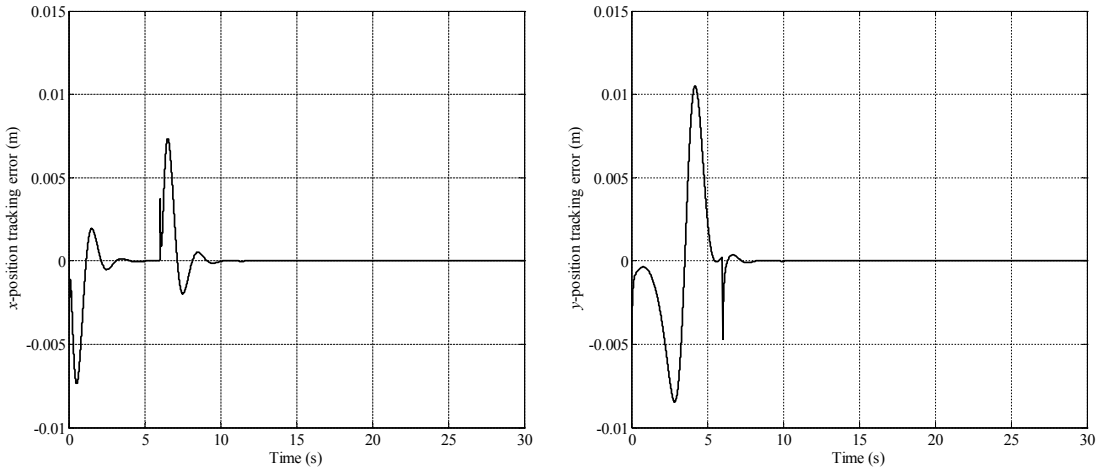

(a) (b)

Figure 4.10 : Trajectory tracking error in (a) X-direction; and (b) Y-direction.

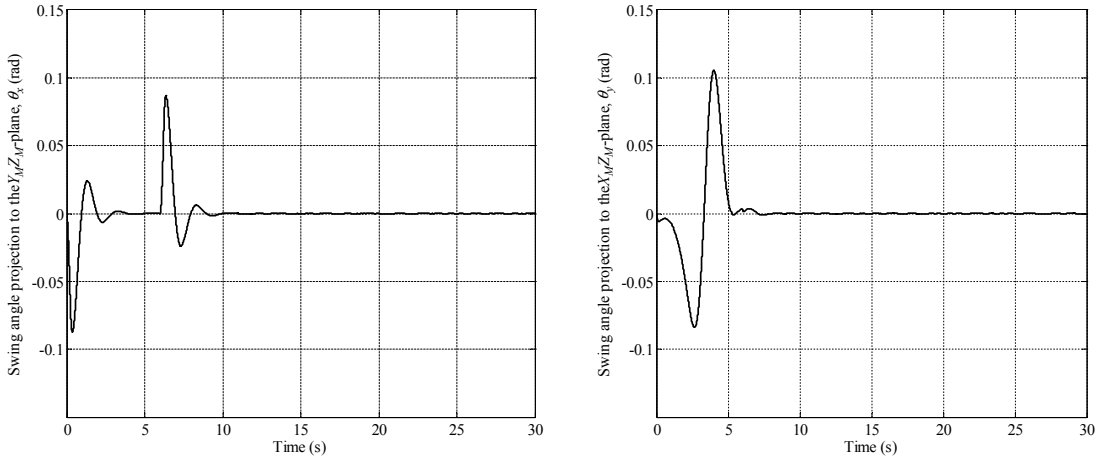

(a) (b)

Figure 4.11 : Swing angle projection to the (a) $Y_M Z_M$-plane; and (b) $X_M Z_M$-plane.

tion end point. The swing angle projections to the $Y_M Z_M$- and $X_M Z_M$-planes are shown in Figure 4.11. The proposed control system appears to be insensitive to the presence of high frequency noise $d(t)$, which demonstrates robustness of the proposed 2-SMO. Figure 4.12 shows the finite-time convergence of the estimated

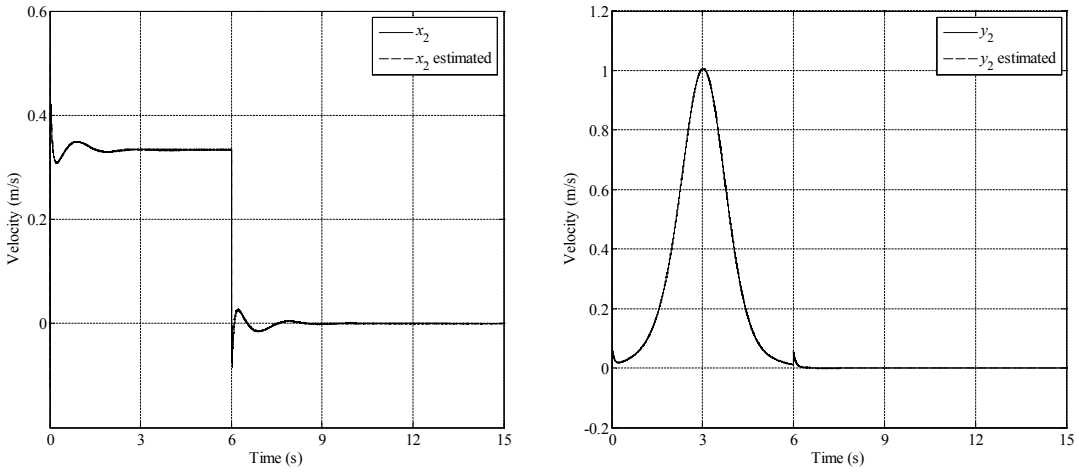

(a) (b)

Figure 4.12 : Real and estimated cart velocities in (a) X-direction; and (b) Y-direction.

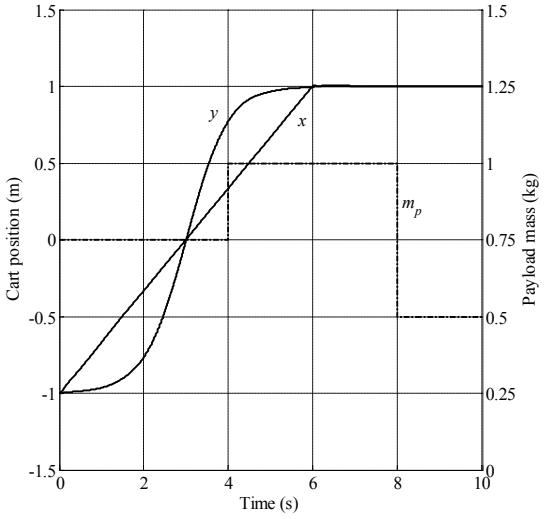

Figure 4.13 : Cart position with payload variation.

velocities in X- and Y-directions to their actual ones over 15 s time duration. Apart from its transient state, the observer produces accurate estimate velocities. For the sake of simulation, arbitrary initial values of velocities have been selected since the

actual initial velocities are unknown. Yet, the estimated velocities have been successfully convergent to the actual measurements from any arbitrary initial values of the observer. To demonstrate the robustness of the controller, the payload is varied between 0.5 to 1 kg, which reflects the process of loading/unloading of the gantry crane. From Figure 4.13, it is shown that the trajectory tracking is unperturbed by the presence of payload variation. It is worth noting that the selection of greater values for the entries of matrix Λ_a will reduce the overshoot but will increase the amplitude of swing angle in the steady state.

4.6 Summary

This chapter has addressed the sliding mode control algorithms for UMS. Firstly, we have proposed an AFSMC for trajectory tracking for a class of UMS. The system dynamic is approximated by using fuzzy model. Then, a sliding function is composed based on the approximated functions of the system dynamics. The adaptive law for the sliding mode control is designed based on the Lyapunov method. The performance of the AFSMC is evaluated by applying the controller to a gantry crane system in the presence of nonlinear frictions. A robust control performance is obtained when the system is subject to external disturbances and parameter variations.

Secondly, we have proposed an observer-based control scheme for trajectory tracking for a class of UMS. The development is based on the second-order sliding mode methodology. The sliding mode observer and then observer-based sliding mode controller are designed to track the pre-specified trajectory based on information of the output positions. The sliding function is constructed from the actual and estimate states. The explicit dependence of the sliding function on the swing angles guarantees zero-swing at the end of transportation as well as the sway angle suppression during the load movement. A robust control performance is obtained

when the system is subject to parametric uncertainties and nonlinear frictions. The 2-SMC scheme is applied to a 3-D gantry crane to demonstrate the efficacy of the proposed method.

Chapter 5

Development of First-order Sliding Mode Control for Offshore Crane Systems

5.1 Introduction

This chapter addresses the problem of robust sliding mode control for 2-D offshore gantry crane and boom crane systems in which their dynamics have been developed in Chapter 3. The linear quadratic regulator (LQR) and linear matrix inequality (LMI) design approaches are utilised to obtain the sliding surface. Robust sliding mode controllers are proposed to track the desired trajectory of the crane systems. Extensive simulation results are given to illustrate the feasibility of the proposed approach, in terms of reducing the effects of disturbances and uncertainties in some practical scenarios coming from the occurrence of strong waves and winds in the open-sea.

5.2 Problem statement

Our objective is to obtain an error dynamics of the offshore crane systems trajectory tracking problems. The 2-D offshore gantry crane and boom crane dynamics are represented by uncertain LTI systems in the form of equations (3.11) and (3.16), respectively. Since both equations have the same form, for convenience, let renumber the equations as follows:

$$\dot{x}(t) = (A + \Delta A(t))x(t) + Bu(t) + D\omega(t). \tag{5.1}$$

It should be noticed that when in the sliding mode, a system completely rejects any signals which satisfy the matching conditions. The inclusion of a tracking require-

ment is thus nontrivial and must always be achieved in such a way as to ensure that the command is not wholly or partly rejected by the sliding system. For this purpose, a reference model is constructed which represents the ideal model of the corresponding LTI system [44, 136].

Let us consider a reference model as follows:

$$\dot{x}_d(t) = A_d x_d(t) + B_d r_d(t), \tag{5.2}$$

where $x_d(t)$ and $r_d(t) \in \mathbb{R}^2$ is the bounded reference input. Matrices A_d and B_d are assumed to satisfy the following matching condition:

$$BK = A_d - A, \quad BN = B_d, \tag{5.3}$$

where matrices K and N are of appropriate dimensions. Let us define the tracking error x_e as the difference between the plant and the reference model states:

$$x_e(t) = x(t) - x_d(t).$$

From (5.1) and (5.2), the following error dynamic system can be obtained as,

$$\begin{aligned} \dot{x}_e(t) =& A_d x_e(t) + (A - A_d)x(t) + \Delta A(t)x(t) + Bu(t) \\ & - B_d r_d(t) + D\omega(t). \end{aligned} \tag{5.4}$$

Without loss of generality, the system disturbances $\Delta A(t)$ and $\omega(t)$ are assumed to be norm-bounded, i.e.,

$$\|\Delta A(t)\| \leq \mu, \quad \|\omega(t)\| \leq \omega_p, \tag{5.5}$$

where μ and ω_p are known positive scalars.

The tracking problem is constituted in finding a control action by using 1-SMC guaranteeing that $\lim_{t\to\infty} x_e(t) = 0$.

5.3 Control design for 2-D offshore gantry crane

In this section, a 1-SMC scheme is proposed to deal with the problem of trajectory tracking for offshore crane system developed in Section 3.3.1. A desired sliding surface is obtained by utilizing the linear quadratic regulator (LQR) design approach. A robust sliding mode controller is proposed to track an optimal trajectory of the crane system during load transfer.

5.3.1 Crane trajectory

The optimal crane trajectory is formulated to minimize the payload residual sway at end points of the cart's motion [64]. For that purpose, a trapezoidal velocity pattern is chosen for the cart's motion and two reference points of the rope length, namely the lower and upper positions, l_D and l_U, are defined. Details of the optimal crane trajectory during container transfer operations are described as follows:

Stage 1 (*Picking up the container with time* t_1): The hoisting rope length decreases from l_D, where the container is on the deck of the mother ship, to l_U where the container is in the upper position, with a maximum lateral velocity v_R. Thus, we have

$$t_1 = \frac{2(l_D - l_U)}{v_R}.$$

It should be noted that the rope length l_D and l_U are assumed to be constant among different containers.

Stage 2 (*Moving the container with a maximum longitudinal velocity* v_y): Assuming the whole distance of travel of lifting, moving and placing the container is y_F with the corresponding time t_F, the moving phase then will take $(t_F - 2t_1)$ in time.

Stage 3 (*Placing the container on the smaller ship with time* t_1): The rope length increases from l_U to l_D. This is the reverse process for lifting the container.

Let $y_d(t)$ and $l_d(t)$ denote the desired trajectories of the cart position and rope length, respectively. The trajectory diagrams are shown in Figure 5.1 and Figure 5.2, from which $y_d(t)$ and $l_d(t)$ are derived from given parameters l_D, l_U, v_R, v_y and y_F as

$$y_d(t) = \begin{cases} \frac{1}{2}at^2, & 0 \le t \le t_1, \\ v_y t - v_y \frac{t_1}{2}, & t_1 < t \le t_2, \\ -\frac{1}{2}at^2 + v_y \frac{t_F}{t_1} t + y_F - \frac{1}{2}at_F^2, & t_2 < t \le t_F, \end{cases}$$

$$\dot{y}_d(t) = \begin{cases} at, & 0 \le t \le t_1, \\ v_y, & t_1 < t \le t_2, \\ -at + v_y \frac{t_F}{t_1}, & t_2 < t \le t_F, \end{cases}$$

where $a = \frac{v_y}{t_1}$ and $t_2 = t_F - t_1$. Similarly, desired trajectories of the rope length and its rate of change are, respectively,

$$l_d(t) = \begin{cases} -\frac{1}{2}bt^2 + l_D, & 0 \le t \le \frac{t_1}{2}, \\ \frac{1}{2}bt^2 - 2v_R t + v_R t_1 + l_U, & \frac{t_1}{2} < t \le t_1, \\ l_U, & t_1 < t \le t_2, \\ \frac{1}{2}bt^2 - bt_2 t + \frac{v_R}{t_1} t_2^2 + l_U, & t_2 < t \le t_F - \frac{t_1}{2}, \\ -\frac{1}{2}bt^2 + bt_F t - \frac{1}{2}bt_F^2 + l_D, & t_F - \frac{t_1}{2} < t \le t_F, \end{cases}$$

$$\dot{l}_d(t) = \begin{cases} -bt, & 0 \le t \le \frac{t_1}{2}, \\ bt - bt_1, & \frac{t_1}{2} < t \le t_1, \\ 0, & t_1 < t \le t_2, \\ bt - bt_2, & t_2 < t \le t_F - \frac{t_1}{2}, \\ -bt + bt_F, & t_F - \frac{t_1}{2} < t \le t_F, \end{cases}$$

where $b = \frac{2v_R}{t_1}$. As described in the previous section, θ is the swing angle with respect to the vessel's coordinates frame. Obviously, θ should be kept at zero if the

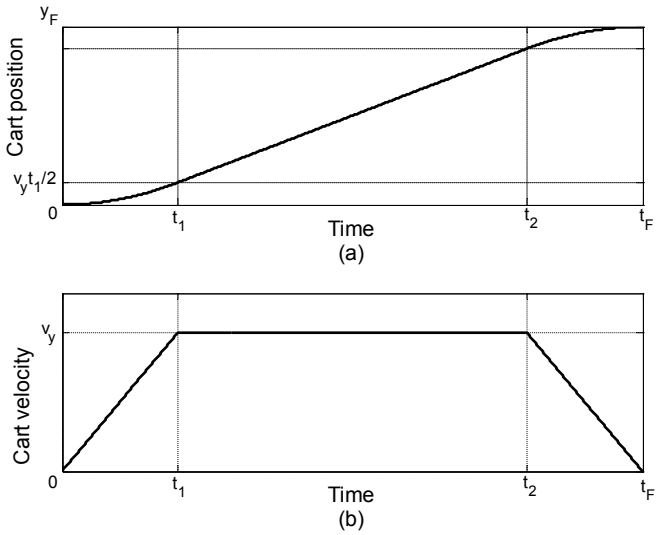

Figure 5.1 : Cart position and velocity reference trajectories.

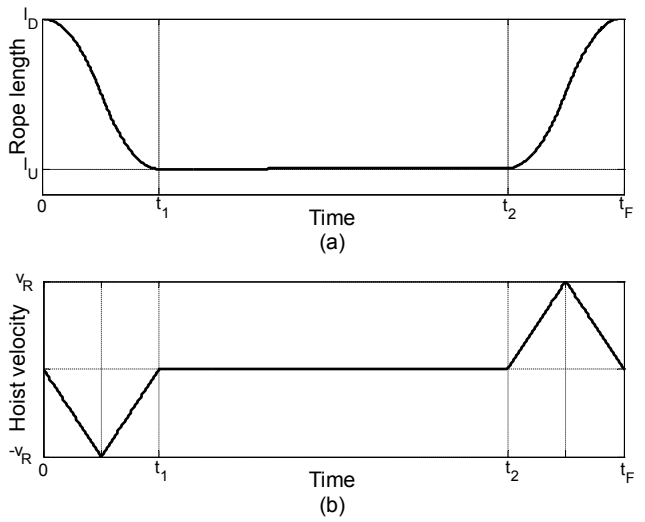

Figure 5.2 : Hoisting rope length and velocity reference trajectories.

vessel is stationary. However, due the to wave-induced motion of the vessel, it can be shown that if the swing angle tracks the roll angle of the vessel $\phi(t)$ during the operation process, the payload will be held on the vertical plane in the ground's coordinate frame. Therefore, the desired payload swing angle trajectory is chosen as $\theta_d(t) = \phi(t)$.

In the following, the desired trajectory for the rope length is denoted as $\Delta l_d(t) = l_d(t) - L$ for the trajectory tracking process. Thus, the state vector of the reference model (5.2) can be defined as $x_d(t) = [y_d \ \Delta l_d \ \theta_d \ \dot{y}_d \ \dot{l}_d \ \dot{\theta}_d]^T$ We are now ready to design a stable sliding surface using the linear quadratic regulator design approach and then a robust control law to guarantee that the system sliding motion converges exponentially to a ball whose radius and the rate of exponential convergence can be chosen arbitrarily.

5.3.2 Sliding surface design using LQR approach

Consider the error dynamic of the 2-D offshore gantry crane in the form of (5.4) with $A_d \in \mathbb{R}^{6\times6}$ and $B \in \mathbb{R}^{6\times2}$. To facilitate the sliding surface design, it is noted that there exists a transformation matrix $T \in \mathbb{R}^{6\times6}$ [44] such that

$$TB = \begin{bmatrix} 0_{4\times2} \\ B_2 \end{bmatrix},$$

where $B_2 \in \mathbb{R}^{2\times2}$ is nonsingular. By using the coordinate transformation $e = Tx_e = z - Tx_d$, (5.4) can be rewritten in the form of the new coordinate:

$$\begin{aligned} \dot{e}(t) =& \overline{A}_d e(t) + (\overline{A} - \overline{A}_d)z(t) + \Delta\overline{A}(t)z(t) + \overline{B}u(t) \\ & - \overline{B}_d r_d(t) + \overline{D}\omega(t), \end{aligned} \tag{5.6}$$

where $z = Tx$, $\overline{A}_d = TA_dT^{-1}$, $\overline{A} = TAT^{-1}$, $\Delta\overline{A}(t) = T\Delta A(t)T^{-1}$, $\overline{B} = TB$, $\overline{B}_d = TB_d$ and $\overline{D} = TD$. It can be assumed that the transformation used to obtain the regular form was an orthogonal one. Hence the Euclidean norm is preserved, in which (5.5) implies

$$\|\Delta\overline{A}(t)\| \leq \mu, \quad \|\omega(t)\| \leq \omega_p.$$

The sliding function is defined in terms of trajectory tracking errors as follows

$$s(t) = \overline{S}e(t) = S_1e_1(t) + S_2e_2(t) = S_2(L_se_1(t) + e_2(t)), \tag{5.7}$$

where $e_1(t) \in \mathbb{R}^4$, $e_2(t) \in \mathbb{R}^2$, $\overline{S} = [S_1 \ S_2] \in \mathbb{R}^{2\times 6}$, and $L_s = S_2^{-1}S_1 \in \mathbb{R}^{2\times 4}$ is a constant matrix to be designed. Consider the following quadratic performance index

$$J = \frac{1}{2}\int_{t_s}^{\infty} e^T(t)Qe(t)dt, \tag{5.8}$$

where $Q \in \mathbb{R}^{6\times 6}$ is a given symmetric positive definite matrix and t_s is the starting time which indicates the induction of the sliding motion. By partitioning Q into subblocks

$$Q = \begin{bmatrix} Q_{11} & Q_{12} \\ Q_{21} & Q_{22} \end{bmatrix}$$

and noting that

$$\begin{aligned} &2e_1^T(t)Q_{12}e_2(t) + e_2^T(t)Q_{22}e_2(t) \\ &= (e_2(t) + Q_{22}^{-1}Q_{21}e_1(t))^T Q_{22}(e_2(t) + Q_{22}^{-1}Q_{21}e_1(t)) - e_1^T(t)Q_{21}^T Q_{22}^{-1}Q_{21}e_1(t), \end{aligned}$$

(5.8) can be rewritten in the form of

$$J = \frac{1}{2}\int_{t_s}^{\infty} \left(e_1^T(t)\overline{Q}e_1(t) + \upsilon^T(t)Q_{22}\upsilon(t)\right) dt,$$

where

$$\begin{aligned} \overline{Q} =& Q_{11} - Q_{12}Q_{22}^{-1}Q_{21}, \\ \upsilon(t) =& e_2(t) + Q_{22}^{-1}Q_{21}e_1(t). \end{aligned}$$

Based on the LQR minimisation of J in association with the nominal system (5.6), we obtain

$$\upsilon(t) = -Q_{22}^{-1}A_{12}^T P e_1(t),$$

where P satisfies the following equation

$$\mathcal{A}^T P + P\mathcal{A} - PA_{12}Q_{22}^{-1}A_{12}^T P + \overline{Q} = 0,$$

in which $\mathcal{A} = A_{11} - A_{12}Q_{22}^{-1}Q_{21}$ and A_{ij} is the subblocks obtained from partitioning matrix $\overline{A}_d$. Consequently, we obtain

$$e_2(t) = -Q_{22}^{-1}(A_{12}^T P + Q_{21})e_1(t). \tag{5.9}$$

During the sliding motion, we have $s(t) = 0$ so that

$$e_2(t) = -L_s e_1(t). \tag{5.10}$$

By comparing (5.9) and (5.10), the design matrix of the sliding function is obtained explicitly as

$$L_s = Q_{22}^{-1}(A_{12}^T P + Q_{21}) = S_2^{-1} S_1. \tag{5.11}$$

Hence, by choosing a suitable matrix for S_2, the sliding function $s(t) = \overline{S}e(t)$, where $\overline{S} = S_2[L_s \ I_2]$ can be obtained.

5.3.3 Sliding mode control

Before presenting our proposed control scheme, the following definition and lemma are introduced.

Definition 1: The solution of system (5.6) is uniformly exponentially convergent to a ball $B(0, r) = \{e \in \mathbb{R}^n : \|e\| \leq r\}$ with rate $\gamma > 0$ if for any $\xi > 0$, there exists $k(\xi) > 0$ such that

$$\|e(t)\| \leq r + k(\xi)\exp(-\gamma t), \ \ \forall t \geq 0.$$

Lemma 1 [108]*:* Let $V(t)$ be a continuous positive definite function for all $t \geq 0$, $k^* \geq 0$. Let

$$\dot{V}(t) \leq -\eta V(t) + \nu, \ \ \forall t \geq 0,$$

where η and ν are positive constants, then

$$V(t) \leq r + k^* \exp(-\gamma t), \ \ \forall t \geq 0,$$

in which $r = \nu/\eta$ and $\gamma = \eta$ is the exponential convergence rate.

Now, the control scheme proposed here has the form of

$$u(t) = u_E(t) + u_R(t), \tag{5.12}$$

where $u_E(t)$ and $u_R(t)$ are respectively the equivalent and switching control. The equivalent control which maintains the sliding motion on the sliding surface is defined as

$$u_E(t) = -\Lambda^{-1}\Big(\overline{S}\,\overline{A}_d e(t) + \Phi s(t)\Big) + \overline{K} z(t) + N r_d(t), \tag{5.13}$$

where $\Lambda = \overline{S}\,\overline{B} = S_2 B_2$, $\overline{K} = KT^{-1}$, and Φ is a design diagonal matrix with real distinct positive eigenvalues chosen such that $\lambda_{\min}(\Phi) = \gamma\|\overline{S}\|^2$, where γ is the chosen convergence rate. The following switching control $u_R(t)$ is designed to drive the system trajectories towards the prescribed sliding surface:

$$u_R(t) = -\Lambda^{-1}\frac{\rho s(t)}{\|s(t)\| + \varepsilon}, \tag{5.14}$$

where

$$\rho = \mu\|\overline{S}\|\|z(t)\|_{\max} + \|\overline{S}\,\overline{D}\|\omega_p, \tag{5.15}$$

in which $\|z(t)\|_{\max}$ is the maximal norm of the transformed state $z(t) = Tx(t)$ of the crane, and $\varepsilon > 0$ is a small positive scalar for chattering reduction to be selected according to the theorem stated below.

Theorem 1: For given bounds of the system disturbances and uncertainties ω_p and μ, as well as a convergence rate γ and positive scalar ε, the state error trajectories of offshore gantry crane system (5.6) are exponentially convergent to the ball $B(0, r_0)$ with rate γ under the following control law:

$$u(t) = -\Lambda^{-1}\left(\overline{S}\,\overline{A}_d e(t) + \Phi s(t) + \frac{\rho s(t)}{\|s(t)\| + \varepsilon}\right) + \overline{K} z(t) + N r_d(t), \tag{5.16}$$

where radius r_0 is determined as

$$r_0 = \sqrt{\frac{\varepsilon\rho}{\lambda_{\min}(\Phi)}}. \tag{5.17}$$

Proof: Consider the Lyapunov function

$$V(t) = \tfrac{1}{2} s^T(t) s(t).$$

By taking its derivative and substituting (5.6) into $\dot{V}(t)$, we obtain

$$\begin{aligned}\dot{V}(t)) =& s^T(t)\dot{s}(t)\\ =& s^T(t)\Big(-\Phi s(t)+\overline{S}\Delta\overline{A}(t)z(t)+\overline{S}\,\overline{D}\omega(t)-\frac{\rho s(t)}{\|s(t)\|+\varepsilon}\Big)\\ \leq& -\lambda_{\min}(\Phi)\|s(t)\|^2+\Big(\mu\|\overline{S}\|\|z(t)\|+\|\overline{S}\,\overline{D}\|\omega_p\Big)\|s(t)\|\\ &-\frac{\rho\|s(t)\|^2}{\|s(t)\|+\varepsilon}\\ =& -\lambda_{\min}(\Phi)\|s(t)\|^2+\Big(\mu\|\overline{S}\|\|z(t)\|+\|\overline{S}\,\overline{D}\|\omega_p\Big)\frac{\|s(t)\|\varepsilon}{\|s(t)\|+\varepsilon}\\ &+\Big(\mu\|\overline{S}\|\|z(t)\|+\|\overline{S}\,\overline{D}\|\omega_p-\rho\Big)\frac{\|s(t)\|^2}{\|s(t)\|+\varepsilon}\end{aligned}\tag{5.18}$$

From (5.15), we have $\rho\geq\mu\|\overline{S}\|\|z(t)\|+\|\overline{S}\,\overline{D}\|\omega_p$, and hence by combining inequality (5.18), it can be verified that

$$\dot{V}(t)\leq-\lambda_{\min}(\Phi)\|s(t)\|^2+\Big(\mu\|\overline{S}\|\|z(t)\|+\|\overline{S}\,\overline{D}\|\omega_p\Big)\frac{\|s(t)\|\varepsilon}{\|s(t)\|+\varepsilon},$$

or

$$\begin{aligned}\dot{V}(t)\leq& -\lambda_{\min}(\Phi)\|s(t)\|^2+\Big(\mu\|\overline{S}\|\|z(t)\|+\|\overline{S}\,\overline{D}\|\omega_p\Big)\varepsilon\\ \leq& -2\gamma V(t)+\rho\varepsilon.\end{aligned}$$

Hence, from Definition 1 and Lemma 1, we get

$$V(t)\leq\frac{\rho\varepsilon}{2\gamma}+k^*\exp(-2\gamma t),\ \ \forall t\geq 0.$$

Thus, from the sliding function $s(t)=\overline{S}e(t)$, we obtain

$$\begin{aligned}\|e(t)\|^2\leq&\frac{2}{\|\overline{S}\|^2}\left(\frac{\rho\varepsilon}{2\gamma}+k^*\exp(-2\gamma t)\right)\\ \leq&\frac{\rho\varepsilon}{\lambda_{\min}(\Phi)}+\frac{2k^*}{\|\overline{S}\|^2}\exp(-2\gamma t),\ \ \forall t\geq 0.\end{aligned}$$

By using the inequality $\sqrt{a+b}\leq\sqrt{a}+\sqrt{b}$, $\forall a,b\geq 0$, we finally obtain

$$\|e(t)\|\leq r_0+k\exp(-\gamma t),\ \ \forall t\geq 0,$$

where $r_0=\sqrt{\frac{\rho\varepsilon}{\lambda_{\min}(\Phi)}}$ and $k=\frac{\sqrt{2k^*}}{\|\overline{S}\|}$. The proof is completed.

5.3.4 Results and discussion

In this work, the numerical values of the offshore gantry crane system parameters are listed as $m_c = 6 \times 10^3$ kg, $m_p = 20 \times 10^3$ kg, $h_t = 15$ m, $d = 5$ m, and $g = 9.81$ m/s. The viscous friction and Coulomb friction coefficients are listed as $K_{cy} = 600$ Ns/m, $K_{cl} = 200$ Ns/m, $K_{c\theta} = 100$ Nms/rad, $P_{cy} = 200$ N, $P_{cl} = 150$ N, and $P_{c\theta} = 800$ Nm. The parameters for wind drag of (3.10) are $\rho_w = 1.225$ kg/m^3, $c_d = 1.05$ and $S_p = 12$ m^2. The nominal state vector is chosen as $x_0 = [0\ 7\ 0\ 0\ 0\ 0]^T$ ($L = 7$ m), with $u_0 = [0 \quad -196.14]^T$ kN. For the sake of illustration, the following parameters are provided as $l_D = 10$ m , $l_U = 4$ m, $v_R = 3$ m/s, $v_y = 0.63$ m/s and $y_F = 10$ m. The matrices K, N and transformation T are obtained as follows:

$$K = \begin{bmatrix} 0 & 0 & -1.962 & 0.006 & 0 & -0.0014 \\ 0 & 0 & 0 & 0 & 0.002 & 0 \end{bmatrix}, \quad N = \begin{bmatrix} 1 & 0 \\ 0 & 1 \end{bmatrix},$$

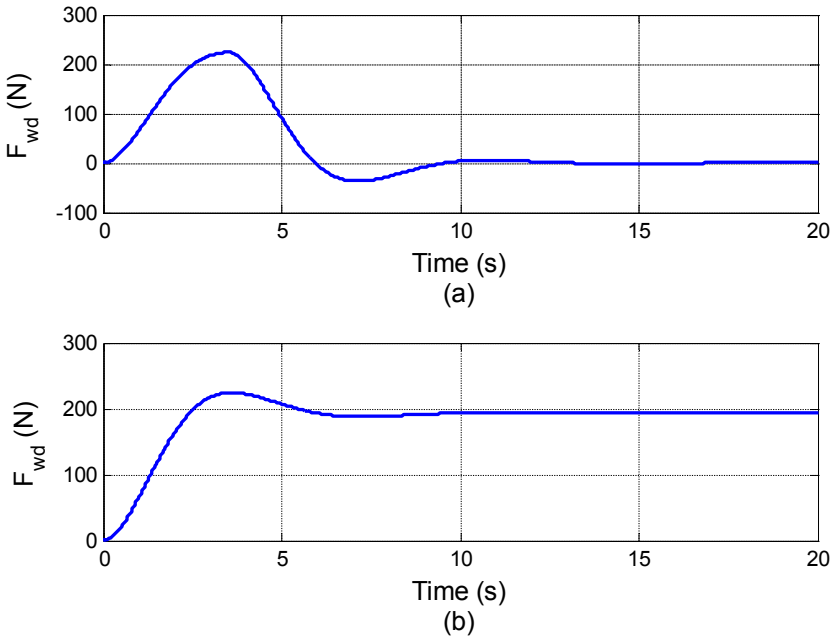

Figure 5.3 : Wind drags due to (a) short burst; and (b) persistent wind disturbances.

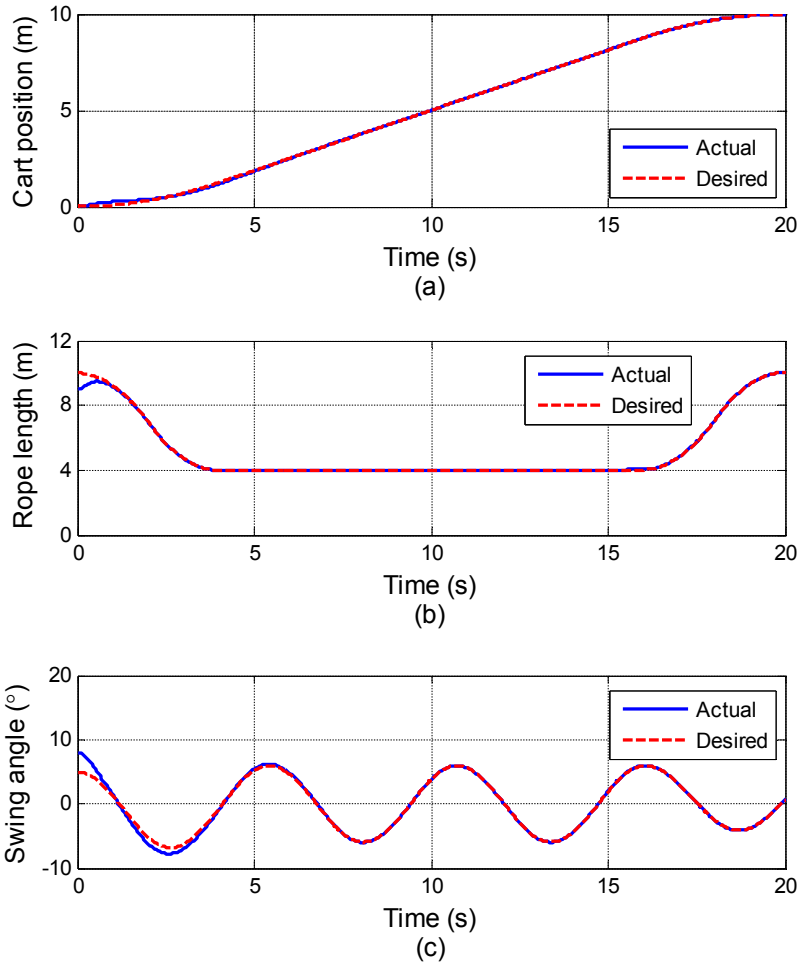

Figure 5.4 : Trajectory tracking responses of the (a) cart position; (b) rope length; and (c) swing angle subject to short burst wind disturbance.

$$T = \begin{bmatrix} 0 & 0 & 1 & 0 & 0 & 0 \\ 0.5735 & 0 & 0 & 0.6711 & 0 & 0.4698 \\ 0 & 1 & 0 & 0 & 0 & 0 \\ -0.8192 & 0 & 0 & 0.4698 & 0 & 0.3289 \\ 0 & 0 & 0 & 0.5735 & 0 & -0.8192 \\ 0 & 0 & 0 & 0 & 1 & 0 \end{bmatrix}.$$

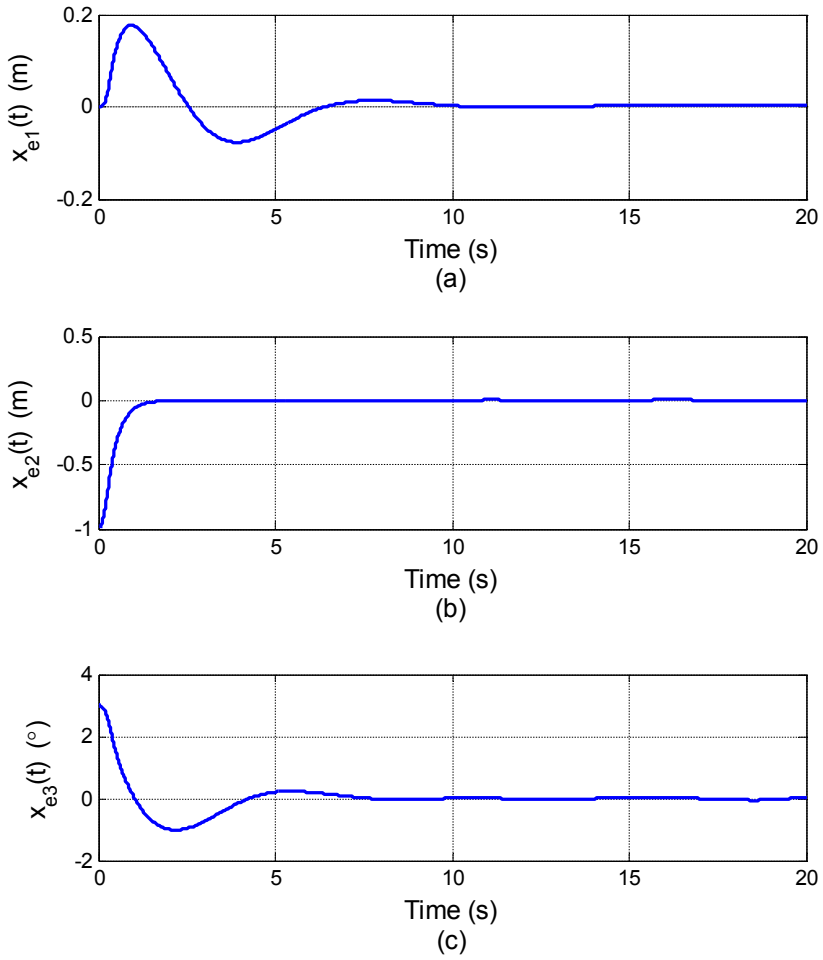

Figure 5.5 : Tracking error responses of the (a) cart position; (b) rope length; and (c) swing angle subject to short burst wind disturbance.

The state weighting matrix Q of the quadratic minimisation is chosen as $Q = TRT^{-1}$, $R = \text{diag}(10, 10, 5, 1, 1, 1)$ which, by choosing $S_2 = I_2$ and using (5.11), provides the sliding function matrix $\overline{S} = S_2[L_s \ I_2]$ as

$$\overline{S} = \begin{bmatrix} -1.9496 & 4.9236 & 0 & -0.4135 & 1 & 0 \\ 0 & 0 & 3.1623 & 0 & 0 & 1 \end{bmatrix}.$$

The upper bounds of the system disturbances and uncertainties, ω_p and μ are *a priori* selected as 2.8×10^3 and 4.5 respectively. From Theorem 1, by choosing the

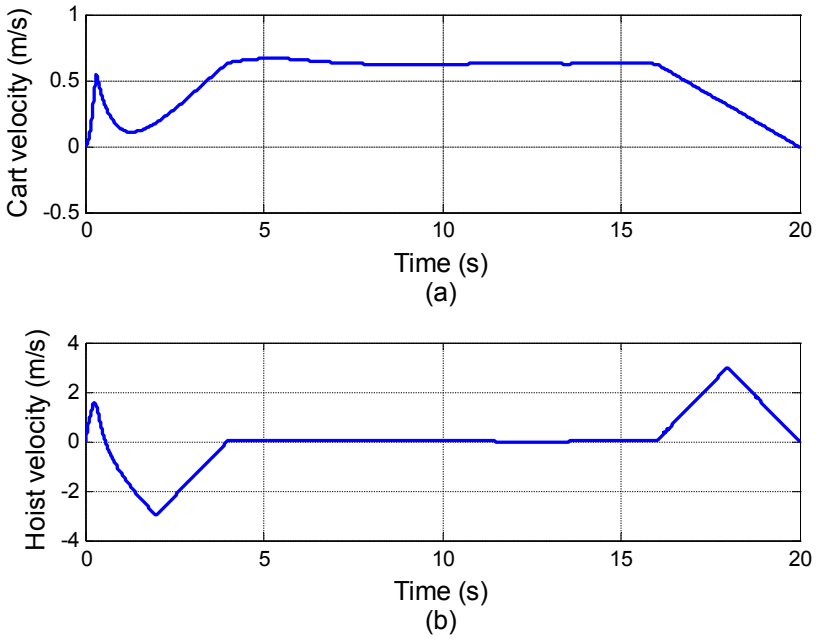

Figure 5.6 : (a) Cart velocity and (b) hoist velocity responses subject to short burst wind disturbance.

exponential decay rate $\gamma = 40$, and $\varepsilon = 10 \times 10^{-3}$, we obtain $\rho = 20$, and radius $r_0 = 13.1 \times 10^{-3}$.

A few scenarios are considered in the simulations to demonstrate the robustness of the designed controller. To accommodate persistent ocean waves in an allowable range, the rolling angular displacement and the heaving acceleration of the vessel are assumed to be respectively $\phi(t) = 7\cos t$ (in degrees) and $\ddot{\zeta}(t) = 2\sin t$ m/s^2. To investigate the effects of high amplitude wind disturbances, two types of wind profiles are considered with respect to time, namely short burst and persistent, with a maximum wind speed of 5.14 m/s or 18.52 km/h corresponding to the limit 10 knots of Sea State 3 conditions [124]. For the short burst wind drag (Figure 5.3(a)), its peak value is set to be 237 N at 3.5 s before it decays to zero. For the persistent wind drag (Figure 5.3(b)), we set its magnitude at around 204 N after it has reached

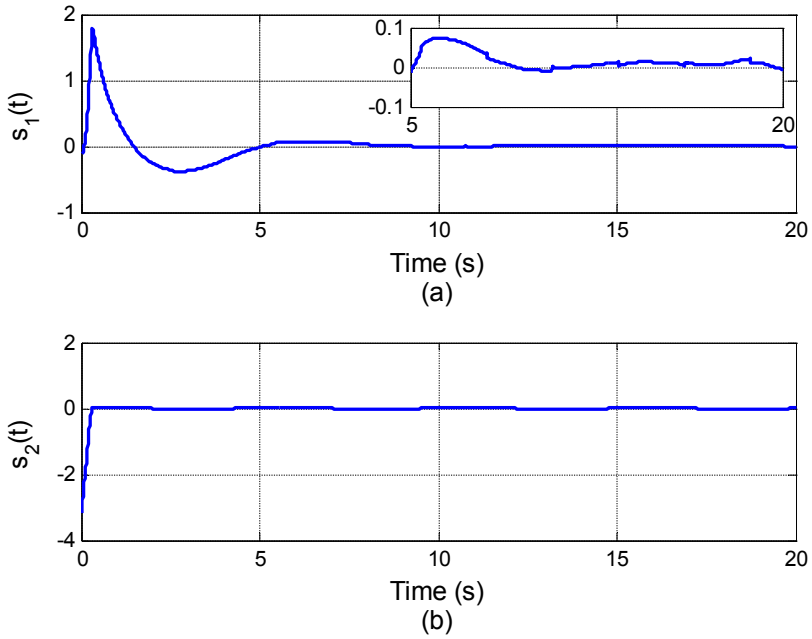

Figure 5.7 : Sliding functions subject to short burst wind disturbance.

the peak value. We also set the initial values of the positions generalized coordinates as $y(0) = 0$ m, $l(0) = 9$ m and $\theta(0) = 8°$. Our simulation is aimed to assess the controller performance to track the optimal crane trajectories as depicted in Figures 5.1 and 5.2.

In the first scenario, we consider the case of the offshore crane system in the presence of short burst wind and ocean waves disturbances. Simulation results for this scenario including the responses of positions, tracking errors, velocities, sliding functions and control forces are presented in Figures 5.4-5.8. As can be seen from Figures 5.4 and 5.5, the cart position and the swing angle track their desired trajectories in about 7 s and the rope length tracks it desired trajectory in a shorter time of about 1.5 s. This is due to higher complexity in the cart input force $F_y(t)$ which is assigned to drive both cart position and swing angle towards their desired trajectories at the same time, as compared to the hoist input force $F_l(t)$. Figure

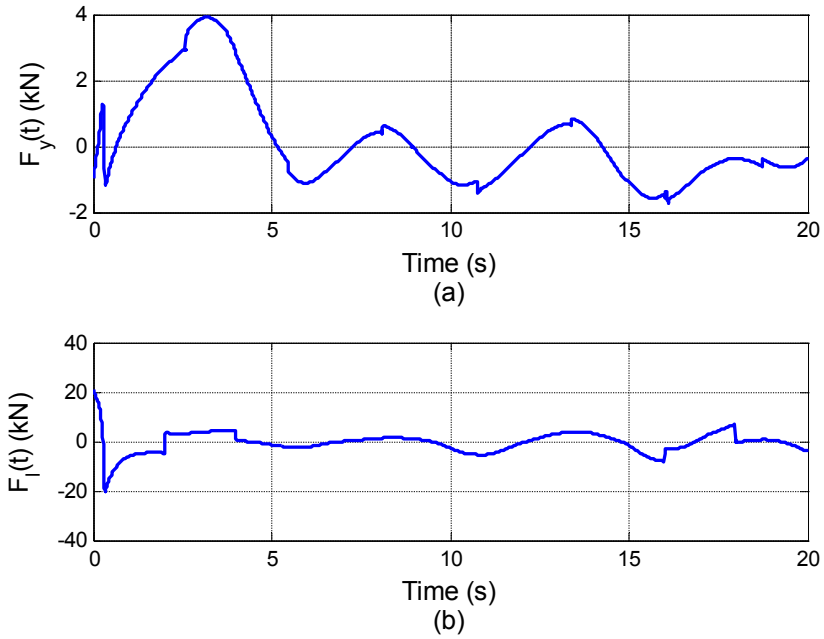

Figure 5.8 : (a) Cart driving force; and (b) hoisting input force subject to short burst wind disturbance.

5.6 shows the trapezoidal and triangular velocity profiles of the cart and hoisting rope motions, respectively, with some overshoots due to nonzero initial values in the swing angle and rope length responses. As can be seen from sliding function responses of Figure 5.7, the trajectory of $s_1(t)$ intercepts the sliding surface for the first time at approximately 1.5 s before it converges, while the trajectory of $s_2(t)$ reaches the sliding surface at approximately 0.3 s. Oscillations can be seen in the input plots of Figure 5.8 after the desired trajectories tracking have been attained due to the effect of the persistent ocean waves. Furthermore, the effect of short burst wind disturbance can be seen from Figure 5.8(a), where the cart driving force produces its peak at around 3 s and decreases gradually after the wind disturbance decayed thanks to the merit of the robust control scheme proposed. From Figure 5.8(b), two peaks can be seen in the hoisting input force response at around 2 s and 18 s which correspond to the process of lifting and lowering the payload.

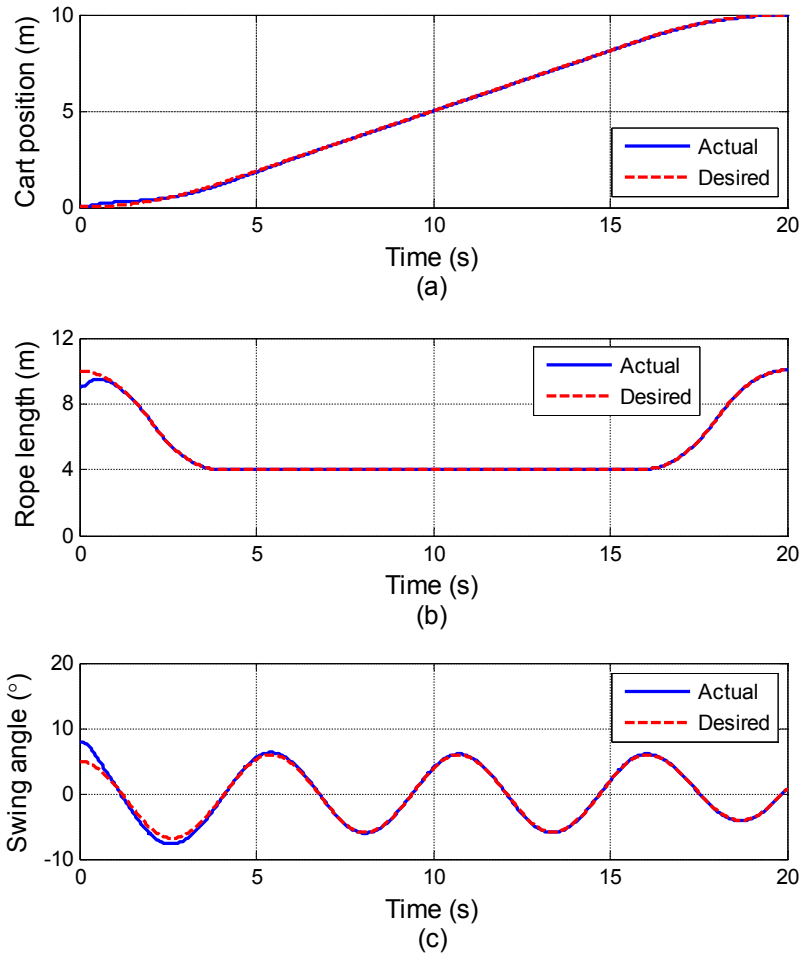

Figure 5.9 : Trajectory tracking responses of the (a) cart position; (b) rope length; and (c) swing angle subject to persistent wind disturbance.

To examine the exponential convergence of the sliding mode, we consider the scenario with the presence of persistent wind and ocean waves disturbances in the system. The simulation results for this scenario are presented in Figures 5.9-5.11. Owing to robustness of the control system, similar trajectory tracking responses (Figure 5.9) with the previous scenario have been obtained. However the effects of persistent wind disturbance can obviously be seen from the plots of sliding function $s_1(t)$ and input force $F_y(t)$. As shown in Figure 5.10(a), the sliding function $s_1(t)$

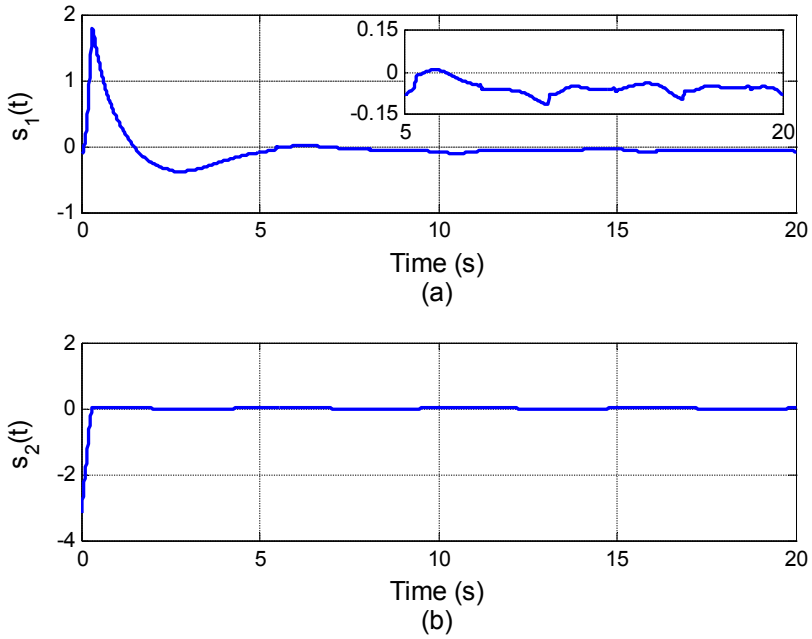

Figure 5.10 : Switching functions subject to persistent wind disturbance.

remains in a small bound within a close vicinity of the sliding surface $s_1(t) = 0$. This subsequently yields persistent magnitude in the input force $F_y(t)$ with an average value about 2.8 kN once the sliding mode is achieved, as can be seen from Figure 5.11(a). On the other hand, the switching function response $s_2(t)$ of Figure 5.10(b) and the hoisting input force response of Figure 5.11(b) are similar with the responses in the previous scenario due to the equivalent rolling and heaving motions in both scenarios. Furthermore, these results have been achieved because the wind disturbance only provides a small effect on the vertical motion of the payload.

Finally, we consider the case when the nominal values of cart and container masses have been perturbed such as $\Delta m_p/m_p = 10\%$, together with the presence of short burst wind and ocean waves disturbances. As can be seen from the responses of Figures 5.12-5.14, the closed-loop system completely rejects the uncertainties caused by these perturbations once sliding has been established. Small differences between

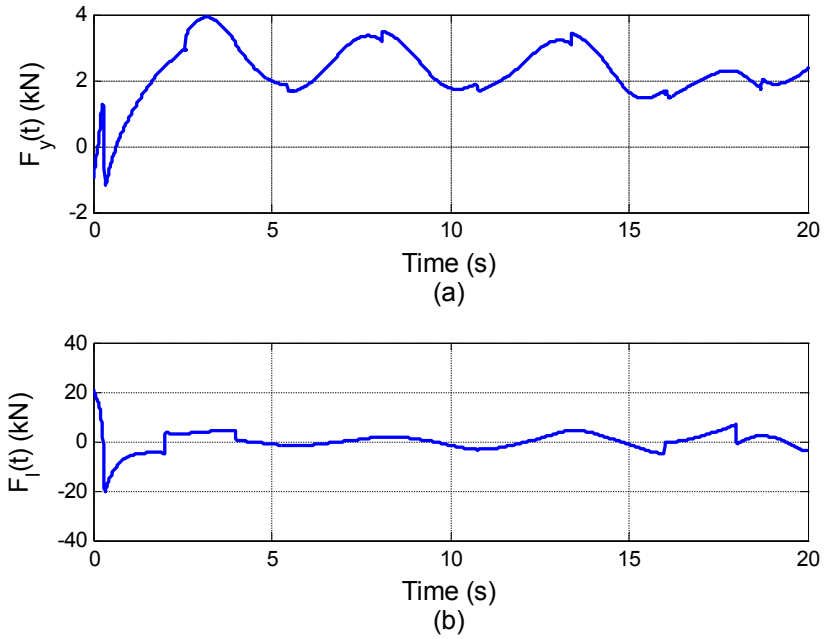

Figure 5.11 : (a) Cart driving force; and (b) hoisting input force subject to persistent wind disturbance.

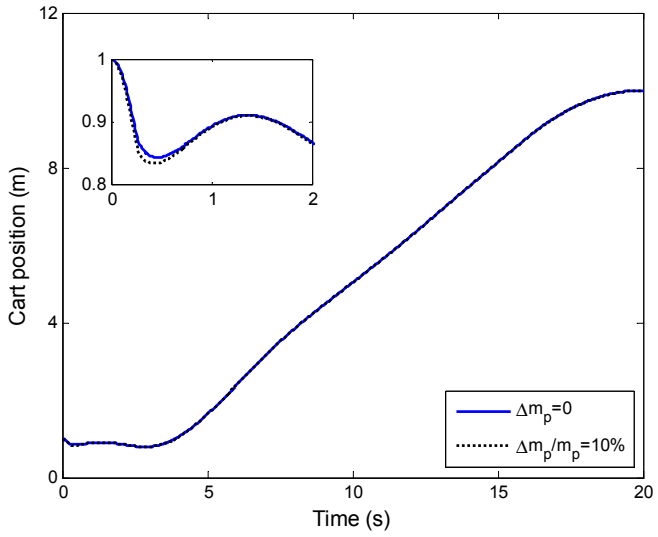

Figure 5.12 : Cart position responses with nominal values of system masses and with $\Delta m_p/m_p = 10\%$.

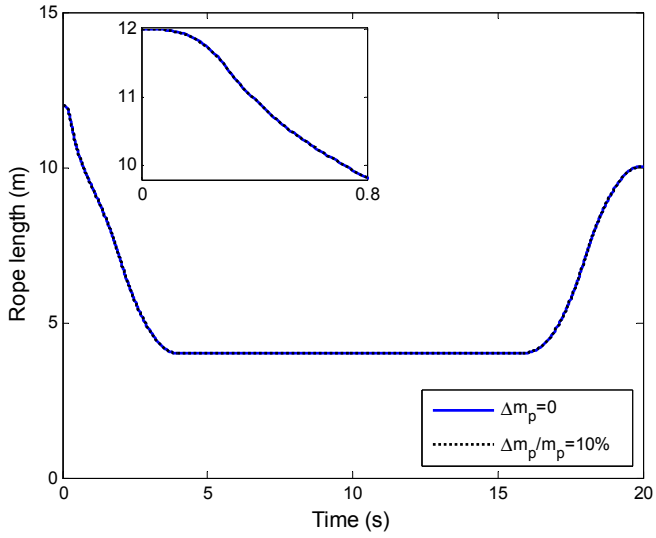

Figure 5.13 : Rope length responses with nominal values of system masses and with $\Delta m_p/m_p = 10\%$.

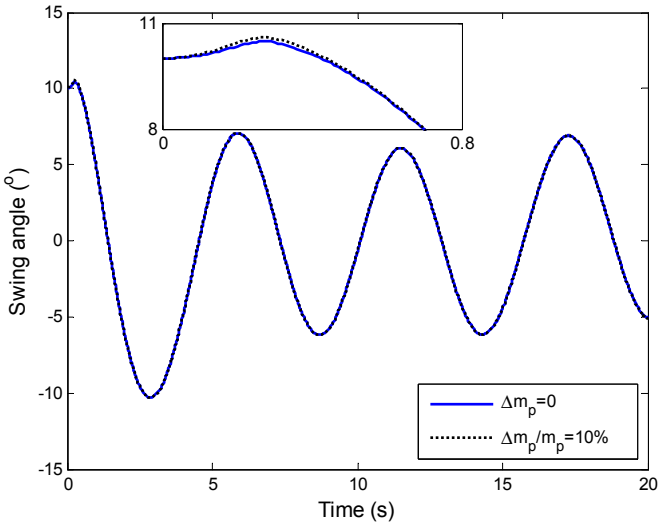

Figure 5.14 : Swing angle responses with nominal values of system masses and with $\Delta m_p/m_p = 10\%$.

the responses with nominal and perturbed parameters can only be seen during the reaching phase of the system. In addition, the rope length response (Figure 5.13) is least affected by these perturbations due to the aforementioned fact, that is, less

complexity in $F_l(t)$ as compared to $F_y(t)$ which contains the decoupling of y- and θ-coordinates.

5.4 Control design for 2-D offshore boom crane

In this section, we propose a 1-SMC scheme for offshore boom crane system developed in Section 3.4.1. Linear matrix inequalities with feasible performance constraints are used to design the sliding surface. A robust sliding mode controller is proposed to for trajectory tracking and the stability of the proposed controller is analytically proven.

5.4.1 Sliding surface design using LMI approach

Consider the error dynamic of the 2-D offshore boom crane in the form of (5.4) with $A_d \in \mathbb{R}^{6\times 6}$ and $B \in \mathbb{R}^{6\times 2}$. For convenience, by taking into account (5.3) and by letting $d(t,x) = \Delta A(t)x(t) + D\omega(t)$, (5.4) can be rewritten as

$$\dot{x}_e(t) = A_d x_e(t) + Bu(t) - BKx(t) - BNr_d(t) + d(t,x). \tag{5.19}$$

The disturbance term $d(t,x)$ is assumed to be norm-bounded, that is,

$$\|d(t,x)\| \leq d_M. \tag{5.20}$$

Let $\Theta \in \mathbb{R}^{6\times r}$ be a matrix whose columns forms an orthonormal basis of null space of matrix B^T, i.e.

$$\Theta^T B = 0_{r\times 2}, \quad \Theta^T\Theta = I_r. \tag{5.21}$$

Matrix Θ can be obtained by using the singular value decomposition (SVD) of B. Let the SVD form of B is

$$B = U_B \Sigma_B V_B,$$

with $U_B \in \mathbb{R}^{6\times 6}$, $\Sigma_B \in \mathbb{R}^{6\times 2}$ and $V_B \in \mathbb{R}^{2\times 2}$. Thus, Θ is formed by the last $(6 - \text{rank}(B))$ columns of U_B. Since $\text{rank}(B) = 2$, we have $r = 4$.

Let the following LMI condition is satisfied:

$$\begin{cases} \Theta^T(A_dP + PA_d^T)\Theta < 0 \\ P > 0 \end{cases} \tag{5.22}$$

Then the sliding surface can be constructed as

$$s(t) = Sx_e(t) = (B^TP^{-1}B)^{-1}B^TP^{-1}x_e(t). \tag{5.23}$$

5.4.2 Sliding mode control

To construct the control law, define a coordinate transformation $w(t) = T_sx_e(t)$, where the transformation matrix T_s is defined as

$$T_s = \begin{bmatrix} (\Theta^TP\Theta)^{-1}\Theta^T \\ (B^TP^{-1}B)^{-1}B^TP^{-1} \end{bmatrix} = \begin{bmatrix} \Pi \\ S \end{bmatrix}.$$

Thus,

$$w(t) = T_sx_e(t) = \begin{bmatrix} \Pi x_e(t) \\ Sx_e(t) \end{bmatrix} = \begin{bmatrix} w_1(t) \\ s(t) \end{bmatrix}.$$

It can be shown that

$$T_s^{-1} = [P\Theta \quad B]$$

and

$$T_sB = \begin{bmatrix} 0_{4\times2} \\ I_2 \end{bmatrix}.$$

Hence, by taking into account (5.19), the derivative of $w(t)$ becomes

$$\begin{aligned} \dot{w}(t) =& T_s\dot{x}_e(t) \\ =& T_sA_dT_s^{-1}w(t) + T_sBu(t) - T_sBKx(t) - T_sBNr_d(t) + T_sd(t,x) \\ \begin{bmatrix} \dot{w}_1(t) \\ \dot{s}(t) \end{bmatrix} =& \begin{bmatrix} \Pi A_dP\Theta & \Pi A_dB \\ SA_dP\Theta & SA_dB \end{bmatrix} \begin{bmatrix} w_1(t) \\ s(t) \end{bmatrix} \\ &+ \begin{bmatrix} 0_{4\times2} \\ I_2 \end{bmatrix} (u(t) - Kx(t) - Nr_d(t)) + \begin{bmatrix} \Pi \\ S \end{bmatrix} d(t,x), \end{aligned}$$

or

$$\dot{w}_1(t) = \Pi A_d P \Theta w_1(t) + \Pi A_d B s(t) + \Pi d(t,x), \tag{5.24}$$

$$\dot{s}(t) = S A_d P \Theta w_1(t) + S A_d B s(t) + u(t) - K x(t) - N r_d(t) + S d(t,x). \tag{5.25}$$

Based on (5.25), the equivalent control which maintains the sliding motion on the sliding surface is obtained as

$$u_E(t) = -S A_d P \Theta \Pi x_e(t) - (S A_d B - \Phi) s(t) + K x_e(t) + N r_d(t), \tag{5.26}$$

where $\Phi \in \mathbb{R}^{2\times 2}$ is any stable design matrix. The switching control which forces the system states to reach the predefined sliding surface is proposed as

$$u_R(t) = -\rho \frac{P_r s(t)}{\|P_r s(t)\|}, \tag{5.27}$$

where $P_r \in \mathbb{R}^{2\times 2}$ is a symmetric positive definite matrix satisfying the Lyapunov equation

$$P_r \Phi + \Phi^T P_r = -I_2,$$

and ρ is a constant satisfying

$$\rho \geq \|S\| d_M. \tag{5.28}$$

Thus, we have the following theorem.

Theorem 2: For given bounds of the system disturbances and uncertainties μ and ω_p, as well as arbitrary radius r_0 and convergence rate γ, the state error trajectories of offshore boom crane system (5.19) converge to zero in finite time under the following control law:

$$u(t) = -S A_d P \Theta \Pi x_e(t) - (S A_d B - \Phi) s(t) + K x_e(t) + N r_d(t) - \rho \frac{P_r s(t)}{\|P_r s(t)\|}. \tag{5.29}$$

Proof: Consider the Lyapunov function

$$V(t) = \tfrac{1}{2} s^T(t) P_r s(t).$$

By taking its derivative and taking into account (5.25) and (5.29), we obtain

$$\begin{aligned}\dot{V}(t) =& 2s^T(t)P_r\dot{s}(t)\\ =& 2s^T(t)P_r\Phi s(t) - \frac{2\rho s^T(t)P_rP_rs(t)}{\|P_rs(t)\|} + 2s^T(t)P_rSd(t,x)\\ =& -\|s(t)\|^2 - 2\rho\|P_rs(t)\| + 2s^T(t)P_rSd(t,x),\end{aligned}$$

since $s^T(t)P_rP_rs(t) = \|P_rs(t)\|^2$. It follows that

$$\dot{V}(t) \leq -\|s(t)\|^2 - 2\|P_rs(t)\|(\rho - \|S\|\|d(t,x)\|), \tag{5.30}$$

Combining inequality (5.28) and (5.30) yields

$$\dot{V}(t) \leq -\|s(t)\|^2,$$

which implies a stable sliding motion is induced in finite time. The proof is completed.

Remark: To eliminate the chattering phenomenon induced by the term $\frac{P_rs(t)}{\|P_rs(t)\|}$ in control law (5.27), a differentiable approximation has been used as follows:

$$u_R(t) = -\rho\frac{P_rs(t)}{\|P_rs(t)\| + \varepsilon},$$

where ε is a small positive constant.

To investigate the dynamical behaviour when the state error trajectories confined to the sliding surface, we substitute $s(t) = 0$ into (5.24) which gives

$$\dot{w}_1(t) = \Pi A_dP\Theta w_1(t) + \Pi d(t,x). \tag{5.31}$$

Let the matrix $P_1 \in \mathbb{R}^4 \times 4$ be the unique symmetric positive definite solution to the following equation:

$$P_1A_1 + A_1^TP_1 = -Q_1, \tag{5.32}$$

where $A_1 = \Pi A_dP\Theta$ and $Q_1 \in \mathbb{R}^4 \times 4$ is a symmetric positive definite matrix. Let $V(w_1) = w_1^T(t)P_1w_1(t)$ be a Lyapunov function for (5.31). Taking the time

derivative of $V(w_1)$ along the system trajectories gives

$$\begin{aligned}
\dot{V}(w_1) =& \dot{w}_1^T(t)P_1w_1(t) + w_1^T(t)P_1\dot{w}_1(t) \\
=& (A_1w_1(t) + \Pi d(t,x))^T P_1w_1(t) + w_1^T(t)P_1(A_1w_1(t) + \Pi d(t,x)) \\
=& w_1^T(t)(A_1^TP_1 + P_1A_1)w_1(t) + 2w_1^T(t)P_1\Pi d(t,x) \\
=& - w_1^T(t)Q_1w_1(t) + 2w_1^T(t)P_1\Pi d(t,x) \\
\leq& - w_1^T(t)Q_1w_1(t) + 2\|P_1w_1(t)\|\|\Pi\|d_M \\
\leq& - \lambda_{\min}(Q_1)\|w_1(t)\|^2 + 2\lambda_{\max}(P_1)\|w_1(t)\|\|\Pi\|d_M \\
=& - \|w_1(t)\|\lambda_{\min}(Q_1)\left[\|w_1(t)\| - \frac{2\lambda_{\max}(P_1)\|\Pi\|d_M}{\lambda_{\min}(Q_1)}\right].
\end{aligned} \tag{5.33}$$

Define

$$\delta = \frac{2\lambda_{\max}(P_1)\|\Pi\|d_M}{\lambda_{\min}(Q_1)}$$

and let $B(0,\delta)$ represent the ball centred at origin given by

$$B(0,\delta) = \{w_1(t) \ : \ \|w_1(t)\| < \delta\}.$$

It follows that, from (5.33) for $w_1(t) \notin B(0,\delta)$, $\dot{V}(w_1) < 0$. Therefore there exists a $t_0 > 0$ such that the states $w_1(t)$ is ultimately bounded with respect to $B(0,\delta)$.

5.4.3 Results and discussion

In this simulation, we consider the lab-scaled offshore boom crane [53]. The numerical values of the system parameters are listed as $M_b = 4$ kg, $m_p = 1$ kg, $L_b = 4$ m, $h_t = 1$ m, and $g = 9.81$ m/s. The viscous friction and Coulomb friction coefficients are listed as $K_{c\beta} = 2$ Nms/rad, $K_{cl} = 1$ Ns/m, $K_{c\theta} = 1$ Nms/rad, $P_{c\beta} = 2$ Nm, $P_{cl} = 1$ N, $P_{c\theta} = 1$ Nm. The parameters for wind drag of (3.10) are $\rho_w = 1.225$ kg/m^3, $c_d = 1.05$ and $S_p = 40$ cm^2. The matrices K and N are obtained as follows:

$$K = \begin{bmatrix} 18.977 & 68.307 & -20.803 & 2 & 0 & 2.8284 \\ -9.3125 & -2.4925 & 7.3549 & 010 & & \end{bmatrix}, \quad N = \begin{bmatrix} 0.0469 & 0.1326 \\ 0.1326 & 1.3750 \end{bmatrix}.$$

The matrices Θ, P, Π and S are obtained as:

$$\Theta = \begin{bmatrix} 0 & 0.2425 & 0.6860 & 0.6860 \\ 0 & -0.2287 & 0.7276 & -0.6468 \\ 1 & 0 & 0 & 0 \\ 0 & 0.8889 & 0 & -0.3143 \\ 0 & 0 & 0 & 0 \\ 0 & -0.3143 & 0 & 0.1111 \end{bmatrix},$$

$$P = \begin{bmatrix} 99.3640 & 102.2222 & -49.6839 & -42.8032 & -3.2398 & -18.5619 \\ 102.2222 & 172.7351 & -15.4513 & -11.6871 & -60.2023 & 0.5128 \\ -49.6839 & -15.4513 & 246.5580 & 7.5874 & -11.6354 & -60.0027 \\ -42.8032 & -11.6871 & 7.5874 & 79.2209 & 16.6665 & 33.4700 \\ -3.2398 & -60.2023 & -11.6354 & 16.6665 & 311.1186 & -111.3354 \\ -18.5619 & 0.5128 & -60.0027 & 33.4700 & -111.3354 & 306.8052 \end{bmatrix},$$

$$\Pi = \begin{bmatrix} 0.0053 & -0.0027 & 0.0049 & 0.0002 & 0 & -0.0001 \\ 0.0254 & -0.0149 & 0.0021 & 0.0179 & 0 & -0.0063 \\ 0.0109 & -0.0019 & 0.0017 & 0.0035 & 0 & -0.0012 \\ 0.0374 & -0.0250 & 0.0053 & 0.0059 & 0 & -0.0021 \end{bmatrix},$$

$$S = \begin{bmatrix} 24.2859 & -13.8708 & 4.5222 & 16.2034 & -2.8284 & 4.6421 \\ -3.6093 & 2.2810 & -0.5066 & -2.3446 & 1 & -0.1711 \end{bmatrix}.$$

The upper bounds of the system disturbances ω_p, μ, and d_M are obtained as 11.225, 2.86, and 25.4 respectively. The control parameters are chosen as $\Phi = \text{diag}(2, 2)$, $\rho = 80$ and $\varepsilon = 0.1$.

Based on the model reference (5.2), the rolling angular displacement $\phi(t)$ is set to be a sinusoidal wave with maximum amplitude 60°. The heaving acceleration of the vessel is assumed to be $\ddot{\zeta}(t) = 0.4 \sin t$ m/s^2. The maximum wind speed is

assumed to be 3 m/s. We also set the initial values of the positions generalized coordinates as $\beta(0) = 50°$, $l(0) = 0.5$ m and $\theta(0) = 30°$.

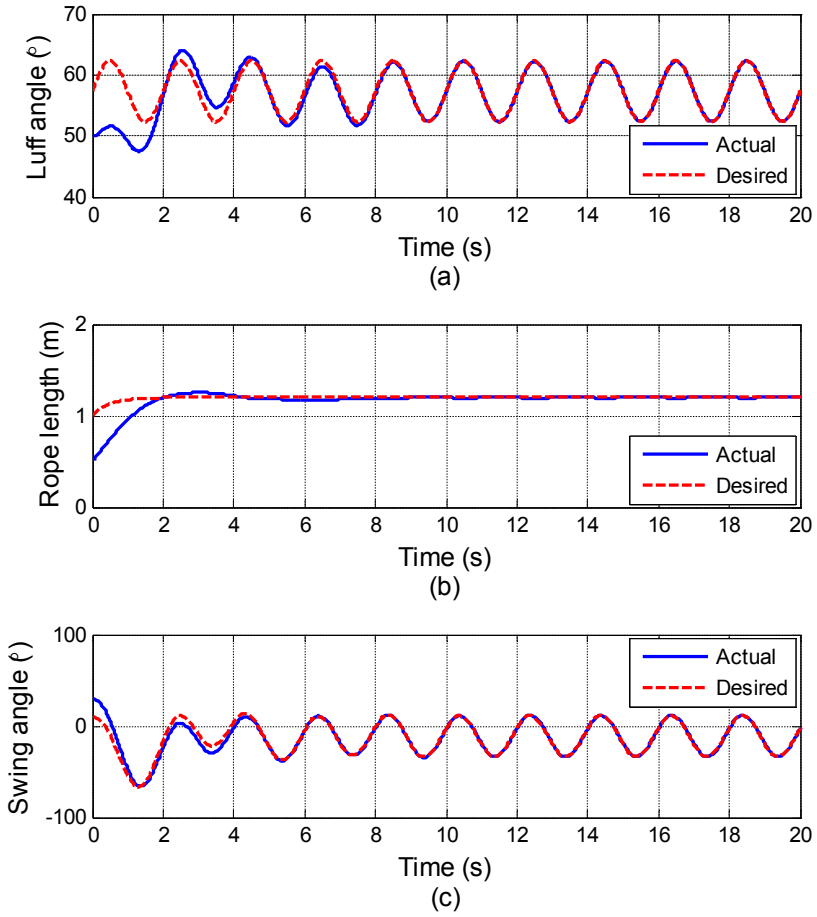

Figure 5.15 : Trajectory tracking responses of the (a) luff angle; (b) rope length; and (c) swing angle.

The tracking response are depicted in Figure 5.15. As can be seen from the results, the luff angle (Figure 5.15(a)) and the payload swing angle (Figure 5.15(c)) track the desired trajectories in about 5 s, despite the relatively large initial error. The rope length (Figure 5.15(b)) tracks the desired trajectory in about 4 s. This is due to higher complexity in the boom input torque $\tau_\beta(t)$ which is assigned to

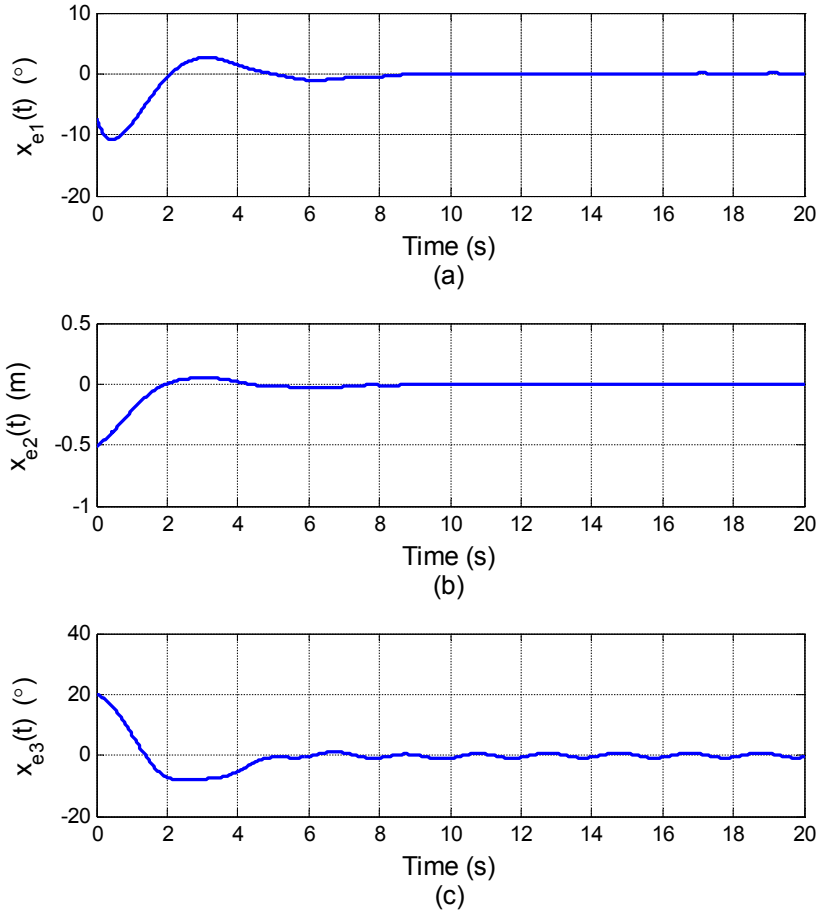

Figure 5.16 : Tracking error responses of the (a) luff angle; (b) rope length; and (c) swing angle.

drive both luff angle and swing angle towards their desired trajectories at the same time, as compared to the hoist input force $F_l(t)$. Figure 5.16 shows the tracking error responses of the control system and Figure 5.17 shows the corresponding sliding functions. Oscillations can be seen in the input plots of Figure 5.18 after the desired trajectories tracking have been attained due to the effect of the persistent disturbances.

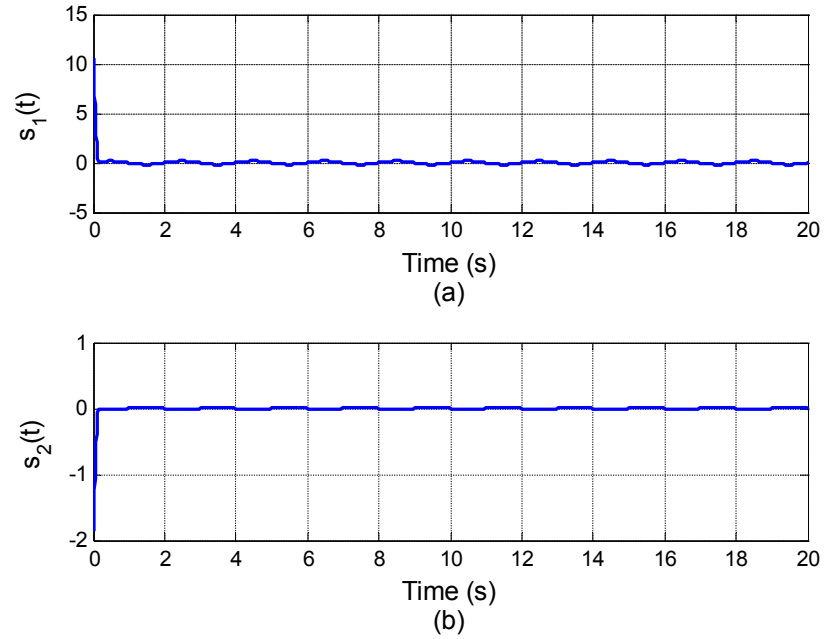

Figure 5.17 : Sliding functions.

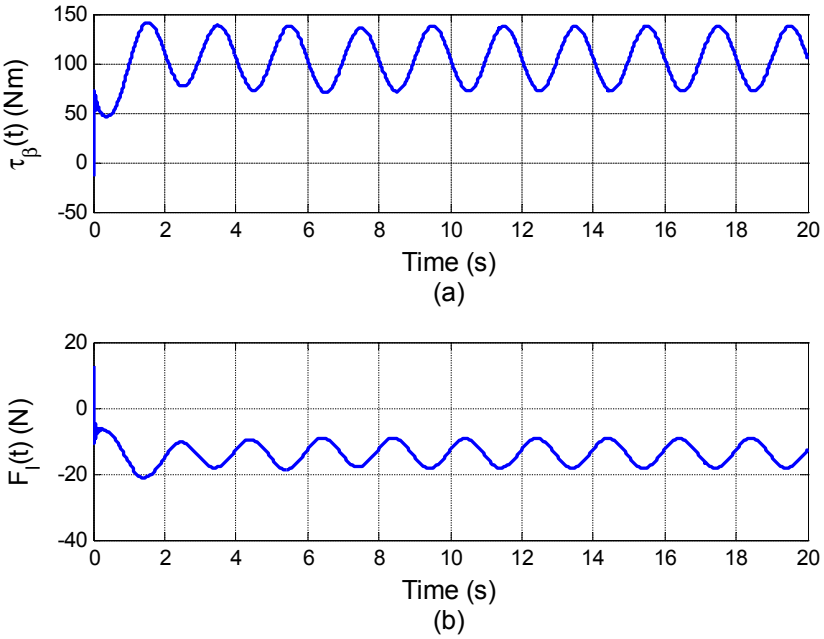

Figure 5.18 : (a) Boom input torque; (b) hoisting input force.

5.5 Summary

In this chapter, we have addressed the problem of robust sliding mode control for 2-D offshore gantry crane and offshore boom crane systems with bounded disturbances and uncertainties. Two design approaches has been utilised to construct the sliding surfaces, namely the LQR and LMI. Robust sliding mode control laws are proposed to drive the state variables of the system towards the sliding surface in finite time and maintain them within an arbitrarily small band in the presence of system disturbances. Extensive simulation results are provided to demonstrate good tracking performance of the proposed controller for offshore crane systems in dealing with the harsh open-sea conditions.

Chapter 6

Development of Second-order Sliding Mode Control for Offshore Crane Systems

6.1 Introduction

This chapter presents a 2-SMC law for trajectory tracking and sway suppression control, making use of its capability of chattering alleviation while achieving high tracking performance and preserving strong robustness. The 2-SMC is designed to deal with 5 DOF offshore crane systems in the presence of vessels' roll, pitch and heave motions. The asymptotic stability of the closed-loop system is guaranteed in the Lyapunov sense. Extensive simulation results are given to illustrate the feasibility of the proposed approach, in terms of reducing the effects of disturbances and model discrepancy.

6.2 Second-order sliding mode control

This section presents the design of the control algorithm for trajectory tracking control of the offshore crane.

6.2.1 The control algorithm

Consider the dynamics of offshore cranes in the form of (3.4)-(3.6) with $q_a \in \mathbb{R}^m$, $q_u \in \mathbb{R}^{n-m}$, and $\tau_a \in \mathbb{R}^m$. For convenience, we renumber the equations as follows:

$$\begin{bmatrix} M_{aa}(q) & M_{au}(q) \\ M_{au}^T(q) & M_{uu}(q) \end{bmatrix} \begin{bmatrix} \ddot{q}_a \\ \ddot{q}_u \end{bmatrix} + \begin{bmatrix} f_a(q,\dot{q}) \\ f_u(q,\dot{q}) \end{bmatrix} = \begin{bmatrix} \tau_a \\ 0_{(n-m)\times 1} \end{bmatrix}, \tag{6.1}$$

$$\ddot{q}_u = M_{uu}^{-1}(q)[-M_{au}^T(q)\ddot{q}_a - f_u(q,\dot{q})], \tag{6.2}$$

$$\ddot{q}_a = \Big(M_{aa}(q) - M_{au}(q)M_{uu}^{-1}(q)M_{au}^T(q)\Big)^{-1} \times \big[- f_a(q,\dot{q}) + M_{au}(q)M_{uu}^{-1}(q)f_u(q,\dot{q}) + \tau_a\big]. \quad (6.3)$$

We assume that all states and vessel coordinates motion are measurable. By using feedback linearisation

$$\tau_a = f_a(q,\dot{q}) - M_{au}(q)M_{uu}^{-1}(q)f_u(q,\dot{q}) + \Big(M_{aa}(q) - M_{au}(q)M_{uu}^{-1}(q)M_{au}^T(q)\Big)u, \quad (6.4)$$

equations (6.3) and (6.2) can be rewritten as

$$\begin{cases} \ddot{q}_a = u, \\ \ddot{q}_u = -M_{uu}^{-1}(q)M_{au}^T(q)u - M_{uu}^{-1}(q)f_u(q,\dot{q}), \end{cases} \quad (6.5)$$

where $u \in \mathbb{R}^m$ is the new control. The tracking problem is constituted in finding a control action guaranteeing that $\lim_{t\to\infty} q_a(t) = q_a^d(t)$ and $\lim_{t\to\infty} q_u(t) = 0$, where $q_a^d(t)$ represents the reference trajectories for the vectors of the actuated generalised coordinates. On the other hand, $q_u(t)$ which represents the system's sway with respect to the ground vertical axis is required to be kept at zero.

Let us define the vector of sliding function $s(t) \in \mathbb{R}^m$ as

$$\begin{aligned} s(t) =& \dot{q}_a - \dot{q}_a^d + \gamma(\dot{q}_u - \dot{q}_u^d) + \lambda_a q_a + \lambda_u q_u \\ =& \dot{q}_a + \gamma\dot{q}_u - \dot{q}^r, \end{aligned} \quad (6.6)$$

where $\dot{q}^r = \dot{q}_a^d - \lambda_a q_a - \lambda_u q_u$. Hence, the second order derivative of the sliding function is obtained as

$$\begin{aligned} \ddot{s}(t) =& \dddot{q}_a + \gamma\dddot{q}_u - \dddot{q}^r \\ =& \Big(I_m - \gamma M_{uu}^{-1}(q)M_{au}^T(q)\Big)\dot{u} + \xi(t,q,\dot{q},u), \end{aligned} \quad (6.7)$$

where

$$\begin{aligned} \xi(t,q,\dot{q},u) =& -\gamma\left[\frac{d}{dt}\Big(M_{uu}^{-1}(q)M_{au}^T(q)\Big)u + \frac{d}{dt}\Big(M_{uu}^{-1}(q)f_u(q,\dot{q})\Big)\right] - \dddot{q}^r \\ =& \gamma M_{uu}^{-1}(q)\left[\Big(\dot{M}_{uu}(q)M_{uu}^{-1}(q)M_{au}^T(q) - \dot{M}_{au}^T(q)\Big)u \right. \\ & \left. + \Big(\dot{M}_{uu}(q)M_{uu}^{-1}(q)f_u(q,\dot{q}) - \dot{f}_u(q,\dot{q})\Big)\right] - \dddot{q}^r, \end{aligned} \quad (6.8)$$

and

$$\begin{aligned}\dddot{q}^r =& \dddot{q}_a^d + \lambda_a \ddot{q}_a^d - \lambda_a \ddot{q}_a - \lambda_u \ddot{q}_u \\ =& \dddot{q}_a^d + \lambda_a \ddot{q}_a^d - \Big(\lambda_a I_m - \lambda_u M_{uu}^{-1}(q) M_{au}^T(q)\Big) u + \lambda_u M_{uu}^{-1}(q) f_u(q, \dot{q}).\end{aligned} \tag{6.9}$$

Next, we consider an auxiliary dynamics constituted by a double integrator with input $v \in \mathbb{R}^m$ and output $w \in \mathbb{R}^m$ as follows:

$$\ddot{w} = v. \tag{6.10}$$

Introduce a function $\sigma \in \mathbb{R}^m$ such that

$$\sigma = s - w. \tag{6.11}$$

Thus, the second derivative of σ is obtained as

$$\ddot{\sigma} = \ddot{s} - v. \tag{6.12}$$

The sliding motion on $\sigma = \dot{\sigma} = 0$ is referred as second-order sliding mode. The theoretical properties of this special class of sliding modes have been thoroughly investigated in [83]. It has been evidenced that the equivalent control for the second-order sliding mode can be defined as the continuous control that solves the equation $\ddot{\sigma} = 0$ [11]. Thus, from (6.12) and (6.7), the equivalent control of the system is obtained as

$$v_{eq} = \ddot{s} = (I_m - \gamma M_{uu}^{-1}(q) M_{au}^T(q))\dot{u} + \xi(t, q, \dot{q}, u). \tag{6.13}$$

Once the second-order sliding mode has been established on $\sigma = \dot{\sigma} = 0$, the equivalent representation of system (6.12) can be obtained by substituting v_{eq} for v [138], yielding to

$$\ddot{w} = v_{eq} = (I_m - \gamma M_{uu}^{-1}(q) M_{au}^T(q))\dot{u} + \xi(t, q, \dot{q}, u). \tag{6.14}$$

The equivalent system (6.14) can be stabilized by 1-SMC law. For this purpose, define the following sliding function:

$$s_w = \dot{w} + \lambda_w w. \tag{6.15}$$

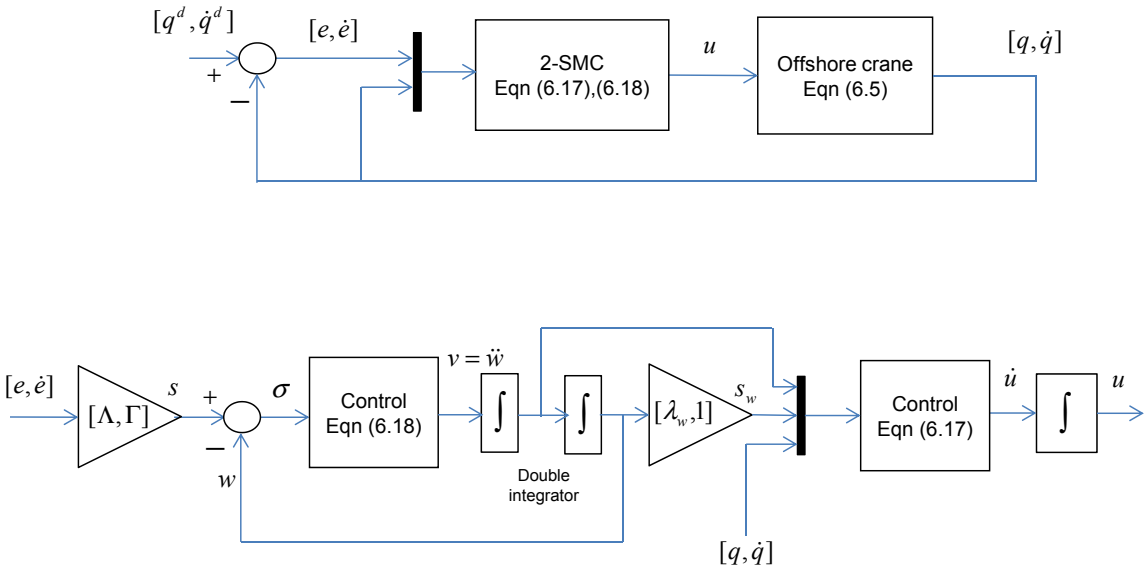

Figure 6.1 : Block diagram of the offshore crane control system

The first derivative of s_w is obtained as

$$\begin{aligned}\dot{s}_w =& \ddot{w} + \lambda_w \dot{w} \\ =& (I_m - \gamma M_{uu}^{-1}(q) M_{au}^T(q))\dot{u} + \xi(t, q, \dot{q}, u) + \lambda_w \dot{w}. \end{aligned} \tag{6.16}$$

The 2-SMC law for the system (6.5), with s, σ and s_w be defined according to (6.6), (6.11) and (6.15) respectively, is proposed as follows:

$$\dot{u} = (I_m - \gamma M_{uu}^{-1}(q) M_{au}^T(q))^{-1}(-\lambda_w \dot{w} - (\Xi_M + \eta)\,\mathrm{sign}\, s_w), \tag{6.17}$$

$$v = (2\Psi_M + \eta)\,\mathrm{sign}\left(\sigma - \tfrac{1}{2}\sigma_M\right). \tag{6.18}$$

Figure 6.1 illustrates the architecture of 2-SMC for offshore crane systems.

6.2.2 Stability analysis

Stabilisation of the system (6.12) on the sliding manifold $\dot{\sigma} = \sigma = 0$ can be determined by the boundedness of the term $\ddot{s}$. From (6.7), (6.8) and (6.9), the second order derivative of the sliding function can be expressed as a function of t, q, $\dot{q}$ and u, that is,

$$\ddot{s} = \Psi(t, q, \dot{q}, u).$$

From the boundedness of matrix $M(q)$ and vector $f(q,\dot{q})$, the entries of the second derivative of the sliding function can be upper bounded such as

$$|\ddot{s}_i| \leq \Psi_{M_i}. \tag{6.19}$$

To prove the stability of the equivalent system by means of control algorithm (6.17), we choose the following Lyapunov function candidate

$$V_w = \frac{1}{2} s_w^T s_w.$$

Then, the derivative of V_w is

$$\begin{aligned}
\dot{V}_w =& s_w^T \dot{s}_w \\
=& s_w^T \left[(I_m - \gamma M_{uu}^{-1}(q) M_{au}^T(q)) \dot{u} + \xi(t,q,\dot{q},u) + \lambda_w \dot{w} \right] \\
=& s_w^T \left[\xi(t,q,\dot{q},u) - (\Xi_M + \eta) \operatorname{sign} s_w \right] \\
\leq& - \sum_{i=1}^{m} \Big((\Xi_{M_i} + \eta_i) - \xi_i(t,q,\dot{q},u) \Big) |s_{w_i}| \\
\leq& - \sum_{i=1}^{m} \eta_i |s_{w_i}|
\end{aligned}$$

which implies that the surface $s_w = 0$ is globally reached in a finite time.

6.3 Results and discussion

The control law (6.17), (6.18) is applied to the offshore gantry crane and offshore boom crane described in Section 3.3.2 and Section 3.4.2, respectively.

6.3.1 Offshore gantry crane

Consider the offshore gantry crane system (3.13). From (6.6), the vector of sliding function is chosen as

$$s = \begin{bmatrix} s_1 \\ s_2 \\ s_3 \end{bmatrix} = \begin{bmatrix} \dot{y} - \dot{y}^d + \lambda_1 (y - y^d) + \gamma \dot{\theta} + \lambda_4 \theta \\ \dot{l} - \dot{l}^d + \lambda_2 (l - l^d) \\ \dot{\delta} + \lambda_3 \delta \end{bmatrix}. \tag{6.20}$$

The values of the offshore gantry crane parameters are listed as $m_c = 6000$ kg, $m_p = 20000$ kg, $h_t = 10$ m, $x = 5$ m, $a = 0.5$ m, $b = 4$ m, $F_{\delta 0} = 8000$ N, and $g = 9.81$ m/s^2. The vessel's motion (ζ, ϕ, ψ) is considered as disturbance in which its amplitude is based on certain scenarios. The controller parameters used in the simulations are $\lambda_1 = 10$, $\lambda_2 = \lambda_3 = 1$, $\lambda_4 = -1$, $\gamma = 0.1$, $\lambda_{w_i} = 1$, $\Xi_{M_i} = 50 \times 10^3$, $\Psi_{M_i} = 10 \times 10^3$, $\eta_i = 30$ and $\sigma_{M_i} = 10$, $\forall i = 1, 2, 3$. The initial value of the generalised coordinates vector is chosen as $(y_0, l_0, \delta_0, \theta_0) = (0\text{m}, 10\text{m}, -0.1\text{rad}, 0\text{rad})$.

Several scenarios are considered for simulation to assess the capability of the proposed controller. The first one is the control with stationary vessel, i.e., its heave, roll and pitch are set to zero ($\zeta = 0$ m and $\phi = \psi = 0$ rad), whose responses are shown in Figure 6.2. In this case, both longitudinal and lateral swing angles are totally suppressed a few seconds after the trolley reached its reference position. The second scenario considered in the study is the control with the presence of vessel's movement such that $\zeta = 0.02 \sin 1.25t$ m, $\phi = 0.02 \sin 1.25t$ rad and $\psi = 0.01 \sin 1.25t$ rad. In practice, this situation can occur due to the presence of ocean currents. As shown in Figure 6.3, the lateral sway is suppressed to zero but the longitudinal sway keep swinging with amplitude 0.03 rad. This is due to the longitudinal sway is controlled indirectly by the control force F_y which is applied to the cart.

To demonstrate the robustness of the controller, the value of payload mass is perturbed by 10% increment. From Figure 6.4, it is shown that the cart position trajectory and swing angles responses are unaffected by the perturbation in payload mass. However, the rope length trajectory of Figure 6.4(b) is slightly affected by the payload variation with 0.02 m steady state error.

In all three scenarios, the proposed 2-SMC has provided a shorter rise time of the trolley position, which is 4.02 s, as compared to [103], which is 8.20 s. However,

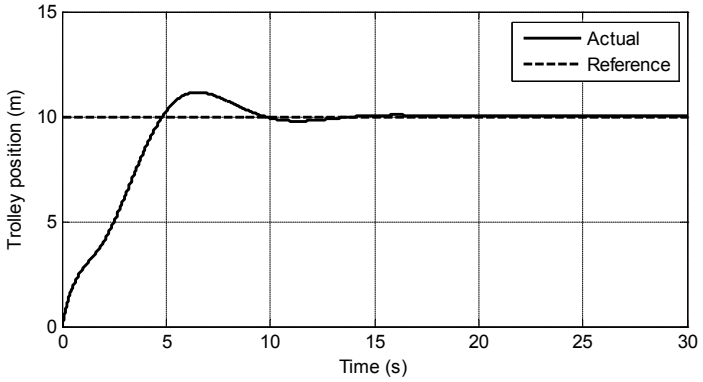

(a)

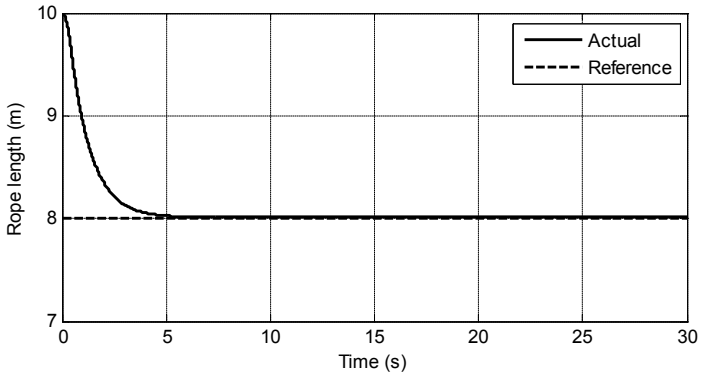

(b)

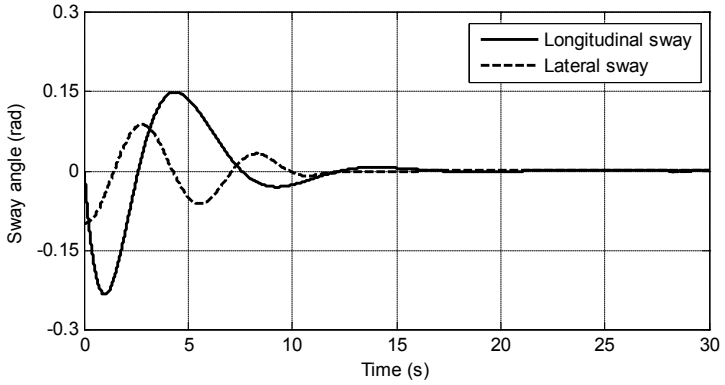

(c)

Figure 6.2 : (a) Trolley position; (b) rope length; and (c) swing angles; when the mobile harbour is stationary, i.e. $\zeta = 0$ m and $\phi = \psi = 0$ rad.

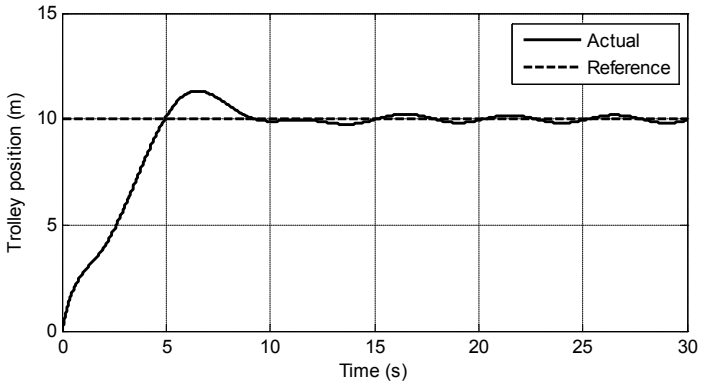

(a)

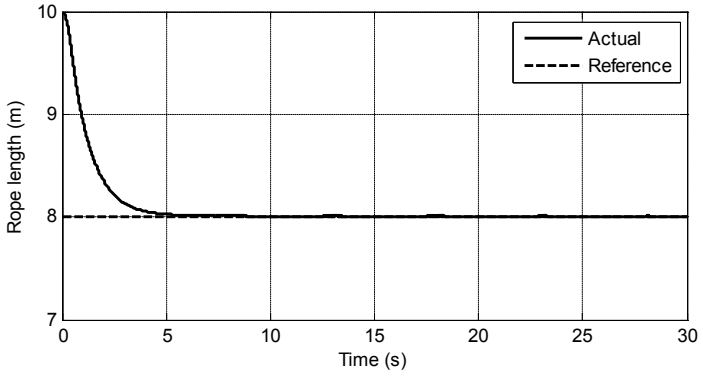

(b)

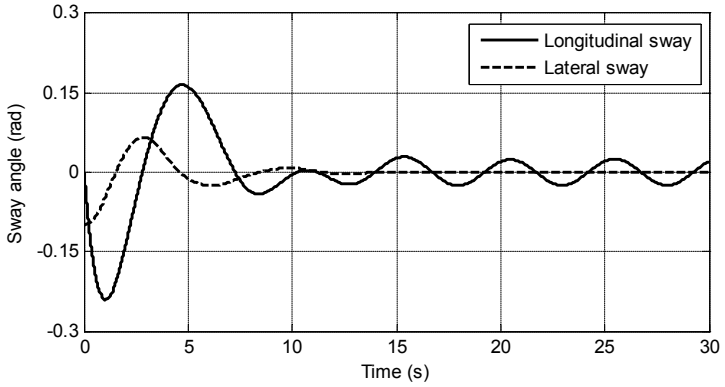

(c)

Figure 6.3 : (a) Trolley position; (b) rope length; and (c) swing angles; when $\zeta = 0.02 \sin 1.25t$ m, $\phi = 0.02 \sin 1.25t$ rad and $\psi = 0.01 \sin 1.25t$ rad.

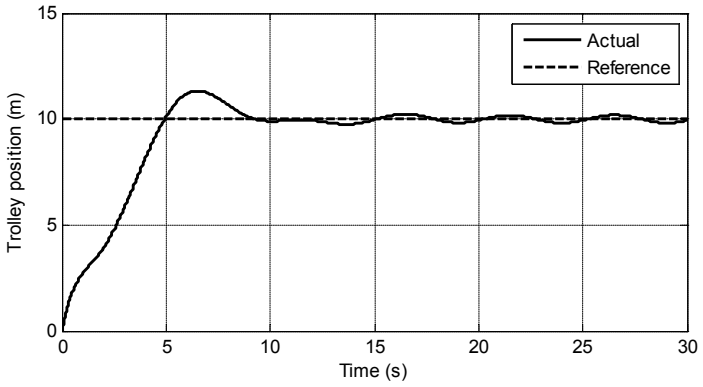

(a)

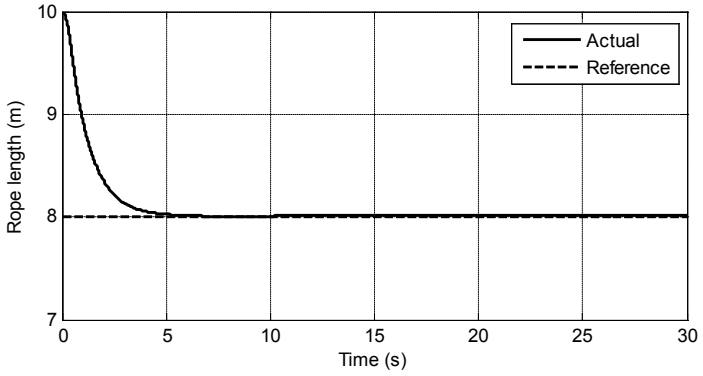

(b)

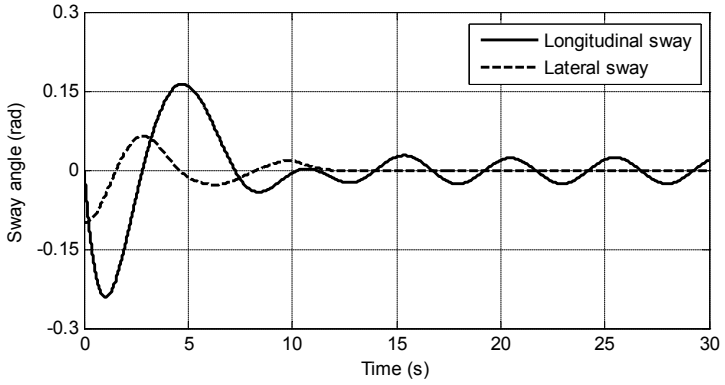

(c)

Figure 6.4 : (a) Trolley position and payload mass; (b) rope length; and (c) swing angles; when $\zeta = 0.02 \sin 1.25t$ m, $\phi = 0.02 \sin 1.25t$ rad, $\psi = 0.01 \sin 1.25t$ rad, and $\Delta m/m = 10\%$.

this faster response comes at the cost of 10.1% overshoot.

6.3.2 Offshore boom crane

Here, we consider the offshore boom crane system (3.17). From (6.6), the sliding function for the 2-SMC is chosen as

$$s = \begin{bmatrix} s_1 \\ s_2 \\ s_3 \end{bmatrix} = \begin{bmatrix} \dot{\alpha} - \dot{\alpha}^d + \lambda_1(\alpha - \alpha^d) + \gamma_1\dot{\delta}_1 - \lambda_4\delta_1 \\ \dot{\beta} - \dot{\beta}^d + \lambda_2(\beta - \beta^d) + \gamma_2\dot{\delta}_2 - \lambda_5\delta_2 \\ \dot{l} - \dot{l}^d + \lambda_3(l - l^d) \end{bmatrix}.$$

The offshore boom crane parameters are listed as $J_\alpha = 120 \times 10^3$ kg-m^2, $J_\beta = 20 \times 10^3$ kg-m^2, $m = 10 \times 10^3$ kg, $h_t = 10$ m, $L_b = 21$ m, $b_1 = b_2 = b_4 = b_5 = 0.1$ N-m/rad-s^{-1}, $b_3 = 0.2$ N/m-s^{-1} and $g = 9.8065$ m-s^{-2}. The crane base is located on the vessel such that $p_{bx} = 20$ m, $p_{by} = 0$ m and $p_{bz} = 10$ m. The vessel's heaving, rolling and pitching are considered as disturbances, where $\zeta = 0.02 \sin 1.25t$ m and $\phi = \psi = 0.01 \sin 1.25t$ rad. The controller parameters used in the simulations are $\lambda_1 = \lambda_2 = 2$, $\lambda_3 = \lambda_4 = \lambda_5 = 1$, $\gamma_1 = \gamma_2 = 0.5$, $\lambda_{w_i} = 1$, $\Xi_{M_i} = 50 \times 10^3$, $\Psi_{M_i} = 10 \times 10^3$, $\eta_i = 30$ and $\sigma_{M_i} = 10$, $i = 1, 2, 3$. The initial value of the generalised coordinates vector are chosen as $(\alpha_0, \beta_0, l_0, \theta_{1_0}, \theta_{2_0}) = (0\text{rad}, 0.5\text{rad}, 10\text{m}, 0\text{rad}, 0\text{rad})$. The swing angles responses which will be presented in this section are the tangential pendulation and radial sway with respect to the ground coordinate frame, namely δ_1 and δ_2 respectively, as defined by (3.18). The reference trajectories are chosen such that $\alpha^d = \beta^d = 1.0$ rad and $l^d = 15$ m.

We consider several scenarios for simulation to assess the capability of the proposed controller. In the first scenario, we consider that the vessel is stationary, i.e., its heaving, rolling and pitching are set to zero ($\zeta = 0$ m, $\phi = \psi = 0$ rad), where the system responses are shown in Figure 6.5. In this case, the swing angles are suppressed to the maximum amplitude of 0.04 rad which results a small amplitude of oscillation on the slew and luff angles after they reach their references. The rope

length response reaches its reference after 4.0 s. The second scenario considered in the study is the control with the presence disturbances in the vessel, i.e., the heaving, rolling and pitching of the vessel are set as nonzero such that $\zeta = 0.02 \sin 1.25t$ m and $\phi = \psi = 0.01 \sin 1.25t$ rad. As shown in Figure 6.6(d), the maximum amplitude of the swing angles increases to 0.07 rad due to the presence of disturbances. This also results small increases in the oscillation amplitude of both slew and luff angles responses as shown in Figures 6.6(a) and Figure 6.6(b), respectively.

Additionally, the payload mass is perturbed by 10% increment in order to demonstrate the robustness of the controller. It can be seen that from Figure 6.7, the slew, the luff and the swing angles, and the rope length responses are unperturbed by the change in payload mass, which is similar with the responses in Figure 6.6.

6.4 Summary

A robust control scheme has been proposed for 3-D offshore gantry crane and boom crane. From a chosen sliding surface vector, a 2-SMC law has been proposed, and the asymptotic stability of the equivalent system in the Lyapunov sense has been presented. Good performance in trajectory tracking and swing angle suppression are obtained either when the vessels are stationary or moving with heave, roll and pitch motions. Robust control performances have been obtained when the systems are subjected to payload variations. Simulation results are provided to demonstrate the effectiveness of the proposed control method.

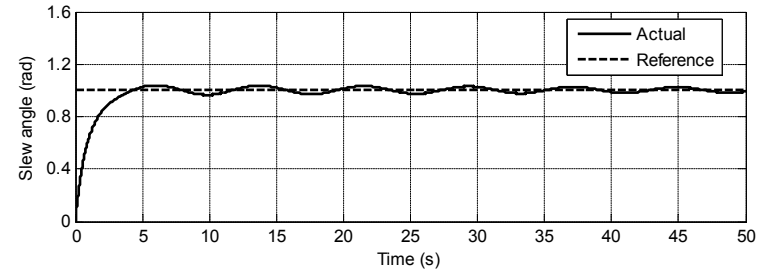

(a)

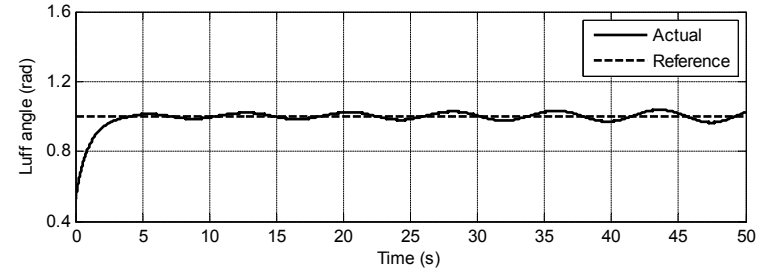

(b)

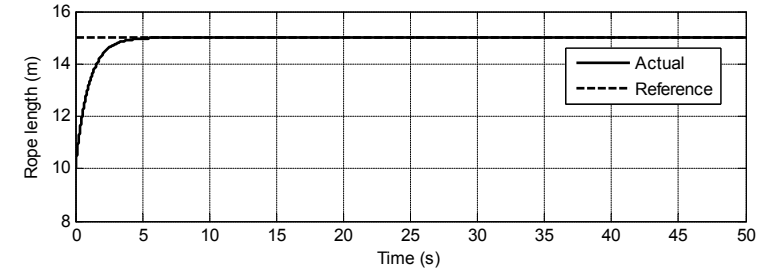

(c)

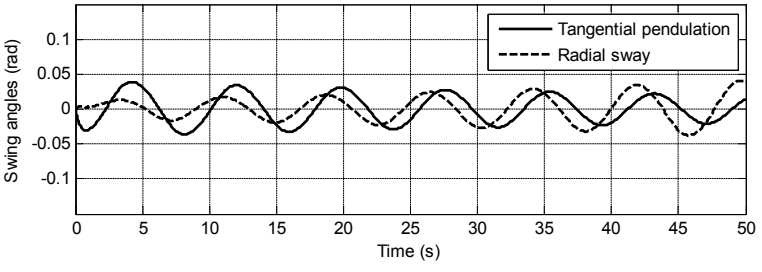

(d)

Figure 6.5 : (a) Slew angle; (b) luff angle; (c) rope length; and (d) swing angles; when the vessel is stationary, i.e. $\zeta = 0$ m and $\phi = \psi = 0$ rad.

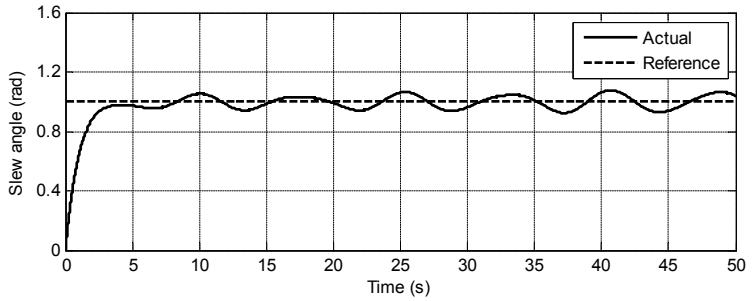

(a)

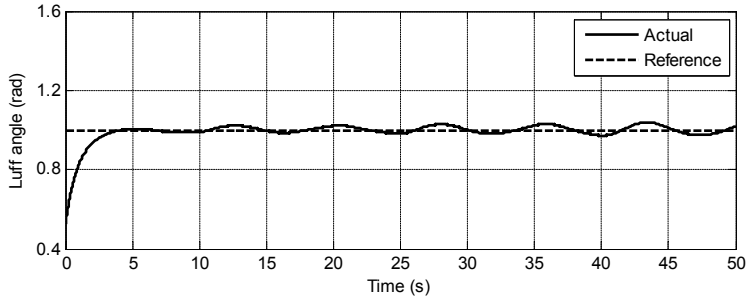

(b)

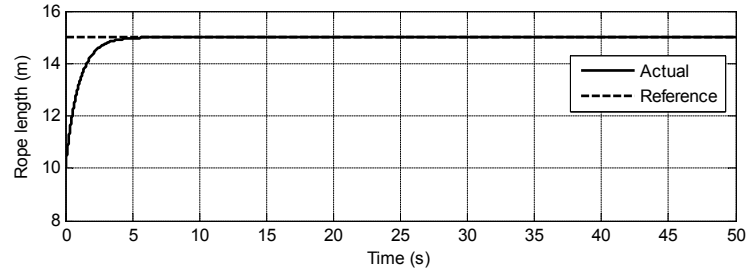

(c)

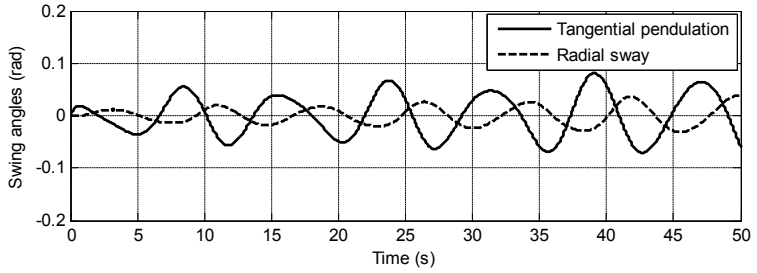

(d)

Figure 6.6 : (a) Slew angle; (b) luff angle; (c) rope length; and (d) swing angles; when $\zeta = 0.02 \sin 1.25t$ m and $\phi = \psi = 0.01 \sin 1.25t$ rad.

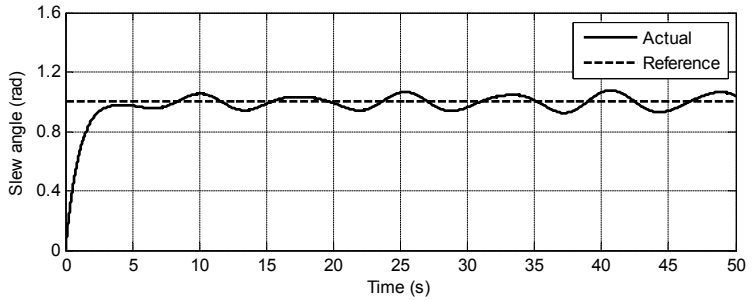

(a)

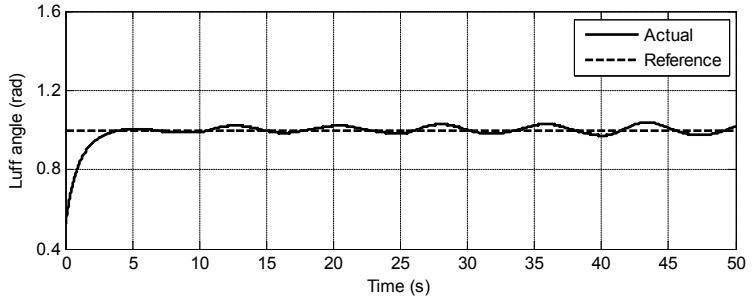

(b)

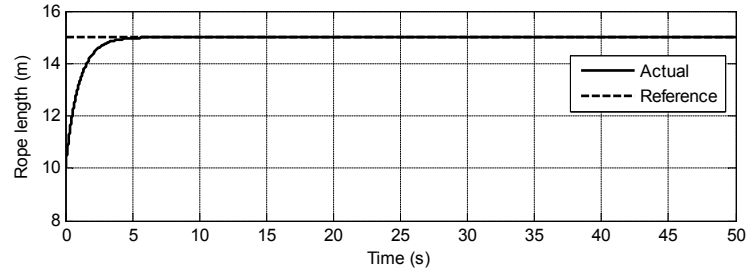

(c)

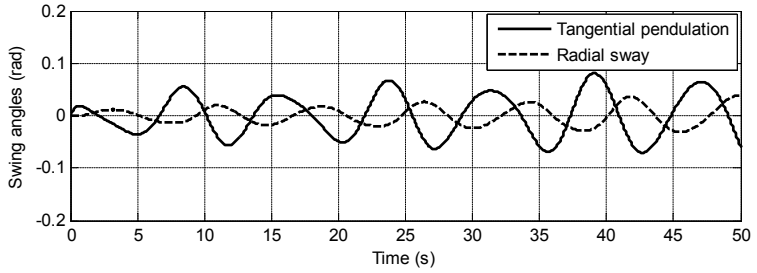

(d)

Figure 6.7 : (a) Slew angle; (b) luff angle; (c) rope length; and (d) swing angles; when $\zeta = 0.02 \sin 1.25t$ m, $\phi = \psi = 0.01 \sin 1.25t$ rad, and $\Delta m/m = 10\%$

Chapter 7

Thesis Contributions and Conclusions

7.1 Thesis contributions

The contributions of the thesis are summarised as follows:

- The two most common types of offshore cranes, namely the gantry crane and boom crane, have been considered in the study. For each crane types, 2-D and 3-D models have been developed with full system dynamics including the rope length variation. Disturbance terms due to wave-induced motion of the vessels are included in the dynamic models. The 2-D offshore crane models have been presented in uncertain linear time-invariant (LTI) forms to facilitate the first-order sliding mode control design.

- A generalisation of the second-order sliding mode control has been formulated for a class of underactuated mechanical systems (UMS) to establish a basic idea of the control technique. A second-order sliding mode observer has been proposed to estimate the state velocities subject to high-frequency noise. A generalisation of the fuzzy first-order sliding mode for a class UMS has also been developed in which the fuzzification technique has been used for model estimation in the construction of the control law.

- First-order sliding mode control laws have been proposed for 2-D offshore gantry crane and boom crane systems. By making use of the LTI forms of the offshore crane models, the sliding surfaces have been constructed based on linear quadratic regulator and linear matrix inequality design approaches.

Robust sliding mode controllers were then proposed to drive the state error trajectories to the sliding surface in a finite time and maintain it there for subsequent time.

- A second-order sliding mode control (2-SMC) law has been proposed for trajectory tracking and pendulation suppression for 3-D offshore gantry crane and boom crane systems. The controller has been constructed to deal with 5 DOF crane systems subject to vessels' roll, pitch and heave motions. From a chosen sliding surface vector, a 2-SMC control laws have been proposed, and the asymptotic stability of the equivalent system has been presented in the Lyapunov sense.

7.2 Conclusions

The main theme of this thesis is the analytical modelling and control design of offshore crane systems. The new topic of offshore crane control systems in crane automation field becomes the motivation to produce this work.

To accomplish the thesis objectives, we have developed nonlinear mathematical models of offshore gantry and boom cranes. Based on the Euler-Lagrange formulation, full system dynamics have been derived for the cranes by considering the effects of roll, pitch and heave motions of the vessels. The linearised models have also been derived to utilise the advantage of linear time invariant theoretical knowledge. In addition, the effect of wind disturbances has been considered in the offshore crane models.

Since cranes are classified as underactuated mechanical systems (UMS), the generic form of problem formulation for UMS can provide a useful conceptual framework for crane control design. For this purpose, an adaptive fuzzy sliding mode controller (AFSMC) has been proposed for a class of UMS, in which, the model with

uncertainties is approximated using fuzzy logic. Based on the Lyapunov method, the adaptive law for the controller is designed. A generic form of second-order sliding mode controller (2-SMC) for UMS has been developed as well. The sliding function for the 2-SMC is obtained from the actual and estimate states. The performances of the proposed AFSMC and 2-SMC are evaluated by applying the control schemes to a conventional gantry crane systems.

In Chapter 5, first-order sliding mode control (1-SMC) laws have been designed for 2-D offshore cranes in the presence of vessel's rolling motion and wind flows. Two sliding function design approaches have been utilised, namely the quadratic minimisation and linear matrix inequalities (LMI) technique. Robust 1-SMC laws are proposed to drive the state variables of the system towards the sliding surface in finite time and maintain them in a small bound within a close vicinity of the sliding surface. The reference signals of crane trajectories are incorporated within the sliding mode design procedure by using the model-reference approach. This approach has been implemented to ensure the reference signals are not rejected by the sliding mode controller. Extensive simulation results are provided to illustrate the feasibility of the proposed design approach in some practical scenarios.

In Chapter 6, we have proposed a second-order sliding mode control (2-SMC) scheme for trajectory tracking and pendulation suppression control for 3-D offshore cranes with full system dynamics. The challenge in this control problem is to deal with 5 DOF crane systems in the presence of vessels' roll, pitch and heave motions. Based on the generalisation of the 2-SMC, a control law has been constructed for offshore gantry and boom cranes, and the asymptotic stability of the equivalent system has been presented. Simulations have been performed for both offshore crane systems to show that the proposed controller can deal with the aforementioned problem.

In conclusion, the sliding mode control developments throughout this thesis have shown high performances against nonlinearities and uncertainties of the systems. The results have shown that chattering alleviation can be achieved whether by using a boundary layer in 1-SMC or exploiting the advantage of 2-SMC. In spite of that, research on crane systems in marine operations remains an open problem due to various considerations can be taken into account in terms of actuator dynamics, path planning, disturbances rejection, and so on.

7.3 Future work

Potential future works in the offshore cranes automation topic can be explored in two main aspects, namely, the system modelling and control design.

Offshore cranes modelling

In the development of offshore cranes model, despite full number of DOF including rope length variation has been considered for cranes model, only three DOF are taken into account for the ships, i.e., roll, pitch and heave. We also assume that the ships are ideally held by moorings, in which, the ships' centres of gravity are only displaced from the ground reference point by heave motions. For future work, the inclusion the other three DOF of ships motion, namely, yaw, surge and sway, is recommended.

The future work may focus on the offshore boom cranes model development since they are widely used in offshore operations. Sway suppression control of boom cranes is more difficult than gantry cranes due to certain constraints in the rotational motion of the boom, such as luff angle range and angular velocity limit. Moreover, research on boom cranes is still preliminary as compared to gantry cranes in terms of the availability of lab-scale model in the experimental setup.

For the purposes of practicality, the offshore cranes model development may

include the actuators dynamics. The actuator mechanisms that commonly used in crane systems are electric, hydraulic and pneumatic actuators. The inclusion of actuator dynamics may add the relative degree in the overall system model. Hence, the higher-order sliding mode can be a good approach to tackling these problems. In addition, time-delay can also be considered in the model development.

Offshore cranes control

In offshore cranes control, more effort is required to construct robust control to deal with the harsh sea conditions. In fact, the magnitude of wind disturbance is more difficult to estimate as compared to ocean waves that can be assumed as sinusoidal.

Offshore cranes control for underwater load placement operations is a challenging, yet an interesting topic to be explored. In this particular problem, the designer must consider the effects of ocean current and buoyancy to payload position underwater. The presence of ship motions during underwater conveying may also be considered as system disturbances.

In most of the works on offshore cranes from the literature and some parts of this thesis, step reference inputs have been used for trajectory tracking problems. Cranes path planning can be important in some circumstances, e.g., to avoid obstacles during load transfer operation. The reference trajectories other than step functions may pose a more challenging problem in terms of sway amplitudes. Additionally, the optimal trajectories for offshore cranes to minimise sway can further be investigated.

Bibliography

[1] E. M. Abdel-Rahman, A. H. Nayfeh, and Z. N. Masoud, "Dynamics and control of cranes: A review," *Journal of Vibration and Control*, vol. 9, no. 7, pp. 863–908, 2003.

[2] M. M. Abdelhameed, "Enhancement of sliding mode controller by fuzzy logic with application to robotic manipulators," *Mechatronics*, vol. 15, no. 4, pp. 439–458, 2005.

[3] J. Adamy and A. Flemming, "Soft variable-structure controls: a survey," *Automatica*, vol. 40, no. 11, pp. 1821–1844, 2004.

[4] Y. M. Al-Sweiti and D. Söffker, "Planar cargo control of elastic ship cranes with the "Maryland rigging" system," *Journal of Vibration and Control*, vol. 13, no. 3, pp. 241–267, 2007.

[5] N. B. Almutairi and M. Zribi, "Sliding mode control of a three-dimensional overhead crane," *Journal of Vibration and Control*, vol. 15, no. 11, pp. 1679–1730, 2009.

[6] J. Alvarez, I. Orlov, and L. Acho, "An invariance principle for discontinuous dynamic systems with application to a coulomb friction oscillator," *Journal of Dynamic Systems, Measurement, and Control*, vol. 122, no. 4, pp. 687–690, 2000.

[7] H. Ashrafiuon, K. Muske, L. McNinch, and R. Soltan, "Sliding-mode tracking control of surface vessels," *IEEE Transactions on Industrial Electronics*,

vol. 55, no. 11, pp. 4004–4012, 2008.

[8] H. Ashrafiuon and R. S. Erwin, "Sliding mode control of underactuated multibody systems and its application to shape change control," *International Journal of Control*, vol. 81, no. 12, pp. 1849–1858, 2008.

[9] A. Astolfi, "Discontinuous control of nonholonomic systems," *Systems & Control Letters*, vol. 27, no. 1, pp. 37–45, 1996.

[10] S. Bag, S. Spurgeon, and C. Edwards, "Output feedback sliding mode design for linear uncertain systems," *IEE Proceedings - Control Theory and Applications*, vol. 144, no. 3, pp. 209–216, 1997.

[11] G. Bartolini, A. Ferrara, A. Pisano, and E. Usai, "Adaptive learning and control using sliding modes," *Journal of Applied Mathematics and Computer Science*, vol. 8, no. 1, pp. 51–71, 1998.

[12] G. Bartolini, A. Ferrara, and E. Punta, "Multi-input second-order sliding-mode hybrid control of constrained manipulators," *Dynamics and Control*, vol. 10, no. 3, pp. 277–296, 2000.

[13] G. Bartolini, A. Pisano, and E. Usai, "First and second derivative estimation by sliding mode technique," *Journal of Signal Processing*, vol. 4, no. 2, pp. 167–176, 2000.

[14] G. Bartolini and A. Pisano, "Black-box position and attitude tracking for underwater vehicles by second-order sliding-mode technique," *International Journal of Robust and Nonlinear Control*, vol. 20, no. 14, pp. 1594–1609, 2010.

[15] G. Bartolini, A. Pisano, E. Punta, and E. Usai, "A survey of applications of second-order sliding mode control to mechanical systems," *International Journal of Control*, vol. 76, no. 9-10, pp. 875–892, 2003.

[16] G. Bartolini, A. Pisano, and E. Usai, "Second-order sliding-mode control of container cranes," *Automatica*, vol. 38, no. 10, pp. 1783–1790, 2002.

[17] G. Bartolini, E. Punta, and T. Zolezzi, "Multi-input sliding mode control of nonlinear uncertain affine systems," *International Journal of Control*, vol. 84, no. 5, pp. 867–875, 2011.

[18] D. Blackburn, W. Singhose, J. Kitchen, V. Patrangenaru, J. Lawrence, T. Kamoi, and A. Taura, "Command shaping for nonlinear crane dynamics," *Journal of Vibration and Control*, vol. 16, no. 4, pp. 477–501, 2010.

[19] A. Bloch, D. E. Chang, N. Leonard, and J. Marsden, "Controlled Lagrangians and the stabilization of mechanical systems. II. Potential shaping," *IEEE Transactions on Automatic Control*, vol. 46, no. 10, pp. 1556–1571, 2001.

[20] A. Bloch, N. Leonard, and J. Marsden, "Controlled lagrangians and the stabilization of mechanical systems. i. the first matching theorem," *IEEE Transactions on Automatic Control*, vol. 45, no. 12, pp. 2253–2270, 2000.

[21] A. Bloch, M. Reyhanoglu, and N. McClamroch, "Control and stabilization of nonholonomic dynamic systems," *IEEE Transactions on Automatic Control*, vol. 37, no. 11, pp. 1746–1757, 1992.

[22] M. Canale, L. Fagiano, A. Ferrara, and C. Vecchio, "Vehicle yaw control via second-order sliding-mode technique," *IEEE Transactions on Industrial Electronics*, vol. 55, no. 11, pp. 3908–3916, 2008.

[23] L. M. Capisani, A. Ferrara, and L. Magnani, "Design and experimental validation of a second-order sliding-mode motion controller for robot manipulators," *International Journal of Control*, vol. 82, no. 2, pp. 365–377, 2009.

[24] O. Cerman and P. Hušek, "Adaptive fuzzy sliding mode control for electro-hydraulic servo mechanism," *Expert Systems with Applications*, vol. 39, no. 11, pp. 10 269–10 277, 2012.

[25] C.-Y. Chang and K.-H. Chiang, "Fuzzy projection control law and its application to the overhead crane," *Mechatronics*, vol. 18, no. 10, pp. 607–615, 2008.

[26] D. E. Chang, "Stabilizability of controlled Lagrangian systems of two degrees of freedom and one degree of under-actuation by the energy-shaping method," *IEEE Transactions on Automatic Control*, vol. 55, no. 8, pp. 1888–1893, 2010.

[27] Y.-F. Chen and A.-C. Huang, "Controller design for a class of underactuated mechanical systems," *IET Control Theory Applications*, vol. 6, no. 1, pp. 103–110, 2012.

[28] Y. Chitour, "Time-varying high-gain observers for numerical differentiation," *IEEE Transactions on Automatic Control*, vol. 47, no. 9, pp. 1565–1569, 2002.

[29] H. H. Choi, "Variable structure output feedback control design for a class of uncertain dynamic systems," *Automatica*, vol. 38, no. 2, pp. 335–341, 2002.

[30] H. H. Choi, "LMI-based sliding surface design for integral sliding mode control of mismatched uncertain systems," *IEEE Transactions on Automatic Control*, vol. 52, no. 4, pp. 736–742, 2007.

[31] C. Cornejo and L. Alvarez-Icaza, "Passivity based control of under-actuated mechanical systems with nonlinear dynamic friction," *Journal of Vibration and Control*, vol. 18, no. 7, pp. 1025–1042, 2012.

[32] B. d'Andréa Novel, F. Boustany, F. Conrad, and B. Rao, "Feedback stabilization of a hybrid PDE-ODE system: Application to an overhead

crane," *Mathematics of Control, Signals and Systems*, vol. 7, no. 1, pp. 1–22, 1994.

[33] M. Das and C. Mahanta, "Optimal second order sliding mode control for linear uncertain systems," *ISA Transactions*, vol. 53, no. 6, pp. 1807–1815, 2014.

[34] J. Davila, L. Fridman, and A. Levant, "Second-order sliding-mode observer for mechanical systems," *IEEE Transactions on Automatic Control*, vol. 50, no. 11, pp. 1785–1789, 2005.

[35] R. Delpoux and T. Floquet, "High-order sliding mode control for sensorless trajectory tracking of a PMSM," *International Journal of Control*, vol. 87, no. 10, pp. 2140–2155, 2014.

[36] K. Do, Z.-P. Jiang, and J. Pan, "Underactuated ship global tracking under relaxed conditions," *IEEE Transactions on Automatic Control*, vol. 47, no. 9, pp. 1529–1536, 2002.

[37] K. Do, Z. Jiang, and J. Pan, "Robust adaptive path following of underactuated ships," *Automatica*, vol. 40, no. 6, pp. 929–944, 2004.

[38] K. Do and J. Pan, "Global tracking control of underactuated ships with nonzero off-diagonal terms in their system matrices," *Automatica*, vol. 41, no. 1, pp. 87–95, 2005.

[39] K. Do and J. Pan, "Global robust adaptive path following of underactuated ships," *Automatica*, vol. 42, no. 10, pp. 1713–1722, 2006.

[40] K. Do and J. Pan, "Nonlinear control of an active heave compensation system," *Ocean Engineering*, vol. 35, no. 56, pp. 558–571, 2008.

[41] W. Dong, "Cooperative control of underactuated surface vessels," *IET Control Theory Applications*, vol. 4, no. 9, pp. 1569–1580, 2010.

[42] W. Dong and Y. Guo, "Global time-varying stabilization of underactuated surface vessel," *IEEE Transactions on Automatic Control*, vol. 50, no. 6, pp. 859–864, 2005.

[43] F. R. Driscoll, M. Nahon, and R. G. Lueck, "A comparison of ship-mounted and cage-mounted passive heave compensation systems," *Journal of Offshore Mechanics and Arctic Engineering*, vol. 122, no. 3, pp. 214–221, 2000.

[44] C. Edwards and S. K. Spurgeon, *Sliding mode control: Theory and applications*. London: Taylor & Francis, 1998.

[45] M. Ö. Efe, C. Ünsal, O. Kaynak, and X. Yu, "Variable structure control of a class of uncertain systems," *Automatica*, vol. 40, no. 1, pp. 59–64, 2004.

[46] M. Efe, "Fractional fuzzy adaptive sliding-mode control of a 2-DOF direct-drive robot arm," *IEEE Transactions on Systems, Man, and Cybernetics, Part B: Cybernetics*, vol. 38, no. 6, pp. 1561–1570, 2008.

[47] S. Emel'yanov, S. Korovin, and A. Levant, "High-order sliding modes in control systems," *Computational Mathematics and Modeling*, vol. 7, pp. 294–318, 1996.

[48] A. Estrada and F. Plestan, "Second order sliding mode output feedback control with switching gains - Application to the control of a pneumatic actuator," *Journal of the Franklin Institute*, vol. 351, no. 4, pp. 2335–2355, 2014, special Issue on 2010-2012 Advances in Variable Structure Systems and Sliding Mode Algorithms.

[49] F. Fahimi, "Sliding-mode formation control for underactuated surface vessels," *IEEE Transactions on Robotics*, vol. 23, no. 3, pp. 617–622, 2007.

[50] L. Fan, W. W. Wilson, and B. Dahl, "Congestion, port expansion and spatial competition for US container imports," *Transportation Research Part E: Logistics and Transportation Review*, vol. 48, no. 6, pp. 1121–1136, 2012.

[51] Y. Fang, W. Dixon, D. Dawson, and E. Zergeroglu, "Nonlinear coupling control laws for an underactuated overhead crane system," *IEEE/ASME Transactions on Mechatronics*, vol. 8, no. 3, pp. 418–423, 2003.

[52] Y. Fang, B. Ma, P. Wang, and X. Zhang, "A motion planning-based adaptive control method for an underactuated crane system," *IEEE Transactions on Control Systems Technology*, vol. 20, no. 1, pp. 241–248, 2012.

[53] Y. Fang, P. Wang, N. Sun, and Y. Zhang, "Dynamics analysis and nonlinear control of an offshore boom crane," *IEEE Transactions on Industrial Electronics*, vol. 61, no. 1, pp. 414–427, 2014.

[54] Y. Feng, X. Han, Y. Wang, and X. Yu, "Second-order terminal sliding mode control of uncertain multivariable systems," *International Journal of Control*, vol. 80, no. 6, pp. 856–862, 2007.

[55] R. Fierro, F. Lewis, and A. Lowe, "Hybrid control for a class of underactuated mechanical systems," *IEEE Transactions on Systems, Man and Cybernetics, Part A: Systems and Humans*, vol. 29, no. 6, pp. 649–654, 1999.

[56] S. Garrido, M. Abderrahim, A. Gimenez, R. Diez, and C. Balaguer, "Anti-swinging input shaping control of an automatic construction crane," *IEEE Transactions on Automation Science and Engineering*, vol. 5, no. 3, pp. 549–557, 2008.

[57] J. Ghommam and F. Mnif, "Coordinated path-following control for a group of underactuated surface vessels," *IEEE Transactions on Industrial Electronics*, vol. 56, no. 10, pp. 3951–3963, 2009.

[58] J. Ghommam, F. Mnif, A. Benali, and N. Derbel, "Asymptotic backstepping stabilization of an underactuated surface vessel," *IEEE Transactions on Control Systems Technology*, vol. 14, no. 6, pp. 1150–1157, 2006.

[59] J. Ghommam, F. Mnif, and N. Derbel, "Global stabilisation and tracking control of underactuated surface vessels," *IET Control Theory Applications*, vol. 4, no. 1, pp. 71–88, 2010.

[60] A. Giua, C. Seatzu, and G. Usai, "Observer-controller design for cranes via Lyapunov equivalence," *Automatica*, vol. 35, no. 4, pp. 669–678, 1999.

[61] Y. Guo and P.-Y. Woo, "An adaptive fuzzy sliding mode controller for robotic manipulators," *IEEE Transactions on Systems, Man and Cybernetics, Part A: Systems and Humans*, vol. 33, no. 2, pp. 149–159, 2003.

[62] Q. P. Ha, D. Rye, and H. Durrant-Whyte, "Fuzzy moving sliding mode control with application to robotic manipulators," *Automatica*, vol. 35, no. 4, pp. 607–616, 1999.

[63] Y. Hacioglu, Y. Z. Arslan, and N. Yagiz, "MIMO fuzzy sliding mode controlled dual arm robot in load transportation," *Journal of the Franklin Institute*, vol. 348, no. 8, pp. 1886–1902, 2011.

[64] J. Hamalainen, A. Marttinen, L. Baharova, and J. Virkkunen, "Optimal path planning for a trolley crane: fast and smooth transfer of load," *IEE Proceedings - Control Theory and Applications*, vol. 142, no. 1, pp. 51–57, 1995.

[65] X. Han, E. Fridman, and S. Spurgeon, "Sliding-mode control of uncertain systems in the presence of unmatched disturbances with applications," *International Journal of Control*, vol. 83, no. 12, pp. 2413–2426, 2010.

[66] J. Hatleskog and M. Dunnigan, "Passive compensator load variation for deep-water drilling," *IEEE Journal of Oceanic Engineering*, vol. 32, no. 3, pp. 593–602, 2007.

[67] R. Henry, Z. Masoud, A. Nayfeh, and D. Mook, "Cargo pendulation reduction on ship-mounted cranes via boom-luff angle actuation," *Journal of Vibration and Control*, vol. 7, no. 8, pp. 1253–1264, 2001.

[68] J. Huang, X. Xie, and Z. Liang, "Control of bridge cranes with distributed-mass payload dynamics," *IEEE/ASME Transactions on Mechatronics*, vol. 20, no. 1, pp. 481–486, 2015.

[69] J. Hung, W. Gao, and J. Hung, "Variable structure control: a survey," *IEEE Transactions on Industrial Electronics*, vol. 40, no. 1, pp. 2–22, 1993.

[70] C.-L. Hwang, "A novel Takagi-Sugeno-based robust adaptive fuzzy sliding-mode controller," *IEEE Transactions on Fuzzy Systems*, vol. 12, no. 5, pp. 676–687, 2004.

[71] C.-L. Hwang, C.-C. Chiang, and Y.-W. Yeh, "Adaptive fuzzy hierarchical sliding-mode control for the trajectory tracking of uncertain underactuated nonlinear dynamic systems," *IEEE Transactions on Fuzzy Systems*, vol. 22, no. 2, pp. 286–299, 2014.

[72] Z.-P. Jiang, "Global tracking control of underactuated ships by Lyapunov's direct method," *Automatica*, vol. 38, no. 2, pp. 301–309, 2002.

[73] T. Johansen, T. Fossen, S. I. Sagatun, and F. Nielsen, "Wave synchronizing crane control during water entry in offshore moonpool operations - experimental results," *IEEE Journal of Oceanic Engineering*, vol. 28, no. 4, pp. 720–728, 2003.

[74] G. Y. Ke, K. W. Li, and K. W. Hipel, "An integrated multiple criteria preference ranking approach to the Canadian west coast port congestion conflict," *Expert Systems with Applications*, vol. 39, no. 10, pp. 9181–9190, 2012.

[75] B. Kimiaghalam, A. Homaifar, M. Bikdash, and B. R. Hunt, "Feedforward control law for a shipboard crane with Maryland rigging system," *Journal of Vibration and Control*, vol. 8, no. 2, pp. 159–188, 2002.

[76] S. Küchler, T. Mahl, J. Neupert, K. Schneider, and O. Sawodny, "Active control for an offshore crane using prediction of the vessel's motion," *IEEE/ASME Transactions on Mechatronics*, vol. 16, no. 2, pp. 297–309, 2011.

[77] P. Kundu, *Fluid mechanics*. Waltham, MA: Academic Press, 2012.

[78] C.-C. Kung and T.-H. Chen, "Observer-based indirect adaptive fuzzy sliding mode control with state variable filters for unknown nonlinear dynamical systems," *Fuzzy Sets and Systems*, vol. 155, no. 2, pp. 292–308, 2005.

[79] C.-L. Kuo, T.-H. Li, and N. Guo, "Design of a novel fuzzy sliding-mode control for magnetic ball levitation system," *Journal of Intelligent and Robotic Systems*, vol. 42, no. 3, pp. 295–316, 2005.

[80] S. Labiod, M. S. Boucherit, and T. M. Guerra, "Adaptive fuzzy control of a class of MIMO nonlinear systems," *Fuzzy Sets and Systems*, vol. 151, no. 1, pp. 59–77, 2005.

[81] E. Lataire, M. Vantorre, G. Delefortrie, and M. Candries, "Mathematical modelling of forces acting on ships during lightering operations," *Ocean Engineering*, vol. 55, pp. 101–115, 2012.

[82] E. Lefeber, K. Pettersen, and H. Nijmeijer, "Tracking control of an underactuated ship," *IEEE Transactions on Control Systems Technology*, vol. 11, no. 1, pp. 52–61, 2003.

[83] A. Levant, "Sliding order and sliding accuracy in sliding mode control," *International Journal of Control*, vol. 58, no. 6, pp. 1247–1263, 1993.

[84] A. Levant, "Robust exact differentiation via sliding mode technique," *Automatica*, vol. 34, no. 3, pp. 379–384, 1998.

[85] A. Levant, "Higher-order sliding modes, differentiation and output-feedback control," *International Journal of Control*, vol. 76, no. 9-10, pp. 924–941, 2003.

[86] A. Levant, "Principles of 2-sliding mode design," *Automatica*, vol. 43, no. 4, pp. 576–586, 2007.

[87] T.-H. S. Li and Y.-C. Huang, "MIMO adaptive fuzzy terminal sliding-mode controller for robotic manipulators," *Information Sciences*, vol. 180, no. 23, pp. 4641–4660, 2010.

[88] W.-S. Lin and C.-S. Chen, "Robust adaptive sliding mode control using fuzzy modelling for a class of uncertain MIMO nonlinear systems," *IEE Proceedings - Control Theory and Applications*, vol. 149, no. 3, pp. 193–201, 2002.

[89] D. Liu, J. Yi, D. Zhao, and W. Wang, "Adaptive sliding mode fuzzy control for a two-dimensional overhead crane," *Mechatronics*, vol. 15, no. 5, pp. 505–522, 2005.

[90] Y. Liu and H. Yu, "A survey of underactuated mechanical systems," *IET Control Theory Applications*, vol. 7, no. 7, pp. 921–935, 2013.

[91] M. López-Martínez, J. Acosta, and J. Cano, "Non-linear sliding mode surfaces for a class of underactuated mechanical systems [Brief Paper]," *IET Control Theory Applications*, vol. 4, no. 10, pp. 2195–2204, 2010.

[92] K. Ma, "Comments on "quasi-continuous higher order sliding-mode controllers for spacecraft-attitude-tracking maneuvers"," *IEEE Transactions on Industrial Electronics*, vol. 60, no. 7, pp. 2771–2773, 2013.

[93] M. Manceur, N. Essounbouli, and A. Hamzaoui, "Second-order sliding fuzzy interval type-2 control for an uncertain system with real application," *IEEE Transactions on Fuzzy Systems*, vol. 20, no. 2, pp. 262–275, 2012.

[94] R. Martinez, J. Alvarez, and Y. Orlov, "Hybrid sliding-mode-based control of underactuated systems with dry friction," *IEEE Transactions on Industrial Electronics*, vol. 55, no. 11, pp. 3998–4003, 2008.

[95] R. Martinez and J. Alvarez, "A controller for 2-DOF underactuated mechanical systems with discontinuous friction," *Nonlinear Dynamics*, vol. 53, no. 3, pp. 191–200, 2008.

[96] Z. Masoud, A. Nayfeh, and D. Mook, "Cargo pendulation reduction of ship-mounted cranes," *Nonlinear Dynamics*, vol. 35, no. 3, pp. 299–311, 2004.

[97] S. Messineo, F. Celani, and O. Egeland, "Crane feedback control in offshore moonpool operations," *Control Engineering Practice*, vol. 16, no. 3, pp. 356–364, 2008.

[98] S. Messineo and A. Serrani, "Offshore crane control based on adaptive external models," *Automatica*, vol. 45, no. 11, pp. 2546–2556, 2009.

[99] S. Mondal and C. Mahanta, "Nonlinear sliding surface based second order sliding mode controller for uncertain linear systems," *Communications in*

Nonlinear Science and Numerical Simulation, vol. 16, no. 9, pp. 3760–3769, 2011.

[100] K. Muske, H. Ashrafiuon, S. Nersesov, and M. Nikkhah, "Optimal sliding mode cascade control for stabilization of underactuated nonlinear systems," *Journal of Dynamic Systems, Measurement, and Control*, vol. 134, no. 2, pp. 021 020–1 – 021 020–11, 2012.

[101] V. Nekoukar and A. Erfanian, "Adaptive fuzzy terminal sliding mode control for a class of MIMO uncertain nonlinear systems," *Fuzzy Sets and Systems*, vol. 179, no. 1, pp. 34–49, 2011.

[102] S. G. Nersesov, H. Ashrafiuon, and P. Ghorbanian, "On estimation of the domain of attraction for sliding mode control of underactuated nonlinear systems," *International Journal of Robust and Nonlinear Control*, 2012.

[103] Q. Ngo and K. Hong, "Sliding-mode antisway control of an offshore container crane," *IEEE/ASME Transactions on Mechatronics*, vol. 17, no. 2, pp. 201–209, 2012.

[104] H. M. Omar and A. H. Nayfeh, "Gantry cranes gain scheduling feedback control with friction compensation," *Journal of Sound and Vibration*, vol. 281, no. 1-2, pp. 1–20, 2005.

[105] Y. Orlov, L. Aguilar, and J. C. Cadiou, "Switched chattering control vs. backlash/friction phenomena in electrical servo-motors," *International Journal of Control*, vol. 76, no. 9-10, pp. 959–967, 2003.

[106] R. Ortega, M. Spong, F. Gomez-Estern, and G. Blankenstein, "Stabilization of a class of underactuated mechanical systems via interconnection and damping assignment," *IEEE Transactions on Automatic Control*, vol. 47, no. 8, pp. 1218–1233, 2002.

[107] M. Osiński and S. Wojciech, "Application of nonlinear optimisation methods to input shaping of the hoist drive of an off-shore crane," *Nonlinear Dynamics*, vol. 17, no. 4, pp. 369–386, 1998.

[108] S. Oucheriah, "Robust exponential convergence of a class of linear delayed systems with bounded controllers and disturbances," *Automatica*, vol. 42, no. 11, pp. 1863–1867, 2006.

[109] V. Panchade, R. Chile, and B. Patre, "A survey on sliding mode control strategies for induction motors," *Annual Reviews in Control*, vol. 37, no. 2, pp. 289–307, 2013.

[110] G. Parker, M. Graziano, F. Leban, J. Green, and J. Bird, "Reducing crane payload swing using a rider block tagline control system," in *OCEANS 2007 - Europe*, June 2007, pp. 1–5.

[111] K. Y. Pettersen and H. Nijmeijer, "Underactuated ship tracking control: Theory and experiments," *International Journal of Control*, vol. 74, no. 14, pp. 1435–1446, 2001.

[112] A. Pisano and E. Usai, "Sliding mode control: A survey with applications in math," *Mathematics and Computers in Simulation*, vol. 81, no. 5, pp. 954–979, 2011.

[113] Port Consultants Rotterdam, "Procurement Container Handling Cranes - Port El Sokhna, Egypt," 2014, [Online; accessed 17-November-2014].

[114] C. D. Rahn, F. Zhang, S. Joshi, and D. M. Dawson, "Asymptotically stabilizing angle feedback for a flexible cable gantry crane," *Journal of Dynamic Systems, Measurement, and Control*, vol. 121, no. 3, pp. 563–566, 1999.

[115] R. Raja Ismail and Q. P. Ha, "Trajectory tracking and anti-sway control of three-dimensional offshore boom cranes using second-order sliding modes,"

in *IEEE International Conference on Automation Science and Engineering (CASE)*, 2013, pp. 996–1001.

[116] R. Raja Ismail, N. D. That, and Q. P. Ha, "Offshore container crane systems with robust optimal sliding mode control," in *International Symposium on Automation and Robotics in Construction and Mining (ISARC)*, 2014, pp. 149–156.

[117] M. Ravichandran and A. Mahindrakar, "Robust stabilization of a class of underactuated mechanical systems using time scaling and Lyapunov redesign," *Industrial Electronics, IEEE Transactions on*, vol. 58, no. 9, pp. 4299–4313, 2011.

[118] M. Roopaei, M. Zolghadri, and S. Meshksar, "Enhanced adaptive fuzzy sliding mode control for uncertain nonlinear systems," *Communications in Nonlinear Science and Numerical Simulation*, vol. 14, no. 910, pp. 3670–3681, 2009.

[119] E. Ryan and M. Corless, "Ultimate boundedness and asymptotic stability of a class of uncertain dynamical systems via continuous and discontinuous feedback control," *IMA Journal of Mathematical Control and Information*, vol. 1, no. 3, pp. 223–242, 1984.

[120] S. I. Sagatun, "Active control of underwater installation," *IEEE Transactions on Control Systems Technology*, vol. 10, no. 5, pp. 743–748, 2002.

[121] V. Sankaranarayanan and A. Mahindrakar, "Control of a class of underactuated mechanical systems using sliding modes," *IEEE Transactions on Robotics*, vol. 25, no. 2, pp. 459–467, 2009.

[122] H. Schaub, "Rate-based ship-mounted crane payload pendulation control system," *Control Engineering Practice*, vol. 16, no. 1, pp. 132–145, 2008.

[123] J. She, A. Zhang, X. Lai, and M. Wu, "Global stabilization of 2-DOF underactuated mechanical systemsan equivalent-input-disturbance approach," *Nonlinear Dynamics*, vol. 69, no. 1-2, pp. 495–509, 2012.

[124] F. Singleton, "The Beaufort scale of winds – its relevance, and its use by sailors," *Weather*, vol. 63, no. 2, pp. 37–41, 2008.

[125] B. Skaare and O. Egeland, "Parallel force/position crane control in marine operations," *IEEE Journal of Oceanic Engineering*, vol. 31, no. 3, pp. 599–613, 2006.

[126] Skaugen PetroTrans Inc., "Lightering 101 Introduction to Lightering," Jan 2004.

[127] J.-J. E. Slotine and W. Li, *Applied nonlinear control*. Englewood Cliffs, New Jersey: Prentice Hall, 1991.

[128] M. W. Spong and M. Vidyasagar, *Robot dynamics and control*. New York: John Wiley & Sons, 1989.

[129] S. K. Spurgeon and R. Davies, "A nonlinear control strategy for robust sliding mode performance in the presence of unmatched uncertainty," *International Journal of Control*, vol. 57, no. 5, pp. 1107–1123, 1993.

[130] N. Sun and Y. Fang, "An efficient online trajectory generating method for underactuated crane systems," *International Journal of Robust and Nonlinear Control*, vol. 24, no. 11, pp. 1653–1663, 2014.

[131] N. Sun, Y. Fang, and X. Zhang, "An increased coupling-based control method for underactuated crane systems: Theoretical design and experimental implementation," *Nonlinear Dynamics*, vol. 70, no. 2, pp. 1135–1146, 2012.

[132] K. Takagi and H. Nishimura, "Control of a jib-type crane mounted on a flexible structure," *IEEE Transactions on Control Systems Technology*, vol. 11, no. 1, pp. 32–42, 2003.

[133] C. Tao, J. Taur, and M.-L. Chan, "Adaptive fuzzy terminal sliding mode controller for linear systems with mismatched time-varying uncertainties," *IEEE Transactions on Systems, Man, and Cybernetics, Part B: Cybernetics*, vol. 34, no. 1, pp. 255–262, 2004.

[134] M. Teixeira and S. Żak, "Stabilizing controller design for uncertain nonlinear systems using fuzzy models," *IEEE Transactions on Fuzzy Systems*, vol. 7, no. 2, pp. 133–142, 1999.

[135] Transportation Safety Board of Canada, "Grounding, Container Ship Horizon (Report no. M04L0092)," Sainte-Anne-de-Sorel, Quebec, Canada, July 2004.

[136] C.-S. Tseng, B.-S. Chen, and H.-J. Uang, "Fuzzy tracking control design for nonlinear dynamic systems via T-S fuzzy model," *IEEE Transactions on Fuzzy Systems*, vol. 9, no. 3, pp. 381–392, 2001.

[137] V. Utkin, "Variable structure systems with sliding modes," *IEEE Transactions on Automatic Control*, vol. 22, no. 2, pp. 212–222, 1977.

[138] V. I. Utkin, *Sliding Modes in Control and Optimization*. Berlin: Springer-Verlag, 1992.

[139] F. Valenciaga, "A second order sliding mode path following control for autonomous surface vessels," *Asian Journal of Control*, vol. 16, no. 5, pp. 1515–1521, 2014.

[140] W. Wang, J. Yi, D. Zhao, and D. Liu, "Design of a stable sliding-mode controller for a class of second-order underactuated systems," *IEE Proceedings - Control Theory and Applications*, vol. 151, no. 6, pp. 683–690, 2004.

[141] L. Wu, C. Wang, H. Gao, and L. Zhang, "Sliding mode H_∞ control for a class of uncertain nonlinear state-delayed systems," *Journal of Systems Engineering and Electronics*, vol. 17, no. 3, pp. 576–585, 2006.

[142] R. Xu and Ü. Özgüner, "Sliding mode control of a class of underactuated systems," *Automatica*, vol. 44, no. 1, pp. 233–241, 2008.

[143] J. H. Yang and K. S. Yang, "Adaptive coupling control for overhead crane systems," *Mechatronics*, vol. 17, no. 2-3, pp. 143–152, 2007.

[144] X. F. Yin, L. P. Khoo, and C.-H. Chen, "A distributed agent system for port planning and scheduling," *Advanced Engineering Informatics*, vol. 25, no. 3, pp. 403–412, 2011.

[145] K.-K. D. Young, "Controller design for a manipulator using theory of variable structure systems," *IEEE Transactions on Systems, Man and Cybernetics*, vol. 8, no. 2, pp. 101–109, 1978.

[146] R. Yu, Q. Zhu, G. Xia, and Z. Liu, "Sliding mode tracking control of an underactuated surface vessel," *IET Control Theory Applications*, vol. 6, no. 3, pp. 461–466, 2012.

[147] X. Zhang, Y. Fang, and N. Sun, "Minimum-time trajectory planning for underactuated overhead crane systems with state and control constraints," *IEEE Transactions on Industrial Electronics*, vol. 61, no. 12, pp. 6915–6925, 2014.